1-13-2017

Coastal Ecosystem Processing of Nitrogen Rich High Explosives

Mark L. Ballentine
University of Connecticut - Avery Point, mark.ballentine@uconn.edu

Coastal Ecosystem Processing of Nitrogen Rich High Explosives

Mark Lewis Ballentine, Ph.D.

University of Connecticut, 2017

2,4,6-trinitrotoluene (TNT) and hexahydro-1,3,5-trinitro-1,3,5 (RDX) have been used extensively by the world's militaries for more than a century. Millions of tons of these compounds have been released into marine environments globally. Contamination levels and biological accumulation of TNT and RDX in marine systems from both legacy and new environmental exposures are neither well documented nor understood.

TNT and RDX synthesized with a stable nitrogen isotope (^{15}N) label were used to trace the uptake, biotransformation, and retention of, both parent compounds, their primary organic derivatives, and associated nitrogen-containing breakdown products in coastal marine biota. The experimental approach consisted of single species dose exposures, multi-species interactive steady state experiments, and cross ecosystem comparisons.

First order modeling of tissue RDX and ^{15}N concentrations revealed high rates of uptake offset by rapid elimination and redistribution of tracer into bulk biomass. Tissue ^{15}N levels varied by a factor of 8 between species in the same habitat, and were similar among the same species across different habitats. For all biota, the tissue ^{15}N tracer concentrations associated with intact RDX were 10-fold lower than the total ^{15}N measured in bulk biomass indicating that the majority of the RDX uptake was biotransformed internally. Four different biotransformation pathways were proposed to explain the observed patterns of ^{15}N retention. Some of these pathways may indicate that some organisms could be using N released from RDX as a nutrient

(e.g. macroalgae), while other pathways consist of accumulation of unknown organic N containing derivatives or adducts that may have further toxicity.

The use of the ^{15}N tracer provided the ability to measure munitions biotransformation more completely than previously possible. It revealed that that marine biota take up more TNT and RDX than previously thought, and retain more breakdown products in largely as yet unidentified forms. This discovery raises new questions about the long term impact of post uptake biotransformation products on coastal marine biota.

Coastal Ecosystem Processing of Nitrogen Rich High Explosives

Mark Lewis Ballentine

B.S., Indiana University, 2005

A Dissertation

Submitted in Partial Fulfillment of the

Requirements for the Degree of Doctor of Philosophy

at the

University of Connecticut

2017

2017

Approval Page

Doctor of Philosophy Dissertation

Coastal Ecosystem Processing of Nitrogen Rich High Explosives

Presented by

Mark Lewis Ballentine, B.S.

Major Advisor _____

Craig Tobias

Associate Advisor _____

Penny Vlahos

Associate Advisor _____

Kevin Brown

University of Connecticut

2017

Preface

Each chapter of this dissertation has been submitted and/or published and stands alone[1]. The dissertation introduction and conclusion tie together the overall theme of the work, but specific introductions and conclusions are presented for each chapter. While the use of introductions and conclusions for each chapter creates some repetition, the repetition facilitates the publication of each chapter individually. All chapters describe the uptake and retention of the munitions on coastal marine biota, but each chapter has a more specialized focus: Bioconcentration factor of TNT and RDX (Chapter 2), uptake and modeling of a RDX derived stable nitrogen isotopic tracer (Chapter 3), and uptake and retention of RDX in three simulated coastal habitats (Chapter 4).

[1] All chapters are formatted for the journals in which they are submitted or published: Archives of Environmental Contamination and Toxicology (Chapter 2), Chemosphere (Chapter 3), and Environmental Toxicology and Chemistry (Chapter 4).

Acknowledgements

I would like to thank my advisor, Dr. Craig Tobias, without his years of guidance, patience, and support I surely would still be sitting at my desk writing. I am thankful to Dr. Penny Vlahos for our many meetings about research ideas, writing help, and pep talks. I would also like to thank Dr. Kevin Brown for his help, modeling guidance, and scientific insight. All of my experiments required the help of many people and without them none of my work would have been possible. I would like to thank Chris Cooper, David Cady, and Veronica Rollins for their scientific knowledge and lab savvy that helped my experiments run smoothly. A special thank you to Charlie Woods whom listened and answered all of my questions about building experimental setups and gave great advice. Most importantly, I would like to thank my wife, Regina Ballentine, and my children for their unwavering guidance, support, and love for without them I could not have accomplish my crazy dream.

The staff and facilities at the University of Connecticut's Department of Marine Sciences are world class. The staff made working, taking classes, and completing research interesting and more importantly fun during my time at Uconn. I would like to thank the administrative team for all of the support throughout the years: Mrs. Pat Evans, Mrs. Elise Hayes, Mrs. Janet Laflamme, and Miss Debra Schuler.

Finally, I would like to thank Strategic Environmental Research and Development Program No. ER-2122 for their support and funding.

Table of Contents

List of Tables

Chapter 2:

Chapter 3:

Chapter 4:

List of Figures

Chapter 1:

Chapter 2:

Chapter 3:

Chapter 4:

Chapter 1: Introduction

Background:

2,4,6-trinitrotoluene (TNT) and hexahydro-1,3,5-trinitro-1,3,5-triazine (RDX) have been used extensively by the world's militaries for more than a century. Introduction of these compounds into the marine environment has occurred for almost as long. Munitions have been released to the environment through detonation, manufacturing, disposal, and leakage of underwater military munitions (UWMMs; Harrison & Vane, 2010; Hovatter et al., 1997; Talmage et al., 1999). In addition, prior to 1970, the accepted method of disposal was to dump the obsolete and unserviceable munitions into the oceans. In total the amount of munitions constituents released to the marine environment is estimated in the millions of tons (Voie & Mariussen, 2016). Managing munitions contaminated sites has become an international problem with only a select few countries that have the expertise to characterize the environmental and human impact (Sunahara et al., 2009). Contamination levels and biological accumulation of TNT and RDX in marine systems from both legacy and new environmental exposure are neither well documented nor understood (Clausen et al., 2004; Rosen & Lotufo, 2007). While there are many munitions that are currently in use by the Department of Defense (DoD), this dissertation focuses on primarily on the interaction of TNT, RDX, and their primary derivatives with macrobiota in the coastal marine environment.

TNT is a nitroaromatic compound (Fig. 1.1A) that was invented in 1863 by German chemist Joseph Wilbrand to be used as a yellow dye. It was not used as an explosive in civil engineering or military applications for several years after its initial discovery. TNT is fairly insensitive to shock and heat, can even burn when exposed to heat without detonation. RDX is a nitroamine (Fig. 1.1B) was first reported in 1898 by Georg Friedrich Henning who applied and obtained a German patent for its synthesis. Much like TNT, RDX is insensitive to shock and

will burn without detonation. TNT and RDX are often mixed and co-occur in munitions. A common example is "Composition B" which contains 60% RDX and 40% TNT. Although TNT and RDX can both be present in munitions, environmental contamination can consist of one or both constituents depending on the nature of the release and differential environmental transport characteristics.

Biotransformation of TNT and RDX:

TNT and RDX can be found around the globe in environments rich with life (Pennington & Brannon, 2002). While millions of tons of munitions have been dumped into the environment, studies of freshwater and terrestrial reveal typically low biotic tissue concentrations for species exposed to munitions (Lotufo et al., 2009). Understanding the ability of how different species biotransform TNT and RDX is important for policy makers in decisions for possible remediation. Munitions transformation pathways have been extensively studied in both terrestrial and freshwater environments (Monteil-Rivera et al., 2009) in very controlled environmental experiments. There are various breakdown pathways for TNT that include transformation via alkaline hydrolysis (Emmrich, 2001), photolysis (Andrews & Osmon, 1975), reduced in the presence of iron (Oh et al., 2002), and can be biotransformed (Monteil-Rivera et al., 2009). While there are many transformation pathways TNT can undergo to produce breakdown derivatives, the aromatic ring at the center of the TNT molecule is stable and does not break apart under most environmental conditions (Monteil-Rivera et al., 2009). The stability of TNT's aromatic ring allows for a large suite of stable TNT derivatives to be measured in the environment. The breakdown plays a role in the potential presence of toxic breakdown products which directly influence macrobiota. The coastal marine environment with high rates of production are in an intensely redox active (both aerobic and anaerobic) environment. Previous

controlled freshwater and terrestrial studies may or may not be an adequate analog for interaction between TNT and coastal marine biota.

RDX much like TNT has both aerobic and anaerobic transformation pathways. Although RDX and TNT both can be transformed in aerobic and anaerobic conditions, RDX has transformation pathways that differ from that of TNT. RDX does not have the stabilizing aromatic ring of TNT which leads to transformation pathways leading to aliphatic derivatives (Hawari et al., 2002). Tracing the biotransformation of RDX will help reveal differences between previous studies (aquatic and terrestrial controlled experiments) and simulated marine mesocosms. Both RDX and TNT have derivatives that contain large amounts of nitrogen that allows for the use of stable nitrogen isotopes as a tool for tracing biotransformation of the munitions compounds.

Stable isotopes:

Stable isotopes are a powerful tool that allow for the tracing of nitrogen, carbon, oxygen, or other molecules in the both laboratory and environmental systems. Stable isotopes have been used previously for toxicological (Rosen & Lotufo, 2005), bioconcentration (Houston & Lotufo, 2005), biodegradation studies (Annamaria et al., 2010; Van Aken et al., 2004), and in marine systems for examining uptake/cycling of dissolved inorganic nitrogen (DIN; Holmes et al., 2000; Tobias et al., 2003). The previous studies using stable isotopes for munitions work focused mainly on ^{14}C and ^{18}O tracer. The use TNT and RDX with a stable nitrogen isotope label is a novel approach of tracking the biotransformation of munitions in experiments that simulate complex coastal marine environments (e.g. mesocosms). The three nitrogen atoms in the nitro groups on the aromatic ring of TNT, along with all of the six nitrogen atoms contained within the RDX molecule, can be traced during compound assimilation and breakdown at organismal to

ecosystem scales. The use of stable nitrogen isotopes opens the possibility to trace a majority of possible biotransformation and mineralization products allowing for a more complete accounting of RDX and TNT uptake and processing within macroorganisms.

Research Objectives:

The overarching goal of this dissertation was to trace the uptake, biotransformation, and elimination of TNT and RDX in coastal marine biota. The following chapters describe evaluation of these processes first under highly controlled exposure conditions, followed by inclusion of competing sediment microbial mineralization reactions, and finally conclude with a mesocosm scale cross ecosystem evaluation.

Chapter 2: Bioconcentration of TNT and RDX in Coastal Marine Biota.

The goal of this chapter was threefold: (1) to experimentally determine steady-state bioconcentration factor (BCF) values for TNT, RDX, and their derivatives in marine biota across a range of trophic levels; (2) to assess metabolism of munitions in organisms that contribute to BCF values; and (3) to assess these experimentally derived values in the context of other approaches for estimating BCF values. These short term experiments were conducted at the benchtop scale under conditions where munitions degradation via microbial breakdown was negligible.

Chapter 3: Uptake and fate of hexahydro-1,3,5-trinitro-1,3,5-triazine (RDX) in coastal marine biota determined using a stable isotopic tracer, ^{15}N-[RDX]

The goal of this chapter was to quantify RDX uptake in 9 different coastal marine species, and assess RDX-derived nitrogen retention in the organism using ^{15}N nitro-labeled RDX in an aquaria where other competing RDX degradation pathways were operating (mineralization). ^{15}N

mass balance modeling was used to evaluate the uptake, transformation, retention, and elimination of RDX in the biota.

Chapter 4: Biotic uptake and retention of hexahydro-1,3,5-trinitro-1,3,5-triazine (RDX) derived nitrogen measured in three simulated coastal habitats

The goal of this chapter was to compare the biotic uptake and retention of RDX derived nitrogen using ^{15}N nitro-labeled RDX in 13 different marine species across marine habitats that exhibited different levels of RDX mineralization. Experimental conditions in the mesocosms simulated three common coastal ecotypes: subtidal sand, subtidal vegetated fine-grained sediment, and intertidal salt marsh. The patterns of biotic processing were compared across these ecotypes.

References

Andrews, C. C., & Osmon, J. L. (1975). *The Effects of Ultraviolet Light on TNT in Aqueous Solutions,* Report WQEC/C 75-197 (AD-B008175), Weapons Quality Engineering Center, Naval Weapons Support Center, Crane, IN.

Annamaria, H., Manno, D., Strand, S. E., Bruce, N. C., & Hawari, J. (2010). Biodegradation of RDX and MNX with *rhodococcus* sp. strain DN22: New insights into the degradation pathway. *Environmental Science & Technology, 44*(24), 9330-9336.

Clausen, J., Robb, J., Curry, D., & Korte, N. (2004). A case study of contaminants on military ranges: Camp Edwards, Massachusetts, USA. *Environmental Pollution, 129*(1), 13-21.

Emmrich, M. (2001). Kinetics of the alkaline hydrolysis of important nitroaromatic co-contaminants of 2, 4, 6-trinitrotoluene in highly contaminated soils. *Environmental Science & Technology, 35*(5), 874-877.

Harrison, I., & Vane, C. (2010). Attenuation of TNT in seawater microcosms. *Water Science and Technology, 61*(10), 2531-2538.

Hawari, J., Halasz, A., Groom, C., Deschamps, S., Paquet, L., Beaulieu, C., & Corriveau, A. (2002). Photodegradation of RDX in aqueous solution: A mechanistic probe for biodegradation with *rhodococcus* sp. *Environmental Science & Technology, 36*(23), 5117-5123.

Holmes, R. M., Peterson, B. J., Deegan, L. A., Hughes, J. E., & Fry, B. (2000). Nitrogen biogeochemistry in the oligohaline zone of a New England estuary. *Ecology, 81*(2), 416-432.

Houston, J. G., & Lotufo, G. R. (2005). Dietary exposure of fathead minnows to the explosives TNT and RDX and to the pesticide DDT using contaminated invertebrates. *International Journal of Environmental Research and Public Health, 2*(2), 286-292.

Hovatter, P. S., Talmage, S. S., Opresko, D. M., & Ross, R. H. (1997). Ecotoxicity of mitroaromatics to aquatic and terrestrial species at army superfund sites. *ASTM Special Technical Publication,* (1317), 117-129.

Lotufo G.R., Lydy M.J., Rorrer G.L., Cruz-Uribe O., Cheney D.P. (2009) Bioconcentration, bioaccumulation, and biotransformation of explosives and related compounds in aquatic organisms. In: Sunahara G.I., Lotufo G., Kuperman R.G., Hawari J. (eds) Ecotoxicology of explosives. CRC press, Boca Raton, pp 123-155.

Monteil-Rivera F., Halasz A., Groom C., Zhao J., Thiboutot S., Ampleman G., Hawari J. (2009) Fate and transport of explosives in the environment: a chemist's view. In: Sunahara G.I., Lotufo G., Kuperman R.G., Hawari J. (eds) Ecotoxicology of explosives. CRC press, Boca Raton, pp 5-33.

Oh, S., Cha, D. K., Kim, B. J., & Chiu, P. C. (2002). Effect of adsorption to elemental iron on the transformation of 2, 4, 6- trinitrotoluene and hexahydro- 1, 3, 5- trinitro- 1, 3, 5-triazine in solution. *Environmental Toxicology and Chemistry, 21*(7), 1384-1389.

Pennington, J. C., & Brannon, J. M. (2002). Environmental fate of explosives. *Thermochimica Acta, 384*(1), 163-172.

Rosen, G., & Lotufo, G. R. (2005). Toxicity and fate of two munitions constituents in spiked sediment exposures with the marine amphipod *Eohaustorius estuarius*. *Environmental Toxicology and Chemistry, 24*(11), 2887-2897.

Rosen, G., & Lotufo, G. R. (2007). Bioaccumulation of explosive compounds in the marine mussel, *Mytilus galloprovincialis*. *Ecotoxicology and Environmental Safety, 68*(2), 237-245.

Sunahara G.I., Kuperman R.G., Lotufo G.R., Hawari J., Thiboutot S., Ampleman G. (2009) Introducion. In: Sunahara G.I., Lotufo G., Kuperman R.G., Hawari J. (eds) Ecotoxicology of explosives. CRC press, Boca Raton, pp 1-3.

Talmage, S. S., Opresko, D. M., Maxwell, C. J., Welsh, C. J., Cretella, F. M., Reno, P. H., & Daniel, F. B. (1999). Nitroaromatic munition compounds: Environmental effects and screening values. *Reviews of environmental contamination and toxicology* (pp. 1-156) Springer.

Tobias, C., Giblin, A., McClelland, J., Tucker, J., & Peterson, B. (2003). Sediment DIN fluxes and preferential recycling of benthic microalgal nitrogen in a shallow macrotidal estuary. *Marine Ecology Progress Series, 257*, 25-36.

Van Aken, B., Yoon, J. M., & Schnoor, J. L. (2004). Biodegradation of nitro-substituted explosives 2,4,6-trinitrotoluene, hexahydro-1,3,5-trinitro-1,3,5-triazine, and octahydro-1,3,5,7-tetranitro-1,3,5-tetrazocine by a phytosymbiotic methylobacterium sp. associated with poplar tissues (*Populus deltoides* x *nigra* DN34). *Applied and Environmental Microbiology, 70*(1), 508-517.

Voie, Ø A., & Mariussen, E. (2016). Risk assessment of sea dumped conventional munitions. *Propellants, Explosives, Pyrotechnics.* DOI 10.1002/prep.201600163

Figure and Table Captions:

Figure 1.1: Molecular structure of TNT and RDX. A. is the molecular structure of the nitroaromatic compound TNT that has a molecular weight of 227.13 g mol^{-1}. B. is the molecular structure of the nitroamine RDX that has a molecular weight of 222.26 g mol^{-1}.

Figure 1: Molecular Structure of TNT and RDX

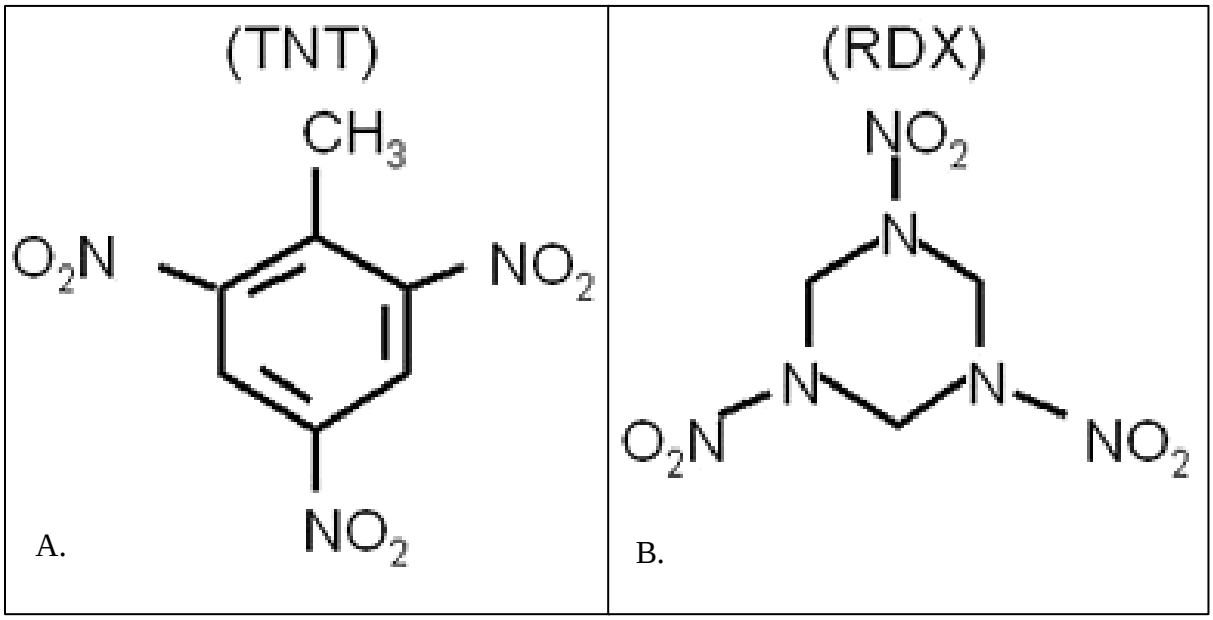

Chapter 2: Bioconcentration of TNT and RDX in Coastal Marine Biota[2]

[2] Ballentine, M., Tobias, C., Vlahos, P., Smith, R., & Cooper, C. (2015). Bioconcentration of TNT and RDX in coastal marine biota. *Archives of Environmental Contamination and Toxicology, 68*(4), 718-728.

Abstract

The bioconcentration factor (BCF) was measured for 2,4,6-trinitrotoluene (TNT) and hexahydro-1,3,5-trinitro-1,3,5-triazine (RDX) in seven different marine species of varying trophic levels. Time series and concentration gradient treatments were used for water column and tissue concentrations of TNT, RDX, and their environmentally important derivatives 2-amino-4,6-dintrotoluene (2-ADNT) and 4-amino-2,6-dinitrotoluene (4-ADNT). BCF values ranged from 0.0031 to 484.5 mL g^{-1} for TNT and 0.023 to 54.83 mL g^{-1} for RDX. The use of log K_{ow} value as an indicator was evaluated by adding marine data from this study to previously published data. For the munitions in this study, log K_{ow} value was a good indicator in the marine environment. The initial uptake and elimination rates of TNT and RDX for *Fucus vesiculosus* were 1.79 and 0.24 h^{-1} for TNT and 0.50 and 0.0035 h^{-1} for RDX respectively. Biotransformation was observed in all biota for both TNT and RDX. Biotransformation of TNT favored 4-ADNT over 2-ADNT at ratios of 2:1 for *Fucus vesiculosus* and 3:1 for *Mytilus edulis*. Although RDX derivatives were measureable, the ratios of RDX derivatives were variable with no detectable trend. Previous approaches for measuring BCF in freshwater systems compare favorably with these experiments with marine biota, yet significant gaps on the ultimate fate of munitions within the biota exist that may be overcome with the use stable isotope labeled munitions substrates.

1. Introduction

Munitions have been released to the environment through detonation, manufacturing, disposal, and leakage of underwater military munitions (UWMMs; Harrison and Vane 2010; Hovatter et al. 1997; Talmage et al. 1999). The United States alone has >50 coastal military sites. Documented contamination in soils, aquatic sediments, surface and groundwaters has been reported (Best et al. 1999; Pennington and Brannon 2002). Disposal of UWMMs into the oceans has been practiced since the Second World War (Darrach et al. 1998; Sunahara et al. 2009), but contamination levels and biological accumulation in marine systems is neither well documented nor understood (Clausen et al. 2004; Rosen and Lotufo 2007; Lotufo et al. 2009). For example, low concentrations of munitions detected in marine sediments (Darrach et al. 1998; Ek et al. 2006) have been linked to increase mortality to *Nitocra spinipes*, a marine copepod, whereas no significant impact was found for either *M. edulis* (blue mussel) or *Platichtys flesus* (European flounder) (Ek et al. 2006).

The munitions most likely to be of concern in marine environments are 2,4,6 trinitrotoluene (TNT), hexahydro-1,3,5-trinitro-1,3,5-triazine (RDX), and octahydro-1,3,5,7-tetranitro-1,3,5,7-tetrazocine (HMX; Lotufo et al. 2010). TNT readily undergoes microbial-mediated transformations along with abiotic processing to produce the mono amino products 2-amino-4,6-dintrotoluene (2-ADNT) and 4-amino-2,6-dinitrotoluene (4-ADNT), but breakdown products of RDX are not often observed (Pennington and Brannon 2002; Smith et al. 2013; Monteil-Rivera et al. 2009). TNT and RDX along with their derivatives are United States Environmental Protection Agency (USEPA) priority pollutants. Toxicity of TNT and its two major degradation products, 2-ADNT and 4-ADNT, along with RDX have been reported for several aquatic and terrestrial species (Lotufo et al. 2001, 2010; Nipper et al. 2009; Talmage et

al. 1999; Yoo et al. 2006). However, the bioconcentration of TNT and RDX in coastal marine biota is not well studied (Lotufo et al. 2009; Talmage et al. 1999).

Bioconcentration factor (BCF) is the most common indicator for the tendency of a substance to partition to exposed biota (Meylan et al. 1999). The BCF value is a ratio of the concentration of the compound in the biota tissue to the concentration of the compound in the surrounding seawater. BCF values can be experimentally derived, as in this study, or they can be estimated from the regression equations of the general form (Meylan et al. 1999):

$$\log BCF = a \log K_{ow} + b \quad (1)$$

where K_{ow} is the octanol/water partition coeffiecient, and terms a and b are empirically derived constants for a wide variety of compounds. Meylan et al. (1999) derived a = 0.86 and b = -0.39 for nonionic compounds with a Log K_{ow} in the range of 1-7 (Meylan et al. 1999). Lotufo et al. (2009) similarly derived an equation relating K_{ow} to BCF from a review of published works for a variety of munition compounds and species (a = 0.53 and b = -0.23) and found that the majority of BCF values for munitions in their study were dramatically lower than the predicted values using Meylan et al. (1999) values (Lotufo et al. 2009). The equation relating BCF to K_{ow} for munitions reported by Lotufo et al. (2009) contains values derived from a relatively small number of primarily freshwater species and only one marine fish. Increasing the range of species evaluated by Lotufo et al. (2009) to include the following marine biota would be valuable for further study of munitions effects on marine organisms and food webs.

The BCF values of coastal marine biota with respect to munitions compounds are not well known. The majority of experiments completed for munitions are toxicity studies that were performed using terrestrial and freshwater organisms with very few BCF studies completed for

marine species (Rosen and Lotufo. 2007; Lotufo et al. 2009, 2010; Ek et al. 2006; Ownby et al. 2005). Expanding munitions BCF characterization to a broader collection of marine organisms is an important first step for constraining reasonable assessments of ecological and human health risks in marine settings associated with these compounds. The objectives of this study were threefold: (1) to experimentally determine minimum approach steady-state BCF values for TNT, RDX, and their derivatives in marine biota across a range of trophic levels similar to studies summarized in Lotufo et al (2009); (2) to assess metabolism of munitions in organisms that contribute to BCF values; and (3) to assess these experimentally derived values in the context of other approaches for estimating BCF values.

2. Methods

2.1 Experimental Design

In total, one phytoplankton species (*Tetraselmis impellucida*), two macroalgae species (*Fucus vesiculosus* and *Ulva lactuca*), two epifaunal species (*Hemigrapsus sanguineus* and *Littorina littorea*), and two bivalve species (*Crassostrea virginica* and *Mytilus edulis*) were used in TNT- and RDX-exposure experiments. The species were chosen to represent several trophic levels of a coastal marine ecosystem.

Two experimental approaches were used to expose organism to the munitions compounds; each designed to address a specific objective. The first approach consisted of exposures to multiple concentrations (concentration gradient) to calculate BCF values. The second approach used a single addition followed by rapid time series sampling to calculate initial uptake and elimination rates and determine metabolism of munitions within the organism.

2.2 BCF Values

The experiments designed to estimate BCF were based on modifications of Rosen and Lotufo (2007). Multiple 18-liter glass aquaria were established with each containing three individuals of a single species. Each aquarium then had an addition of different munitions concentrations (Table 2.1). All organisms were sampled once after a 24 hour exposure period. This concentration gradient approach was performed on *F. vesiculosus* (macroalgae), *U. lactuca* (macroalgae), *H. sanguineus* (green crab), *L. littorea* (periwinkle), *C. virginica* (eastern oyster), and *M. edulis* (blue mussel), as well as on the phytoplankton *T. impellucida*, where the incubation was performed in culture flasks instead of aquaria. *T. impellucida* had munitions added in 250 mL Corning culturing flasks (Cole-Parmer, USA) and were held in an 18°C temperature- and light-controlled room. *T. impellucida* was gifted by Gary Wikfors from a pure stock grown in the National Oceanic and Atmospheric Administration laboratory (Milford, Connecticut, USA). All biota, with the exception of *T. impellucida,* were collected from eastern Long Island Sound Connecticut and held in flow through seawater tanks sourced from Long Island Sound before experimentation.

2.3 Rates and Munitions Biotransformation

The experiments designed to quantify munitions biotransformation consisted of a concentrated single addition of the munitions TNT and RDX dissolved together in methanol (~0.05 percent of total aqueous volume, Table 2.1) into 75 liter glass aquaria containing several individuals of a single species. Aqueous and biota sampling occurred 1 h after the initial spike and then once every 24 h for 168 h for *M. edulis*. For *F. vesiculosus,* aqueous and biotic sampling occurred at 15, 30 min, 1, 4, 24, 48 h, and finally at 120 h. The initial uptake rates are defined for this experiment as the increase of munitions in biota from the time of the spike until the

concentration in the tissue reached a maximum and started to decrease. Initial uptake rates were calculated using plots of log concentration versus time during the first few time points during which the water concentration was relatively constant and matched requirements of a "constant" concentration exposure according to American Society for Testing and Materials (ASTM) E1022-94 (2013). This is method differs from Cruz-Uribe et al. (2007) and Makris et al. (2007) where uptake rates were modeled using removal rates of munitions from water. The elimination rates in this study were calculated using plots of log concentration versus time plots starting at the time point with the highest concentration of munitions until the end of the experiment. The elimination rate in this study differed from Lotufo and Lydy (2005) and Rosen and Lotufo (2007) who calculated depuration rates from a decrease in tissue munitions concentrations in organisms that had been exposed but subsequently moved to munitions-free water (ASTM E1022-94 ,2003). Two organisms, the bivalve *M. edulis* and the macroalgae *F. vesiculosus,* were used in this experiment, both of which, according to existing literature, are believed to possibly represent disparate magnitudes of storage versus processing of munitions (Cruz-Uribe et al. 2007; Makris et al. 2007; Rosen and Lotufo 2007; Vila et al. 2007).

Seawater for all experiments (~30 ppt) was supplied from Long Island Sound and was sand-filtered before addition to the tanks. Temperature, salinity, and dissolved oxygen in the tanks were monitored with an YSI 556 MPS multiparameter instrument (YSI Inc., Yellow Springs, OH) during the experiments. All treatments, except for *T. impellucida,* were exposed to ambient light conditions and room temperatures (16° to 18°C). These ambient conditions were previously shown to have minimal photo degradation effect on the munitions during the time period of the experiments (Smith et al. 2013). *T. impellucida* were kept in a climate-controlled environmental room with a constant temperature of 18°C and a 12-hour light-to-dark cycle.

2.4 Sampling and Analysis

Water and biota collected from the experimental aquaria were analyzed for TNT, 2A-DNT, 4A-DNT, RDX, hexahydro-1,3,5-trinitroso-1,3,5-triazine (TNX), hexahydro-5-nitro-1,3-dinitroso-1,3,5-triazine (DNX), and hexahydro-3,5-dinitro-1-nitroso-1,3,5-triazine (MNX). For water samples, all experiments, except those with *F. vesiculosus*, 5-mL seawater samples were taken and immediately added to 5 mL of high-performance liquid chromatography (HPLC)-grade methanol, shaken, and filtered using 0.45-µm polytetrafluoroethylene (PTFE) syringe-tip filters. Samples were then analyzed by HPLC using USEPA method 8330 (USEPA 1994) as modified by Smith et al. (2013).

To accommodate smaller sampling volumes, water samples for *F. vesiculosus* incubations used a modified "salting out" technique adapted from (Miyares and Jenkins 1990). The change in water-sampling method was introduced to detect munition at lower concentrations. Two mL of seawater sample were added to 1.3 grams of NaCl and shaken. American Chemical Society (ACS)-grade acetonitrile, 1.5 mL, was added then shaken for 5 min. Once the acetonitrile separated from the seawater, the acetonitrile was siphoned off using a 10-mL syringe. The process was repeated two more times using 1 mL of the ACS-grade acetonitrile. Final extract, 1 mL, was then placed into a chromatography vial and run using the gas chromatographer (GC)/electron-capture detector (ECD) with the same method detailed later in the text.

For biota samples, immediately after harvesting the biota were rinsed for 5 min with clean filtered seawater to remove dissolved and weakly sorbed munitions from the tissue surfaces. In the case of *T. impellucida*, the growth media was filtered to collect the species, and then the filters were rinsed with clean filtered seawater. The shells of *M. edulis, H. sanguineus,*

C. virginica, and L. littorea were opened before being rinsed. Once rinsed, tissues were removed, freeze-dried, and weighed. The *H. sanguineus* eggs were found attached to the crab before the experiment and were left in place. The entire sample (crab and eggs) was frozen, and then the eggs were removed from the crabs before the freeze-drying step. The eggs were then prepared the same as all other samples. Samples were then extracted using methods modified from (Conder et al. 2004). ACS-grade acetonitrile, 10 mL, was added to the samples and homogenized using a Tissue Master 125 (Omni International, Kennesaw, GA). Homogenates were then spiked with 0.01 mg L^{-1} of aldrin as an internal standard. The homogenate was sonicated for 1 h and then centrifuged for 10 min at 10,000 rpms. The supernatant was removed and filtered through 0.22-µm PTFE syringe-tip filter.

GC/ECD analysis on the extracts was performed according to methods described by Pan et al. (2005). One microliter of the solution was injected into an Agilent GC/ECD equipped with a HP-DB5 column (30 m x 320 µm, 0.25 µm; Agilent). A pulsed splitless liner was used with helium as the carrier gas at a flow rate of 11.9 mL min^{-1}. The oven temperature was maintained at 90°C with two ramps: ramp 1 at 10.9 min to 200°C held for 1.5 min and ramp 2 at 14.2 min to 250°C held for 1.9 min. Quantification was based on an external calibration curve of available standard munitions TNT, 2-ADNT, 4-ADNT, RDX, MNX, DNX, and TNX (Accustandard, New Haven, Connecticut, USA). The reporting limit for all compounds was 0.7 ng mL^{-1} because this is the lowest point on the calibration curve, and recoveries of munitions from tissue samples were 82 ± 15 %.

3. Results

3.1 Aqueous Concentrations

For the single addition time series experiments (*F. vesiculosus* and *M. edulis*), TNT decreased over the incubation period with a loss of 93% in the *F. vesiculosus* treatment and 70% in the *M. edulis* treatment by the 120- and 168-hour mark, respectively (Fig. 2.1a, b). RDX concentrations remained relatively constant through both incubations. During the course of the incubation, RDX breakdown products TNX, DNX, and MNX were not detected, but TNT derivatives 4-ADNT and 2-ADNT were measurable and increased during the exposure (Fig. 2.1a, b). By the end of the incubation, 4-ADNT and 2-ADNT reached concentrations of 0.29 mg L^{-1} and 0.15 mg L^{-1} for the *F. vesiculosus* treatment (Fig. 2.1a) , and 0.29 mg L^{-1} and 0.10 mg L^{-1} for the *M. edulis* (Fig. 2.1b), i.e., 21 and 18% of the initial TNT concentration, respectively. The ratio of 4-ADNT to 2-ADNT in the water was initially measured at 15 min at 1:1 increasing to 2:1 over the incubation for the *F. vesiculosus* and 2.3:1 to 2.8:1 for *M. edulis*.

Aqueous concentrations of munitions in the 24-hour concentration gradient experiments varied little from the initial spike concentration (Table 2.1). Initial munitions concentrations were compromised before analysis, but repeat experiments indicated good fidelity between measured initial concentrations, target concentrations, and TNT and RDX concentrations over the 24 hour duration (Table 2.1).

3.2 Tissue concentrations

No mortality or sublethal effects were observed in any of the experiments. Extractable munitions concentrations were normalized to organism gram dry weight (g dw) to account for differences in size. For the single-addition time series experiment, the *F. vesiculosus* TNT uptake rate was 3.5 times faster than that for RDX. TNT concentrations in *F. vesiculosus* followed a pattern of

initial uptake followed by a decrease until they reach a constant value of approximately 0.1 µg TNT g dw^{-1} (Fig. 2.2a). 4-ADNT and 2-ADNT increased rapidly to reach a peak value after 1 h of 2 µg 4-ADNT g dw^{-1} and 1.4 µg 2-ADNT gdw^{-1}, respectively. TNT derivatives were measured at greater values then TNT in *F. vesiculosus* tissue at every time point. At the final time point of 120 h, 4-ADNT was 10 times more concentrated in tissue than TNT, and 2-ADNT was 5 times greater. The ratio of 4-ADNT to 2-ADNT increased with time to a maximum ratio of 2.7 to 1. RDX, however, experienced an initial uptake without any subsequent decrease in concentration in the tissue and remained constant (Fig. 2.2b). There were no derivatives of RDX in *F. vesiculosus.* The initial uptake of TNT and RDX were calculated for *F. vesiculosus* from plots of log concentration versus time (Table 2.2). Although the TNT concentration in the water was added as a single addition, the first 4 h the concentration remained within 24% of the initial concentration, thereby permitting a calculation of uptake rates according to ASTM E1022-94 (2013). Only RDX-elimination rates (Table 2.2) were calculated for *M. edulis* because there were not enough data points to calculate initial uptake rates and because the TNT concentration decreased too quickly to permit calculation of TNT-elimination rates according to ASTM E1022-94 (2013). The single-addition time series for *M. edulis*, however, showed quick uptake of TNT within the first hour of exposure and then a near constant amount of TNT and derivatives (Fig 2.2c, d) even though the water concentration continued to decrease. 4-ADNT was the dominant TNT derivative with concentrations that were constantly 2 to 3 times higher than measured TNT. The ratio of 4-ADNT to 2-ADNT in *M. edulis* increases from 1.4:1 to 2:1 over the time series. Rapid incorporation of RDX into tissues during the first hour was followed by a decrease to a lower constant value of approximately 5 µg RDX g dw^{-1} (Fig 2d). Only trace RDX derivative concentrations were measured. MNX and TNX were 5-10 times less than the RDX with the

ratio of MNX to TNX ranging from 0.5:1 to 2:1. The ratios for the RDX derivatives were variable with no clear trend over the time series.

In the concentration gradient experiments, the 24-hour TNT tissue concentrations varied between species by one order of magnitude for any given concentration though tissue concentrations in all species increased with higher aqueous concentrations. The variability in tissue concentrations measured among replicates was dependent on species type. For example, differences as low as 4% were measured in *M. edulis*, whereas tissue concentrations varied ≥89% in *C. virginica.* With the exception of *H. sanguineus*, all species showed a large amount of TNT derivatives relative to TNT (Table 2.3). *H. sanguineus* and its eggs contained ≥15 times more TNT than derivatives. Ratios of 4-ADNT to 2-ADNT in all species had a narrow range from 1.1:1 to 2.1:1, respectively (Table 2.3). The *H. sanguineus eggs* contained 9 times the amount of 4-ADNT than 2-ADNT. Ratios of RDX and its derivatives in tissue varied greatly between and within species. In *Crassostrea virginica* for example, RDX would range from 27 to 83% the sum total of RDX and derivatives. DNX (and no MNX) was detected in two species, *H. sanguineus* eggs and *L. littorea*. MNX was detected in all other species tissues tested.

3.3 BCF Determination

Measured concentrations and subsequent BCF values calculated are reported for parent explosives and the sum of parent explosives and their primary derivative products ∑TNT or ∑RDX (Table 2.4), where the ∑TNT = TNT + 2-ADNT + 4-ADNT and ∑RDX = RDX + DNX + MNX + TNX. BCF values were calculated in two ways from the concentration gradient data as follows: (1) Linear regressions were used to express BCF value as a ratio of munitions with the concentration of munitions in tissue in the numerator divided by the denominator of the concentration of munitions in the seawater (Fig. 2.3) or (2) a portion of the RDX and ∑RDX -

BCF values from the concentration gradient experiments were calculated using single point values instead of linear regressions. In this case, single time point BCF values were derived by dividing the tissue munitions concentrations by the aqueous munitions concentrations for a given time point. These single time point BCF values were then averaged to yield a single species-specific BCF estimate (Table 2.4). This approach was used when the tissue concentration did not yield a significant linear regression as a function of aqueous concentration. BCF values were used to calculate the ∑RDX BCF values in all species except *F. vesiculosus, M. edulis, H. sanguineus,* and *H. sanguineus* eggs (Table 2.4). This approach was not used for any TNT BCF values. The BCF values for TNT and RDX ranged over several orders of magnitude (Table 2.4). The lipid rich *H. sanguineus* eggs had the highest BCF for ∑TNT at 484.5 mL g^{-1}, whereas *U. lactuca* had the lowest value at 0.40 mL g^{-1}. For the ∑RDX, *T. impellucida* had the largest BCF value at 54.83 mL g^{-1} and *U. lactuca* the lowest at 0.21 mL g^{-1}.

4. Discussion

4.1 Rates

Overall, the measured initial uptake rates for TNT and RDX fell within published uptake values for fresh and marine biota (Lotufo and Lydy 2005; Makris et al. 2007; Rosen and Lotufo 2007). In the time series experiments, the initial uptake rates were a function of compound type but not organism type. The parent compounds TNT and RDX showed a rapid initial uptake in tissues of *M. edulis* and *F. vesiculosus* within the first hour. This result is more consistent with the different chemical properties of the munitions controlling uptake rather than some species-specific to difference in organisms. This result is surprising given the dissimilarities between *M. edulis* and *F. vesiculosus* tissues with respect to C:N ratios, lipid content, differences in metabolism, and behavior (Jones and Harwood 1992; Smaal and Vonck 1997; Thompson and

Bayne 1974; Yates and Peckol 1993). Elimination rates of RDX differed substantially between *M. edulis* and *F. vesiculosus*. Like previous reports, RDX elimination rates measured in this marine study were faster than those reported for aquatic organisms (Conder et al. 2004; Lotufo and Lydy 2005; Rosen and Lotufo 2007). The slower elimination rate of RDX in *F. vesiculosus* could be caused by intracellular storage of RDX being a more important factor than biotransformation of the compound in the tissue similar to reports in argonomic plants (Vila et al. 2007). RDX elimination rates measured were similar to TNT elimination rates found by Cruz-Uribe et al. (2007) using three species of marine macroalgae. *M. edulis* does not seem to have a storage mechanism for RDX. Instead the rates for uptake and elimination quickly yielded an apparent steady-state concentration of RDX within the *M. edulis* (Fig. 2d). The appearance rate for TNT derivatives reported in Table 2.2 is the rate that TNT derivatives initially appear and then increase over the time series. Appearance rate in this experiment could include the internal biotransformation of TNT to its derivatives and/or production of derivatives in the water that are repartitioned. Half-lives reported (Table 2.2) reflect the balance among uptake, breakdown, and elimination rates.

4.2 Biotransformation

The time series experiments showed measureable amounts of 4-ADNT and 2-ADNT detected within the first hour in both water and tissue depending on organism and compound. TNT transformation in the water column within this first hour was likely bacterially mediated. Photodegradation was discounted by both a control and by previous experiments (Smith et al., 2013) wherein the control tank (water only) showed a loss of only 27% of the parent munitions in the water. Ratios of the TNT derivatives in tissues shifted over time. Initially, *F. vesiculosus* tissue had the same 1:1 ratio of 4-ADNT to 2-ADNT as did the water column. Over the time

series, biotransformation occurred within the organism, and the ratio increased as high as 3:1 in the *F. vesiculosus* tissue, whereas the water column shifted to a 2:1 ratio. Similarly, in the *M. edulis* treatment, the ratio of 4-ADNT to 2-ADNT did increase in both the tissue and the water column over the time series. The ratio in the water increased from 2:1 to 3:1, whereas the ratio in the tissue also increased from 1.5:1 to 2:1, respectively. For both *M. edulis* and *F. vesiculosus*, the lower TNT derivatives ratio in tissue relative to the water indicate that TNT biotransformed within the organisms, and this is consistent with similar reports (Lotufo et al. 2009). The ratios of 4-ADNT to 2-ADNT for all the biota exposed to an addition of munitions show a non-organism specific preferential biotransformation pathway to 4-ADNT (Table 2.3).

For both the *F. vesiculosus* and *M. edulis* treatments, the water column had no detectable RDX derivatives indicating little breakdown, microbial or otherwise, in the aqueous phase. The high RDX and lack of derivatives measured in *F. vesiculosus* may reflect uptake and storage, with little biotransformation, as observed in vascular plants (Vila et al. 2007). In contrast, *M. edulis* tissue was found to contain RDX derivatives. Because there were no RDX derivatives in the water, the RDX derivatives detected in *M. edulis* tissues were due to internal biotransformation. MNX and TNX were found in *M. edulis* tissue at a ratio ranging from 0.5:1 to 2:1, respectively. The lack of DNX in the tissue might suggest that the production of DNX from MNX is a rate-limiting step in the breakdown of RDX. The relatively small amounts of MNX, DNX, and TNX compared with those of RDX also suggest that the biota do not readily breakdown RDX on these time scales although the capacity for detoxifying enzymes' ability to process all these compounds has been documented (Cho et al. 2008; Kitts et al. 2000; Levine et al. 1990; Macek et al. 2000). For RDX, despite increasing knowledge of transformation

pathways in groundwaters and sediments, clear mechanisms of derivative production from RDX in biota remains unresolved.

4.3 BCF Values

BCF values calculated fall within ranges of published experimental values for a variety of freshwater and limited number of saltwater species (Belden et al. 2005; Lotufo and Lydy 2005; Ownby et al. 2005; Yoo et al. 2006). The majority of the BCF values reported in this study are within one order of magnitude of each other (Table 2.4), and are all lower than BCF of 1000, which is typically considered the threshold above which high bioaccumulation potential should be significant (Singh 2013). The *H. sanguineus* eggs were found to have a much higher BCF for TNT than whole biota. Furthermore, the similarity of the ∑TNT (484.5 mL g^{-1}) and TNT (466.4 mL g^{-1}) BCF values, along with the ratio of TNT to 2-ADNT and 4-ADNT (Table 2.3), indicate that biotransformation of TNT in eggs was much less than the extent in the biota. This greater egg BCF value is likely due to greater lipid content and is consistent with a greater K_{ow} of TNT than that of RDX. Greater amounts of TNT also are found in the viscera of fish that contain relative more lipid content than other parts of the organism (Lotufo 2011). The greater lipid content and possible missing biotransformation framework of the eggs could be of ecological interest since the BCF is greater. The toxicological effects of the TNT on the eggs were not evaluated here, but they might be important for egg development and to organisms that eat the eggs. Although the BCF values measured in this study are greater than other BCF values reported for terrestrial and aquatic organisms, they remain <1,000 and are not considered to be indicative of high bioaccumulation potential (Singh 2013).

Here we calculated BCF values for parent and parent plus derivatives based on direct analysis of these compounds, but there are a variety of approaches used to determine the BCF

value that must be clear when comparing BCF estimates. The BCF can be calculated with only the extractable parent compound, the sum of parent and derivatives, or from extractable (or total) radioactivity following exposure to a radiolabeled parent compound. BCF values calculated from the radiotracer approach have been shown to be greater because ^{14}C tissues measurement includes both the label attributable to parent compound plus the derivatives but also any of the labelled C that may have been metabolized and retained (Belden et al. 2005; Lotufo 2011; Ownby et al. 2005). The fraction metabolized and retained in tissues, however, no longer represents the potential for bioconcentration and/or extant toxicity. Our results provide evidence of compound breakdown within the organisms, and our BCF values are indeed lower than those reported based on a radiotracer. The approach of directly measuring parent compound along with derivatives would give a better, or at least a more conservative, measure of true BCF value.

4.4 Kow

BCF values derived experimentally, including those reported in this study, are normally lower than those predicted from log K_{ow} values (Fig. 2.4; Ownby et al. 2005). Variations in estimated BCF values using log K_{ow} values may result from differences in life stages, metabolism, and lipid content (Jones and Harwood 1992; Smaal and Vonck 1997; Thompson and Bayne 1974; Yates and Peckol 1993). However, these variations in predicted BCF value for TNT and RDX do not seem significant because all estimates, including their variances, are several orders of magnitude lower than BCF values that would indicate bioaccumulation. The dashed-dotted lines on figure 2.4 represents a ± factor of 10 uncertainty about the linear best fit line of the log K_{ow} equation. The majority of BCF values previously reported and added from this study fall within those boundaries with the only outlier being the eggs measured in this study. When values from this study are added to those from previous studies that studied mainly freshwater species, the

linear fit relating BCF value to log K_{ow} value does not substantially change (Lotufo et al. 2009). Therefore, it remains that the log K_{ow} value is a reasonable predictor of the BCF value for these munitions compounds in marine organisms.

5. Conclusion

Results from the time series and concentration gradient experiments support four major findings: (1) the rapid initial uptake of RDX into tissues is consistent with rates reported for marine and freshwater species; (2) TNT and RDX are transformed into multiple derivatives within biota; (3) BCF values are low and do not indicate a high potential for bioconcentration; (4) the use of existing log K_{ow} formulas as predictor of munitions BCF value is reasonable for coastal marine organisms.

BCF values found in this study were low for both TNT and RDX in marine coastal biota. These low BCF values suggest that for TNT, RDX, and their derivatives have a similarly low bioaccumulation potential. Initial uptake and elimination rates calculated in this study also fall within previously published values of both marine and non-marine biota. The use of log K_{ow} value as a predictor of BCF values works well as well for marine biota as it does for fresh and terrestrial biota. The ultimate fate of munitions is still not well known in marine systems, and further experiments particularly using ^{15}N- or ^{13}C-labeled munitions, might shed some light on the metabolic pathways and the fate of the munitions that do make it into the biota. Further research in the fate of munitions within more realistic systems must be performed to fully evaluate and understand the fate and process involved with TNT and RDX in coastal marine environments.

Acknowledgments

This work was supported with funds from the Strategic Environmental Research and Development Program # ER-2122. We would also like to thank Charlie Woods, Dave Cady, and Veronica Rollinson for their lab support.

References

ASTM E1022-94, 2013. Standard Guide for Conducting Bioconcentration Tests with Fishes and Saltwater Bivalve Mollusks, ASTM International, West Conshohocken, PA

Belden JB, Ownby DR, Lotufo GR, Lydy MJ. 2005. Accumulation of trinitrotoluene (TNT) in aquatic organisms: Part 2—Bioconcentration in aquatic invertebrates and potential for trophic transfer to channel catfish (*Ictalurus punctatus*). Chemosphere 58(9):1161-8.

Best EP, Sprecher SL, Larson SL, Fredrickson HL, Darlene BF. 1999. Environmental behavior of explosives in groundwater in groundwater from the Milan Army ammunition plant in aquatic and wetland plant treatments. removal, mass balances and fate in groundwater of TNT and RDX. Chemosphere 38(14):3383-96.

Cho Y, Lee B, Oh K. 2008. Simultaneous degradation of nitroaromatic compounds TNT, RDX, atrazine, and simazine by *Pseudomonas putida* HK-6 in bench-scale bioreactors. Journal of Chemical Technology and Biotechnology 83(9):1211-7.

Clausen J, Robb J, Curry D, Korte N. 2004. A case study of contaminants on military ranges: Camp edwards, massachusetts, USA. Environmental Pollution 129(1):13-21.

Conder JM, Point TWL, Bowen AT. 2004. Preliminary kinetics and metabolism of 2, 4, 6-trinitrotoluene and its reduced metabolites in an aquatic oligochaete. Aquatic Toxicology 69(3):199-213.

Cruz-Uribe O, Cheney DP, Rorrer GL. 2007. Comparison of TNT removal from seawater by three marine macroalgae. Chemosphere 67(8):1469-76.

Darrach M, Chutjian A, Plett G. 1998. Trace explosives signatures from World War II unexploded undersea ordnance. Environ Sci Technol 32(9):1354-8.

Ek H, Dave G, Nilsson E, Sturve J, Birgersson G. 2006. Fate and effects of 2, 4, 6-trinitrotoluene (TNT) from dumped ammunition in a field study with fish and invertebrates. Arch Environ Contam Toxicol 51(2):244-52.

Harrison I and Vane C. 2010. Attenuation of TNT in seawater microcosms. Water Science & Technology 61(10).

Hovatter PS, Talmage SS, Opresko DM, Ross RH. 1997. Ecotoxicity of nitroaromatics to aquatic and terrestrial species at Army superfund sites. ASTM Spec Tech Publ (1317):117-29.

Jones AL and Harwood JL. 1992. Lipid composition of the brown algae *Fucus vesiculosus* and *Ascophyllum nodosum*. Phytochemistry 31(10):3397-403.

Kitts CL, Green CE, Otley RA, Alvarez MA, Unkefer PJ. 2000. Type I nitroreductases in soil enterobacteria reduce TNT (2, 4, 6-trinitrotoluene) and RDX (hexahydro-1, 3, 5-trinitro-1, 3, 5-triazine). Can J Microbiol 46(3):278-82.

Levine B, Furedi E, Gordon D, Barkley J, Lish P. 1990. Toxic interactions of the munitions compounds TNT and RDX in F344 rats. Fundamental and Applied Toxicology 15(2):373-80.

Lotufo G and Lydy M. 2005. Comparative toxicokinetics of explosive compounds in sheepshead minnows. Arch Environ Contam Toxicol 49(2):206-14.

Lotufo GR. 2011. Whole-body and body-part-specific bioconcentration of explosive compounds in sheepshead minnows. Ecotoxicol Environ Saf 74(3):301-6.

Lotufo GR, Gibson AB, Leslie Yoo J. 2010. Toxicity and bioconcentration evaluation of RDX and HMX using sheepshead minnows in water exposures. Ecotoxicol Environ Saf 73(7):1653-7.

Lotufo GR, Farrar JD, Inouye LS, Bridges TS, Ringelberg DB. 2001. Toxicity of sediment-associated nitroaromatic and cyclonitramine compounds to benthic invertebrates. Environmental Toxicology and Chemistry 20(8):1762-71.

Lotufo GR, Lydy MJ, Rorrer GL, Cruz-Uribe O, Cheney DP 2009 Bioconcentration, bioaccumulation, and biotransformation of explosives and related compounds in aquatic organisms. In: Sunahara GI, Lotufo G, Kuperman RG, Hawari J (eds) Ecotoxicology of explosives. CRC Press, Boca Raton, pp 123-155

Macek T, Mackova M, Káš J. 2000. Exploitation of plants for the removal of organics in environmental remediation. Biotechnol Adv 18(1):23-34.

Makris KC, Shakya KM, Datta R, Sarkar D, Pachanoor D. 2007. Chemically catalyzed uptake of 2, 4, 6-trinitrotoluene by *Vetiveria zizanioides*. Environmental Pollution 148(1):101-6.

Meylan WM, Howard PH, Boethling RS, Aronson D, Printup H, Gouchie S. 1999. Improved method for estimating bioconcentration/bioaccumulation factor from octanol/water partition coefficient. Environmental Toxicology and Chemistry 18(4):664-72.

Miyares P and Jenkins T. 1990. Salting-out solvent extraction for determining low levels of nitroaromatics and nitramines in water. USA Cold Regions Research and Engineering Laboratory, Special Report :90-30.

Monteil-Rivera F, Halasz A, Groom C, Zhao J, Thiboutot S, Ampleman G, Hawari J 2009. Fate and transport of explosives in the environment; a chemist's view. In: Sunahara GI, Lotufo G, Kuperman RG, Hawari J (eds) Ecotoxicology of explosives. CRC Press, Boca Raton, pp 5-33

Nipper M, Carr RS, Lotufo GR. 2009. Aquatic toxicology of explosives. Ecotoxicology of Explosives 1:77-115.

Ownby DR, Belden JB, Lotufo GR, Lydy MJ. 2005. Accumulation of trinitrotoluene (TNT) in aquatic organisms: Part 1—Bioconcentration and distribution in channel catfish (*Ictalurus punctatus*). Chemosphere 58(9):1153-9.

Pan X, Zhang B, Cobb GP. 2005. Extraction and analysis of trace amounts of cyclonite (RDX) and its nitroso-metabolites in animal liver tissue using gas chromatography with electron capture detection (GC–ECD). Talanta 67(4):816-23.

Pennington JC and Brannon JM. 2002. Environmental fate of explosives. Thermochimica Acta 384(1):163-72.

Rosen G and Lotufo GR. 2007. Bioaccumulation of explosive compounds in the marine mussel, *Mytilus galloprovincialis*. Ecotoxicol Environ Saf 68(2):237-45.

Singh SN. 2013. Biological remediation of explosive residues. Springer, New York

Smaal A and Vonck A. 1997. Seasonal variation in C, N and P budgets and tissue composition of the mussel *Mytilus edulis*. Mar Ecol Prog Ser 153(7):167-79.

Smith RW, Vlahos P, Tobias C, Ballentine M, Ariyarathna T, Cooper C. 2013. Removal rates of dissolved munitions compounds in seawater. Chemosphere 92(8):898-904.

Sunahara GI, Lotufo G, Kuperman RG, Hawari J. 2009. Introduction, *In Ecotoxicology of explosives* In: Sunahara GI, Lotufo G, Kuperman RG, Hawari J (eds) Ecotoxicology of explosives. CRC Press, Boca Raton, pp 1-3

Talmage SS, Opresko DM, Maxwell CJ, Welsh CJ, Cretella FM, Reno PH, Daniel FB. 1999. Nitroaromatic munition compounds: Environmental effects and screening values. In: Reviews of environmental contamination and toxicology. Springer. 1 p.

Thompson R and Bayne B. 1974. Some relationships between growth, metabolism and food in the mussel *Mytilus edulis*. Mar Biol 27(4):317-26.

Vila M, Lorber-Pascal S, Laurent F. 2007. Fate of RDX and TNT in agronomic plants. Environmental Pollution 148(1):148-54.

Yates J and Peckol P. 1993. Effects of nutrient availability and herbivory on polyphenolics in the seaweed *Fucus versiculosus*. Ecology :1757-66.

Yoo LJ, Lotufo GR, Gibson AB, Steevens JA, Sims JG. 2006. Toxicity and bioaccumulation of 2, 4, 6-trinitrotoluene in fathead minnow (*Pimephales promelas*). Environmental Toxicology and Chemistry 25(12):3253-60.

Figure and Table Captions:

Table 2.1: Concentration gradient experiment aqueous spike concentrations. *A selection of water samples was lost due to error. Precision experiments were run and completed in replicate to test the amount of munitions after 24 hours. The combinations of precision experimental and actual measured values are reported with standard deviations between precision and BCF water values.

Table 2.2: Time series experiment calculated rates. Initial uptake, elimination, and appearance rates were calculated using a plot of Log concentration vs. time. Appearance rate for this experiment is defined as the rate at which 4-ADNT and 2-ADNT increased over the time series. Not determined values (ND) were due to the lack of data points within the first hour. Values in parentheses are coefficients of determination.

Table 2.3: Ratios of TNT and derivatives. Concentration gradient ratio values are calculated by taking the average of the species in all of the separate aquaria (n=12).

Table 2.4: TNT and RDX Bioconcentration factors (BCF). BCF values are given the units mL g^{-1}. ∑TNT = (TNT + 4-ADNT + 2-ADNT). ∑RDX = (RDX + MNX + TNX + DNX) when detected. BCF values indicated by an (*) were not calculated with a best fit line but as an average of single point values. Values in parentheses are coefficients of determination.

Figure 2.1: Aqueous munition concentrations for single dose time series treatment. Panels a and b represent separate aquaria that were dosed with a mixture of TNT and RDX.

Figure 2.2: Tissue concentrations for single dose time series treatment. Solid line shows extractable parent explosive for both parent explosive and ∑ of the parent explosive as detailed in Table 4. Values with error bars consist of the average of 3 separate individual samples (n=3) while points without are single samples (n=1). The bar graph shows the breakdown percent of parent compound and derivatives measured for *Fucus vesiculosus* and *Mytilus edulis*.

Figure 2.3: Example derivation of BCF from the concentration gradient experiments: *Crassostrea virginica*. Each value consists of the average of 3 separate individual specimens (n=3). The solid lines are best fit regressions. ∑TNT and ∑RDX values consist of sum of parent compound and the respective derivatives. BCFs derived from these plots for all organisms are summarized in Table 4.

Figure 2.4: Log BCF vs. Log K_{ow} regression. The solid filled markers and all macroalgae values are from this study. Empty markers are from previously published values. The solid line is a best fit regression line with previous and this study's values (log BCF = 0.66 log K_{ow} – 0.49, r^2 = 0.19). The 2 dotted-dashed lines are lines that have the same slope as the solid line and represent one order of magnitude difference from the best fit linear regression. The dotted best fit

regression is from previously summary of data by Sunahara et. al (2009; log BCF = 0.53 log K_{ow} – 0.23, r^2 = 0.37).

Table 2.1: Concentration gradient experiment aqueous spike concentrations

Tank #	TNT (mg/L)	Measured (mg/L)*	RDX (mg/L)	Measured (mg/L)*
1	3	2.82 ± 0.17	1	1.01 ± 0.09
2	2	1.92 ± 0.21	0.75	0.71 ± 0.09
3	1	1.14 ± 0.04	0.5	0.52 ± 0.06
4	0.5	0.54 ± 0.07	0.25	0.24 ± 0.02
5	0	0	0	0

Table 2.2: Time series experiment calculated rates

Initial uptake rate (hours^{-1})	***Fucus vesiculosus***	***Mytilus edulis***
TNT	1.79 (0.67)	ND
RDX	0.50 (0.99)	ND
Elimination rate (hours^{-1})		
RDX	0.0035 (0.45)	0.013 (0.73)
Half-life (hours)		
RDX	198.6	53.3
Appearance rate (hours^{-1})		
4-ADNT	0.75 (0.93)	ND
2-ADNT	0.58 (0.98)	ND

Table 2.3: Ratio of TNT and derivatives

Species	Ratio of TNT to derivatives	Ratio of 4-ADNT to 2-ADNT	Ratio of ∑TNT to 4-ADNT	Ratio of ∑TNT to 2-ADNT
Tetraselmis impellucida	0.17 ± 0.11	1.1 ± 0.40	0.81 ± 0.16	0.79 ± 0.40
Fucus vesiculosus	0.03 ± 0.02	2.1 ± 0.15	1.51 ± 0.04	3.22 ± 0.17
Ulva lactuca	0.12 ± 0.08	2.1 ± 0.41	1.69 ± 0.23	3.44 ± 0.25
Hemigrapsus sanguineus	4.1 ± 0.59	1.7 ± 0.50	8.35 ± 1.76	13.58 ± 1.73
Hemigrapsus sanguineus eggs	15.5 ± 8.24	9.4 ± 4.29	18.7 ± 9.03	164 ± 91.8
Crassostrea virginica	0.29 ± 0.23	1.5 ± 0.10	3.25 ± 0.46	2.14 ± 0.45
Littorina littorea	0.07 ± 0.05	1.1 ± 0.09	2.15 ± 0.34	2.17 ± 0.11

Table 2.4: TNT and RDX Bioconcentration factors (BCFs)

Species	**Common Name**	**TNT**	**∑TNT**	**RDX**	**∑RDX**
Tetraselmis impellucida	PLY 429	0.25 (0.02)	1.53 (0.66)	8.15 (0.42)	54.83 ± 26.85*
Fucus vesiculosus	Bladder wrack	0.0031 (0.60)	1.85 (0.99)	0.73 (0.65)	0.68 (0.84)
Ulva lactuca	Sea lettuce	0.0056 (0.071)	0.40 (0.70)	0.023 (0.32)	0.21 ± 0.12*
Hemigrapsus sanguineus	Asian shore crab	23.51 (0.61)	28.1 (0.61)	1.97 (0.64)	2.29 (0.56)
Hemigrapsus sanguineus	Asian shore crab external eggs	466.4 (0.92)	484.5 (0.93)	5.55 (0.91)	5.29 (0.67)
Crassostrea virginica	Eastern oyster	0.59 (0.31)	8.61 (0.97)	0.21 (0.44)	2.42 ± 1.76*
Mytilus edulis	Blue mussel	1.0 (0.80)	14.2 (0.98)	0.43 (0.59)	0.33 (0.28)
Littorina littorea	Common periwinkle	0.20 (0.89)	12.30 (0.99)	0.45 (0.82)	4.03 ± 2.01*

Figure 2.1: Aqueous munition concentrations

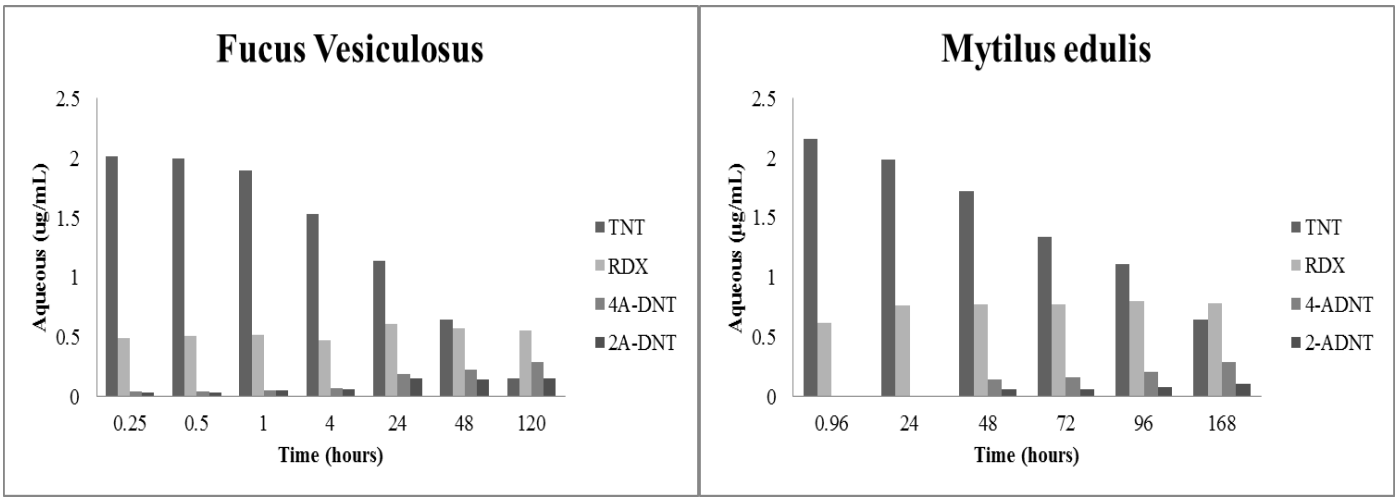

Figure 2.2: Tissue concentration

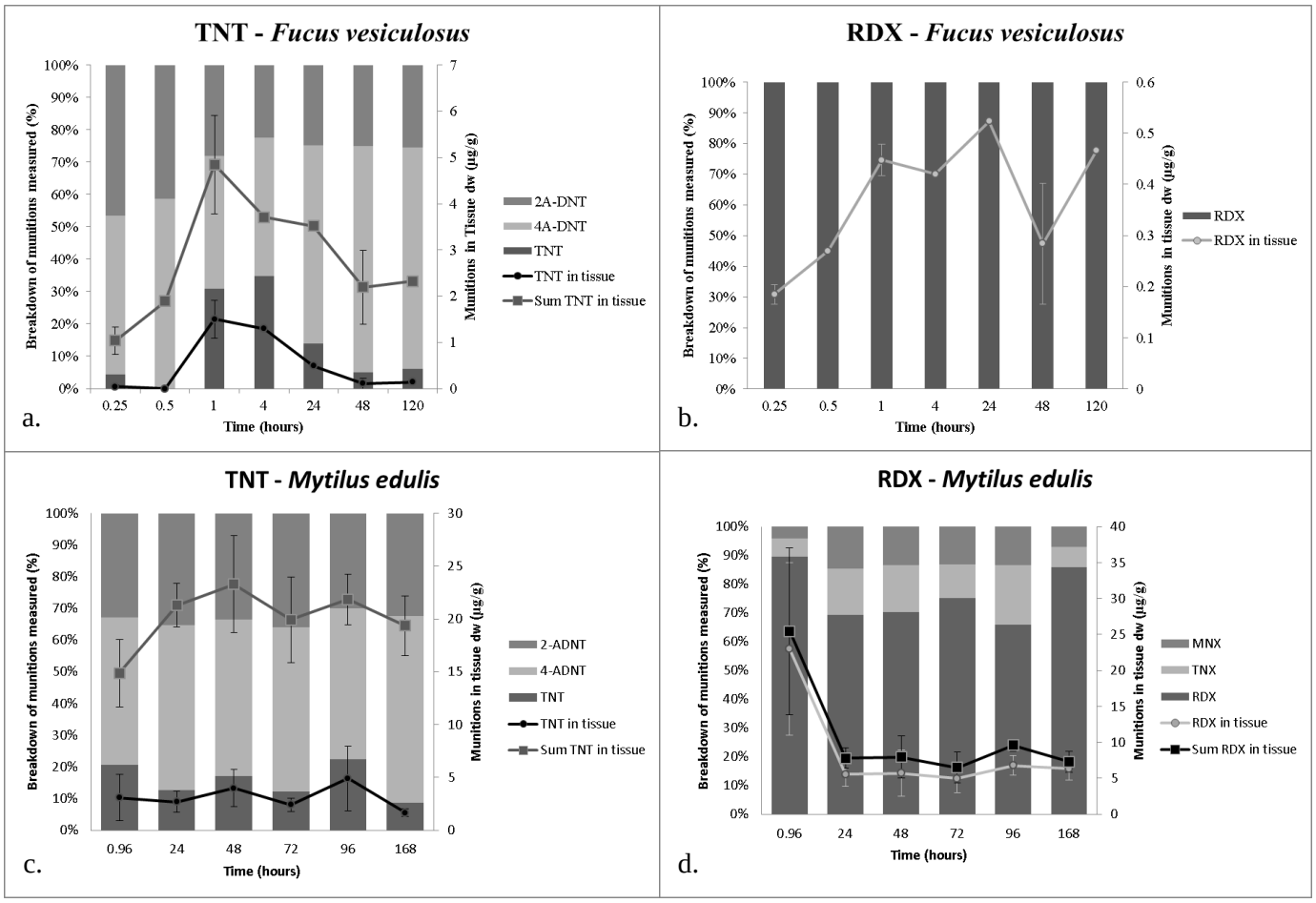

Figure 2.3: Example derivation of BCF

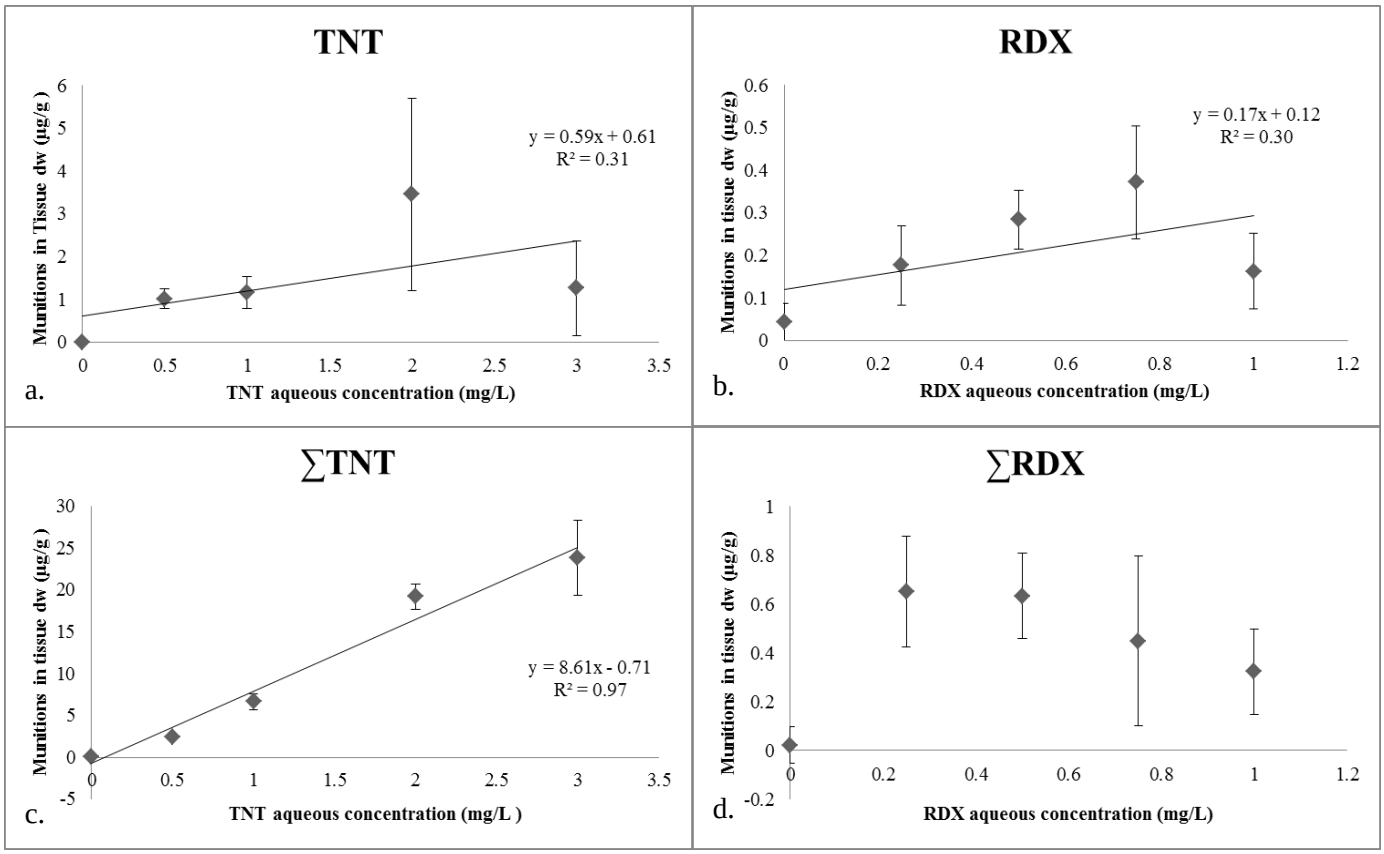

Figure 2.4: Log BCF vs. Log K_{ow} regression

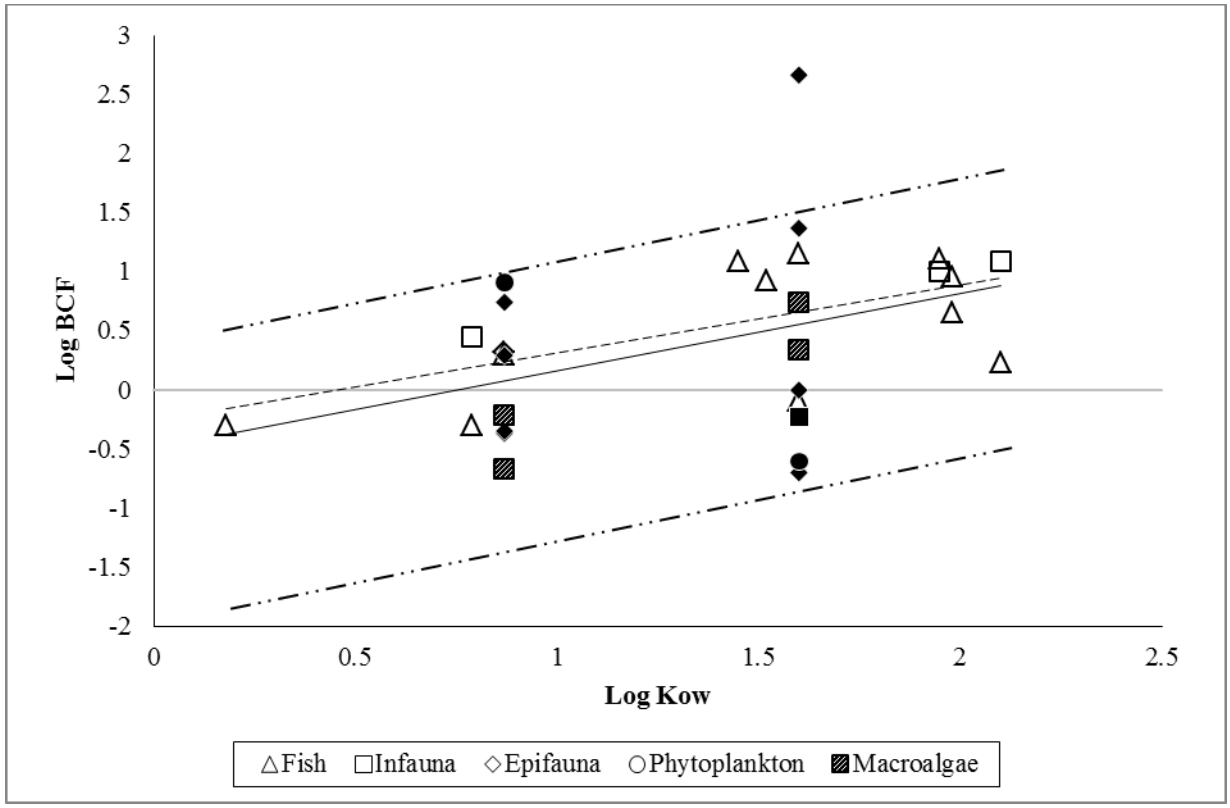

Chapter 3: Uptake and fate of hexahydro-1,3,5-trinitro-1,3,5-triazine (RDX) in coastal marine biota determined using a stable isotopic tracer, ^{15}N-[RDX][3]

[3] Ballentine, M., Ariyarathna, T., Smith, R. W., Cooper, C., Vlahos, P., Fallis, S., Groshens, T., Tobias, C. (2016). Uptake and fate of hexahydro-1, 3, 5-trinitro-1, 3, 5-triazine (RDX) in coastal marine biota determined using a stable isotopic tracer, 15 N–[RDX]. *Chemosphere*, *153*, 28-38.

Abstract

Hexahydro-1,3,5-trinitro-1,3,5-triazine (RDX) is globally one of the most commonly used military explosives and an environmental contaminant. ^{15}N labelled RDX was added into a mesocosm containing 9 different coastal marine species in a time series experiment to quantify the uptake of RDX and assess the RDX derived ^{15}N retention into biota tissue. The ^{15}N attributed to munitions compounds reached steady state concentrations ranging from 0.04 to 0.67 μg ^{15}N g dw^{-1}, the bulk ^{15}N tissue concentration for all species was 1-2 orders of magnitude higher suggesting a common mechanism or pathway of RDX biotransformation and retention of ^{15}N. A toxicokinetic model was created that described the ^{15}N uptake, elimination, and transformation rates. While modeled uptake rates were within previous published values, elimination rates were several orders of magnitude smaller than previous studies ranging from 0.05 to 0.7 $days^{-1}$. These small elimination rates were offset by high rates of retention of ^{15}N previously not measured. Bioconcentration factors and related aqueous:organism ratios and tracer calculated using different tracer and non-tracer methods and yielded a broad range of values (0.35-101.6 mL g^{-1}) that were largely method dependent. Despite the method-derived variability, all values were general low and consistent with little bioaccumulation potential. The use of ^{15}N labelled RDX in this study indicates four possible explanations for the observed distribution of compounds and tracer; each with unique potential implications for possible toxicological impacts in the coastal marine environment.

1. Introduction

Hexahydro-1,3,5-trinitro-1,3,5-triazine (RDX) is a cyclic nitramine military explosive that has been extensively used since World War II (Darrach et al. 1998; Roh et al. 2009). The global use of RDX has resulted in its introduction into the environment through detonation, production, storage, disposal, and leakage of underwater military munitions (Harrison and Vane 2010; Hovatter et al. 1997; Jenkins et al. 2006; Talmage et al. 1999). RDX is a contaminant in terrestrial (Pennington and Brannon 2002) and marine (Darrach et al. 1998) ecosystems and has been shown to be persistent (Smith et al. 2013). Toxicological studies have been reported for terrestrial (Simini et al. 2003), freshwater (Bentley et al. 1977; Mukhi et al. 2005; Mukhi and Patiño 2008; Steevens et al. 2002), and marine systems (Lotufo et al. 2001, 2010; Nipper et al. 2001; Rosen and Lotufo 2007a). The presence of RDX is likely to be of concern in marine environments due to RDX being a possible human carcinogen and a convulsant (Sweeney et al. 2012). Yet, marine systems have not been fully characterized for contamination levels and biological accumulation, nor is the ecological fate of RDX fully understood (Rosen and Lotufo 2007b; Lotufo et al. 2009).

Direct uptake and bioconcentration for several species of marine coastal biota have been measured directly and show that RDX has a very small bioconcentration potential (Ballentine et al. 2015; Lotufo et al. 2010; Rosen and Lotufo 2007b). Similarly low bioconcentration potential can also be predicted for coastal marine systems using octanol/water-partitioning coefficient of RDX (log K_{ow} = 0.87; Burken and Schnoor 1998). The use of carbon isotopes incorporated into RDX as tracers (Lotufo et al. 2009) has shown that a greater amount of RDX is taken up into tissues relative to measures based on direct uptake or predicted from log K_{ow} values. This larger amount of RDX uptake observed in carbon isotope tracer studies is often attributed to munitions

transformations to non-extractable compounds (Lotufo et al. 2009). The non-extractable compounds formed are assumed to be solvent-resistant or possibly tissue bound but surmised to be RDX, RDX derivatives, and/or adducts. The use of the stable nitrogen isotope as a tracer has been used in a variety of marine systems for examining uptake/cycling of dissolved inorganic nitrogen (DIN; Tobias et al. 2001, Holmes et al. 2000), and has potential utility for study of RDX uptake. The RDX ring is broken in several possible biotic pathways (Crocker et al. 2006; Pennington and Brannon 2002) allowing for the possibility of more nitrogen containing products being bound as non-extractable derivatives, adducts, or incorporated into tissue. The use of ^{15}N labeled RDX may show greater sensitivity compared with uptake studies that only use non-labeled RDX or carbon labelled RDX since there is twice the amount of nitrogen in a RDX molecule relative to carbon.

Past studies using bacteria (Annamaria et al. 2010; Bhatt et al. 2006; Van Aken et al. 2004), fungi (Bhatt et al. 2006), terrestrial (Just and Schnoor 2004; Thompson et al. 2005), and freshwater biota (Houston and Lotufo 2005) have used ^{18}O and ^{14}C labeled RDX to primarily show biodegradation or mineralization of RDX. Our study builds upon a few select studies that track the fate of munitions compounds in complex multi-compartmental experiments (Rosen and Lotufo 2010; Lotufo et al. 2001) by the addition of ^{15}N as a tracer. By comparing total amounts of RDX plus the metabolites to total amounts RDX-derived ^{15}N tracer in organisms we can assess gross uptake and retention of compound. The use of ^{15}N allows for the tracking of breakdown of the RDX and its main derivatives and identify amounts of these compounds transformed and retained in tissues in forms other than RDX and its primary nitroso metabolites (MNX, DNX, and TNX). The objective of this study was to quantify RDX uptake in 9 different coastal marine species, and assess RDX-derived nitrogen retention in the organism using ^{15}N

nitro-labeled RDX in an aquaria scale simulation of a coastal marine ecosystem where other competing RDX degradation pathways are operating (mineralization). ^{15}N mass balance modeling was used to evaluate the uptake, transformation, retention, and elimination of biota.

2. Methods

2.1 Experimental Design

Two 70 L glass aquaria containing seawater and sandy sediments from Long Island Sound, Connecticut, USA were connected to a common recirculating glass aquarium reservoir. The sandy sediments were collected from a single site and were primarily consisted of medium sand (50%) and coarse sand (33%) with the remaining percentage consisting of smaller particles. The sediments used had a density of 2.02 g mL^{-1}, porosity of 40%, total organic carbon and total nitrogen of 1.233 mg g sed^{-1} and 0.176 mg g sed^{-1} respectively. The experimental aquaria design was similar to aquaria setup from Smith et al. (2013). Sediments were collected from a nearby subtidal habitat in Long Island Sound (LIS) and added to the aquaria to an average depth of 10 cm. Seawater was then added from LIS. The system was allowed to stabilize over a period of two weeks with flow through water from the LIS. 24 h before the start of the experiment the system was switched to recirculation mode and biota was added. In total, two macroalgae species (*Fucus vesiculosus* and *Ulva lactuca*), two epifaunal species (*Littorina littorea* and *Carcinus maenas*), three bivalve species (*Crassostrea virginica*, *Mytilus edulis*, and *Mercenaria mercenaria*), and two fish species (*Pseudopleuronectes americanus* and *Fundulus heteroclitus*) were used. ^{15}N nitro labelled-RDX (^{15}N-RDX) was synthesized by S. Fallis and T. Groshens at the Naval Air Warfare Center Weapons Division, Chemistry Division, China Lake, CA and was added to the reservoir in single 1 mL addition of methanol for an initial target tank RDX concentration of 0.4 mg L^{-1}, and then added throughout the time series experiment with the use

of a peristaltic pump to target steady state at a rate of 0.037 mL min^{-1}. The pump rate was designed to maintain a steady state RDX at the same initial concentration of 0.4 mg L^{-1} based on measured rates of RDX removed measured in preliminary experiments. Water and biota collected from the experimental aquaria were analyzed for RDX, hexahydro-1,3,5-trinitroso-1,3,5-triazine (TNX), hexahydro-5-nitro-1,3-dinitroso-1,3,5-triazine (DNX), and hexahydro-3,5-dinitro-1-nitroso-1,3,5-triazine (MNX).

2.2 Aqueous sampling

Time series (21 days) water column aqueous munition samples (2 mL) were taken from the experimental tank and placed in 15 mL centrifuge tubes at each time point (days 7, 14, and 21 n=3). Water samples measured for munitions used a modified "salting out" technique adapted from Miyares and Jenkins (1990) and used by Ballentine et al. (2015). Briefly, the 2 mL of sample were added to 1.3 g of NaCl and shaken. American Chemical Society (ACS) – grade acetonitrile, 1.5 mL, was then added and shaken for 5 min. The separated acetonitrile was removed and the process was repeated two more times using 1 mL of ACS-grade acetonitrile. The final extract was then placed into a gas chromatography vial and run using a gas chromatograph (GC) equipped with an electron-capture detector (ECD) as detailed in Ballentine et al. (2015).

2.3 Biota sampling

Biota samples were removed from the experimental aquaria then immediately rinsed for 5 min with clean filtered seawater to remove dissolved and weakly sorbed munitions compounds from the tissue surfaces. The shells of *L. littorea, C. virginica*, *M. edulis*, and *M. mercenaria* were opened before being rinsed. *C. maenas* eggs were removed prior to freeze drying and separated into their own sample vials then freeze-dried. Once rinsed, tissues were removed, freeze-dried,

and weighed. Freeze-dried samples were homogenized using a mortar and pestle and then separated into a fraction for measuring munitions compounds concentrations in the tissue and a fraction for bulk ^{15}N isotope. Samples analyzed for munitions compounds concentrations were extracted using methods modified from Conder et al. (2004). ACS-grade acetonitrile, 10 mL, was added to the samples and then sonicated for 1 h. The homogenate was then centrifuged for 10 min at 10,000 rpm. The supernatant was removed, filtered through 0.22-µm PTFE syringe-tip filter, and 0.01 mg L^{-1} of 3,4-dinitrobenzene (3,4-DNB) as an recovery standard. GC/ECD analysis was conducted with the same method as the water samples (Ballentine et al. 2015). Quantification was based on an external calibration curve of standard munitions RDX, MNX, DNX, and TNX (AccuStandard, New Haven, Connecticut, USA). The recoveries of munitions from tissue samples (n=3) ranged between 42 and 138% with a mean of 97% and standard deviation of 21% with a reporting limit for all compounds of 0.7 ng mL^{-1}. To account for various sizes of organisms extractable munitions concentrations were normalized to organism dry weight (g dw). In addition to munitions concentrations, biota were analyzed for total ^{15}N tracer.

2.4 ^{15}N analysis

Total ^{15}N in all solid samples (sediments, biota tissues, and suspended particulate matter) were analyzed by elemental analyzer – isotope ratio mass spectrometry (EA/IRMS: Delta V, Thermofisher). Samples were freeze-dried and weighed into tin capsules. Sufficient sample mass was used to achieve 40-80 µg N for isotope analyses. Isotope values were normalized with a 2-endpoint correction using United States Geological Survey reference materials L-glutamic acid (USGS40 and USGS41) accompanying each analytical batch and also served as check standards for drift correction. Analytical precision on ^{15}N measurements was 0.3 per mil which is

equivalent to approximately 1/5000th of one percent excess ^{15}N. ^{15}N enrichments were reported in $\delta^{15}N$ using equation 3.1:

$$\delta^{15}N = (R_{sample} / R_{standard} - 1) \cdot 1000 \quad [3.1]$$

where R_{sample} is the $^{15}N/^{14}N$ ratio of the sample and $R_{standard}$ is the $^{15}N/^{14}N$ ratio of atmospheric nitrogen. All $\delta^{15}N$ values are reported as per mil (‰) with an EA/IRMS sensitivity of 0.3‰.

2.5 Nitrogen isotope modeling

The model mass balanced ^{15}N tracer. For the model, the munitions compounds concentrations measured in the biota and aqueous samples were converted to units of μg ^{15}N g dw^{-1}. The units were derived from the molar munitions compounds concentrations (both biota and aqueous samples) times the molar stoichiometry between munitions and ^{15}N tracer (1:3). This conversion was done to enable direct comparison (and unit compatibility) with bulk measurements of ^{15}N in tissue provided by the corrected EA-IRMS values.

Uptake and elimination rates of labeled nitrogen (^{15}N) derived from RDX were determined from a three compartment box model (Fig. 3.1) consisting of the ^{15}N attributable to tissue parent compound (C_p), the ^{15}N attributable tissue metabolites (C_m), and the ^{15}N in tissue, not accounted for either the parent nor metabolite (C_m). MATLAB R2013b by Mathworks was the software used to construct the three box model used. This model was modified from a simpler two box model (Lydy et al. 2000) that directly modeled concentrations of only the parent and metabolite. The root mean square error (RMSE) is a common and well used statistical method to calculate how well the model fits experimental data and was calculated for the 15N three box model (Chai and Draxler, 2014; Table 3.1) Box 1 (Fig. 3.1; C_p) of the model was fit to the experimental data with equation 3.2:

$$\frac{dC_p}{dt} = (k_u \cdot C_w) - \left(k_{ep} \cdot C_p\right) - \left(k_m \cdot C_p\right) - (k_{pN} \cdot C_p) \quad [3.2]$$

where C_w = concentration of ^{15}N in water (µg N mL^{-1}) derived from aqueous RDX concentration, C_p = concentration of labeled nitrogen isotope attributed to the parent compound in the biota (µg N g dw^{-1}), k_u = uptake clearance coefficient (mL g^{-1} d^{-1}), k_{ep} = elimination rate constant (d^{-1}), k_m = uptake rate constant nitrogen derived from RDX (d^{-1}), k_{pN} = nitrogen incorporation rate constant from parent compound (d^{-1}), and t = time (d). Box 2 (Fig. 3.1; C_m) of the model is the ^{15}N derived from RDX metabolites fit to experimental data with equation 3.3:

$$\frac{dC_m}{dt} = \left(k_m \cdot C_p\right) - (k_{em} \cdot C_m) - (k_{mN} \cdot C_m) \quad [3.3]$$

where C_m = concentration of labeled nitrogen attributed to metabolized derivatives in the biota (µg N g dw^{-1}), k_{em} = metabolite derived nitrogen elimination rate constant (d^{-1}), and k_{mN} = nitrogen incorporation rate constant from metabolites (d^{-1}). Box 3 (Fig. 3.1) is the ^{15}N not attributed to RDX or the derivatives MNX, TNX, or DNX. Box 3 (Fig. 3.1; C_N) of the model was fit to experimental data using equation 3.4.

$$\frac{dC_N}{dt} = (k_{mN} \cdot C_m) + \left(k_{pN} \cdot C_p\right) + (k_{DN} \cdot C_{DIN}) - (k_{eN} \cdot C_N) \quad [3.4]$$

C_N = concentration of total labeled nitrogen in the biota (µg N g dw^{-1}), C_{DIN} = concentration of nitrogen from DIN (µg N mL^{-1}), k_{eN} = nitrogen elimination rate constant (d^{-1}), and k_{DN} = uptake of nitrogen from aqueous medium rate constant (d^{-1}). The rate constant k_{DN} is only included for the macroalgae due to the ability to directly uptake DIN from the water column. The model equations (3.2-3.4) were simultaneously fit to experimental data for the concentrations of munitions and ^{15}N-DIN in the system (Fig. 3.1).

In addition to providing the gross rate of exchange between boxes within the organism and with its environment, the model output was also used to calculate bioconcentration factors (BCFs) for comparison to other approaches. BCFs were calculated four ways, three of which were similar to other studies for comparison to other species (Belden et al. 2005; Lotufo et al. 2010; Nuutinen et al. 2003). The first method (BCF_m) used concentrations of munitions in tissue and water (Eqn. 3.5; ASTM E1022-94, 2013). The next three methods represent a deviation from the standard ASTM E1022-94 (2013) definition of a BCF and represent a more specific partitioning ratio. The second method (BCF_T), used concentrations of total ^{15}N in tissue and water (Eqn. 3.6) similar to Belden et al. (2005b) who used ^{14}C. The third method (BCF_{kow}) used the log K_{ow} of RDX in equation 3.7 derived by Meylan et al. (1999). The forth approach was model derived and used the uptake coefficients and elimination rates including k_{eN} (Eqn. 3.8). This approach has previously not been used to calculate BCF and collectively includes the uptake and elimination of RDX and all of its derivatives.

$$BCF_m = \frac{C_p}{C_w} \quad [3.5]$$

$$BCF_T = \frac{C_{15p}}{C_{15w}} \quad [3.6]$$

$$BCF_{kow} = log_{BCF} = 0.86 \cdot log_{K_{ow}} - 0.39 \quad [3.7]$$

$$BCF_R = \frac{k_u}{k_{ep} + k_{em} + k_{eN}} \quad [3.8]$$

3. Results

3.1 Aqueous concentrations

Over the 21 day incubation period RDX decreased by 31% below the target concentration of 0.4 mg L^{-1} (Fig. 3.2) with a new RDX quasi-steady state concentration of 0.25 ± 0.04 mg L^{-1} achieved by day 9. The temporal changes in nitroso derivative concentrations differed from RDX. The derivatives measured reached a steady state 2 days before RDX on day 7. The derivatives declined in concentration late in the experiment when RDX had a slight increase (Fig 3.2). TNX peaked on day 9 at 0.028 ± 0.005 mg L^{-1} until decreasing to an average concentration of 0.013 ± 0.001 mg L^{-1} for days 16 through 21. MNX maintained a concentration of 0.012 ± 0.002 mg L^{-1} for the first 14 days after which MNX could no longer be detected. DNX was not measured in the water column during the 21 day incubation period.

During the 14 days that MNX remained in the water column, TNX and MNX had an average ratio of 2.35 to 1 with respect to each other. The measured derivatives never had a combined concentration greater than RDX. The ratio of RDX to TNX and MNX combined started at 13 to 1 and decreased over the 14 days when MNX was no longer measured to a ratio of 5 to 1. As TNX and MNX degraded and RDX remained steady, the ratio increased to 21 to 1.

3.2 Tissue concentrations – munitions and ^{15}N

$^{15}N_R$ (^{15}N attributed to RDX) and $^{15}N_D$ (^{15}N attributed to MNX + TNX + DNX) were measured in all species. The concentration of $^{15}N_D$ did not exceeded that of $^{15}N_R$ at any time point. Total bulk ^{15}N retained in biota was measured at an average of 1 order of magnitude greater than both $^{15}N_R$ and $^{15}N_D$ in all species (Fig. 3.3). Although certain species retained a greater amount of total ^{15}N than other species, there was no distinguishable pattern between uptake and retention of

total ^{15}N. The $^{15}N_R$ and $^{15}N_D$ reached steady states typically by day 1, which was much faster than the rate at which total ^{15}N in each species attained steady state.

3.2.1 Primary Producers

Both autotrophic species had a rapid initial uptake of munitions and reached a steady state of $^{15}N_R$ on day 1. *F. vesiculosus* obtained a measured steady state of 0.09 ± 0.03 µg $^{15}N_R$ g dw^{-1} while *U. lactuca* reached a steady state of 0.17 ± 0.8 µg $^{15}N_R$ g dw^{-1} (Fig. 3.3). The $^{15}N_D$ ratio to $^{15}N_R$ in *U. lactuca* ranged from 0.6 – 6.5 to 1. No clear pattern of the ratios of $^{15}N_D$ to $^{15}N_R$ was apparent. In both macroalgae species the total µg ^{15}N g dw^{-1} measured was 1-2 orders of magnitude greater than both $^{15}N_D$ and $^{15}N_R$ combined (Fig. 3.3). MNX, DNX, and TNX were not detected in *F. vesiculosus* tissue. TNX was detected throughout the incubation for *U. lactuca* with MNX only detected in the first 2 days. The total ^{15}N in the macroalgae also reach a steady state much later than the $^{15}N_R$ (Fig. 3.3). *U. lactuca* ^{15}N value on day 21 increases beyond the steady state. The total ^{15}N in *U. lactuca* reached a peak value twice as high as *F. vesiculosus.*

3.2.2 Epifauna

L. littorea reached a steady state of 0.12 ± 0.06 µg $^{15}N_R$ g dw^{-1} after day 5 while *C. maenas* steady state value of 0.04 ± 0.01 µg $^{15}N_R$ g dw^{-1} was obtained on day 7 (Fig. 3.3). Derivative to RDX ratios showed no clear pattern for either epifaunal species. The $^{15}N_D$ measured values in *L. littorea* are very similar to the $^{15}N_R$ values for *L. littorea*. *C. maenas* ratio of $^{15}N_D$ to $^{15}N_R$ ranged from 0.2 – 2.4 to 1. There were 2 *C. maenas* egg samples analyzed. $^{15}N_R$ in the *C. maenas* eggs measured 0.14 ± 0.01 µg $^{15}N_R$ g dw^{-1}. The ratio of $^{15}N_D$ to $^{15}N_R$ for *C. maenas* eggs was 0.26 to 1. MNX was found in both epifaunal species while DNX was found only in *L. littorea* and TNX was only found in *C. maenas*. The epifaunal species had an initial uptake of ^{15}N that then increased to a steady state. The total ^{15}N in *L. littorea* reached a steady state value 5 times higher

than the ^{15}N in *C. maenas*. Total ^{15}N for *C. maenas* eggs was 2 orders of magnitudes greater than $^{15}N_D$ and $^{15}N_R$ combined for all other *C. maenas* tissues.

3.2.3 Bivalves

C. virginica tissue concentrations of $^{15}N_R$ were highly variable between time points and within triplicates likely reflecting the variable amount of active pumping observed between individuals. An average concentration of 0.26 ± 0.30 µg $^{15}N_R$ g dw^{-1} was reached after day 2 of the incubation (Fig. 3.3). Both *M. edulis* and *M. mercenaria* reached steady state values of 0.44 ± 0.21 µg $^{15}N_R$ g dw^{-1} and 0.05 ± 0.03 µg $^{15}N_R$ g dw^{-1} respectively. MNX was measured in both *C. virginica* and *M. mercenaria* throughout the incubation. DNX was found only at the day 1 time point in *C. virginica* and *M. edulis*. Measured concentrations of all the derivatives were found only at the day 1 time point in *M. edulis* after which no other derivatives were measured in *M. edulis*. Total ^{15}N was measured 2 orders of magnitude greater than $^{15}N_D$ and $^{15}N_R$ for *M. edulis* and *M. mercenaria* while the total ^{15}N measured in *C. virginica* was measured 1 order of magnitude greater than that of $^{15}N_D$ and $^{15}N_R$ combined. ^{15}N did reach a steady state in *C. virginica* on day 3 of the incubation at a value of 7.6 ± 2.4 µg ^{15}N g dw^{-1} (Fig. 3.3). The total ^{15}N measured in *M. edulis* measured twice the concentration than that measured in *M. mercenaria* and *C. virginica*.

3.2.4 Fish

$^{15}N_D$ for *P. americanus* had an average steady state value reached after 1 day of 0.37 ± 0.15 µg $^{15}N_D$ g dw^{-1}. $^{15}N_R$ reached a steady state for *P. americanus* after day 1 with a value of 0.67 ± 0.29 µg $^{15}N_R$ g dw^{-1}. Due to unidentifiable interference with the GC /ECD analysis tissue concentrations of $^{15}N_D$ and $^{15}N_R$ for *F. heteroclitus* were not able to be determined. MNX, DNX, and TNX were measured in *P. americanus*. DNX and TNX were measured values were

sporadic. On average the total ^{15}N measured in *P. americanus* was 1 order of magnitude greater than that of $^{15}N_D$ and $^{15}N_R$ combined over the time series. *F. heteroclitus* total ^{15}N reached a steady state after 1 day of an average value of 7.6 ± 1.3 μg ^{15}N g dw^{-1}.

3.2.5 Total ^{15}N distribution across biota

The species can be divided into two groups with respect to uptake and retention of total ^{15}N. The first group (*M. edulis, P. americanus, L. littorea, F. vesiculosus, U. lactuca,* and *F. heteroclitus*) had double the average amount of uptake and retention of ^{15}N normalized to mass throughout the experiment than the second group (Fig. 3.4). While the second group (*C. virginica, C. maenas,* and *M. mercenaria*) only retained half the amount of ^{15}N normalized to mass (Fig. 3.4). *U. lactuca* and *L. littorea* contributed the largest percent of ^{15}N attributed to the biota with 17 ± 9 % and 16 ± 4% respectively (Fig. 3.4). *C. maenas* contributed the lowest amount of ^{15}N retained with 6 ± 1% of the total ^{15}N retained by all species. The contribution to the total ^{15}N in each species remained at a steady state starting at day 1 with the exception of a transient spike of ^{15}N measured in *P. americanus* at day 14 (Fig. 3.4).

After the initial incorporation of ^{15}N tracer into biota between day 0 and 1, the ^{15}N found in the biota decreased over time. On day 1 the ^{15}N in the biota only accounted for 8% of the total ^{15}N added to the system initially in the form of ^{15}N-RDX (Fig. 3.5). At the end of the experiment on day 21 the biota accounted for only 4% of the total ^{15}N added to the system. Of the small 8% of the ^{15}N accounted for by the biota, the combined $^{15}N_D$ and $^{15}N_R$ percent found in all species tissues was 11% at day 1. The contribution of $^{15}N_D$ and $^{15}N_R$ to the total ^{15}N in the biota steadily decreases over the time series to a final value of 1% (Fig. 3.5). Majority of the ^{15}N measured in the biota were unknown retained pools of ^{15}N and is much larger than the $^{15}N_R$ and $^{15}N_D$.

3.3 Modeling

The RDX uptake (k_u) varied up to 10 fold among the different species. *M. edulis* had the largest k_u at 38.2 mL g^{-1} day^{-1} while *F. Vesiculosus* had the slowest at 2.3 mL g^{-1} day^{-1} (Table 3.1). There was no pattern to the modeled k_u for the various species with respect to organism group, trophic position, or niche. The two macroalgae species showed markedly different k_u from each other, spanning the whole range of k_u seen across species. The bivalves showed similar k_u rates, ranging from 6 to 36; about the same amount as the periphyton supported *L. littorea* and higher than the infaunal filter feeding *M. mercenaria*. *C. maenas* had among the lowest k_u values and there were similar values between *P. americanus* and *F. heteroclitus* despite their benthic vs pelagic positions. The rate constants for elimination of RDX (k_{ep}) for each species were similar with values ranging from 0.2 to 0.7 $days^{-1}$. The modeled values for k_m varied greatly between some species, ranging from 0 to 5 $days^{-1}$ and mainly reflecting large differences in metabolite concentrations among biota. In comparison to the other parameters, k_{pN} and k_{mN} were much larger. Modeled values for k_{pN} ranged from 1.6 to 7 $days^{-1}$ while k_{mN} ranged from 0 to 3 $days^{-1}$ (Table 3.1). Uptake of RDX derived N mineralized through the DIN pool (k_{DN}) values were small and only existed for three of the species: *F. Vesiculosus*, *U. lactuca*, and *L. littorea*.

BCFs were calculated with 4 different methods. Variation in BCF values were more dependent upon how the BCF was calculated rather than organism type. (1) The BCF calculated with the concentrations of parent munitions (BCF_m) using equation 3.5 were low. (2) The BCF based on total ^{15}N (BCF_T) was calculated by using the total ^{15}N concentrations (Eqn. 3.6) were on average 2 orders of magnitude greater than BCF_m values (Table 3.1). (3) The BCF_R calculated from the model fell between BCF_m and BCF_T values. (4) Finally, a BCF_{kow} calculated from the Log K_{ow} of RDX is shown in Table 3.1 for comparison (Meylan et al. 1999).

4. Discussion

Results from the ^{15}N RDX experiments and modeling support two major findings: (1) RDX was transformed into multiple derivatives, with subsequent ^{15}N retention in the organism; (2) ^{15}N toxicokinetic parameters and BCFs values calculated using ^{15}N labeled RDX, MNX, TNX, and DNX were larger and more variable than previous studies have indicated.

4.1 RDX uptake and transformations in biota

RDX has been shown to be degraded by bacteria (Bhatt et al. 2005; Hawari et al. 2000; Vila et al. 2004) and fungi (Bhatt et al. 2006; Sheremata and Hawari 2000), and taken up into freshwater fish (Belden et al. 2005b) and terrestrial biota (Just and Schnoor 2004; Sarrazin et al. 2009; Vila et al., 2007), but few studies have discussed the fate of RDX in coastal marine biota or generally the fate of RDX in macrobiota after uptake. The previous use of ^{14}C and ^{15}N labeled RDX in aerobic bacterial or fungal studies have been useful in demonstrating mineralization to CO_2 and DIN (NO_x, and N_2O; Fournier et al. 2002; Sheremata and Hawari 2000; Thompson et al. 2005). While many previous toxicological studies have focused on uptake rates, removal rates, and BCF values of RDX, MNX, TNX, and DNX in single organism simplified experiments, but as presented in a few previous similar studies (Rosen and Lotufo 2005, 2010) the environmental uptake of RDX into organisms operates within a host of other transformation and degradation pathways. Here we created experimental conditions whereby both microbial breakdown pathways could operate side by side with macrobiotic uptake and transformations. This study shows that the ^{15}N derived from RDX was found in biota in much larger concentrations than could be attributed to munitions compounds and the ^{15}N concentration should be considered conservative estimates because only the nitro groups were labeled on the RDX and not the ring N. In this study, the amount of total ^{15}N in biota was 1-2 orders of magnitudes greater than can

be accounted for by measureable tissue RDX indicating that a significant amount of the RDX taken up into the biota is being processed into various nitrogen retention pathways.

Despite rapidly attaining a quasi-steady state (maximum but variable concentrations) for RDX and its main derivatives, the munitions derived N was transformed more slowly within the organisms and then retained in the larger total bulk N pool of each organism. This process was evidenced by the slowly increasing total ^{15}N enrichment that required days to weeks before the ^{15}N enrichment leveled to a steady state (Fig. 3.3). The difference in trajectory and pattern between ^{15}N attributed to RDX and total ^{15}N along with the small percentage attributable to RDX (Fig. 3.5) can be seen in all the biota in this study. This result suggests that the mechanisms or pathways responsible for these patterns may be common across biota types.

The data suggests that there are four possible explanations for the difference in pattern between ^{15}N attributed to RDX and total ^{15}N uptake in the biota. (A) The first possible explanation is that the RDX was mineralized to DIN externally in the environment and taken up by macrobiota as DIN. Autotrophs can readily take up DIN, and the model showed that the uptake of DIN (k_{DN}; Table 3.1) was needed to appropriately model the total ^{15}N trajectories in the autotrophs (*F. vesiculosus and U. lactuca*) and the one species heavily grazing on autotrophic periphyton (*L. littorea*). While autotrophic uptake of DIN is common, heterotrophs cannot directly assimilate DIN. Therefore such a pathway cannot explain the ^{15}N subsidy in heterotrophs, and the model validated that k_{DN} for heterotrophs were nonexistent. (B) The second possible explanation is that RDX was rapidly partitioned into the biota and then transformed and retained in tissue as unknown free breakdown products of RDX. Peak MNX, DNX, and TNX concentrations as well as the rate of change in those concentrations varied widely across species. The highly variable patterns of metabolite composition and concentration trajectories between

organisms suggest that organism-specific transformations were important determinants of net tissue metabolite concentrations. It may also be indicative of the multiple different biodegradation pathways that produce secondary ^{15}N containing metabolites beyond MNX, TNX, and DNX. Several pathways have been documented for fungi and prokaryotes, and some have been attributed to the action of cytochrome P450 (Seth-Smith et al. 2008). Similar reactions may also be operating in macrobiota (Bhatt et al. 2006; Crocker et al. 2006). Cytochrome P450 belongs to a protein family that is highly evolutionarily conserved and is found in different types of both prokaryotic (Seth-Smith et al. 2008) and eukaryotic cells (Bhushan et al. 2003). The P450 protein has been shown to produce RDX metabolites (nitrite, 4-Nitro-2,4-diazabutanal, formaldehyde, and ammonium) by consuming RDX and NADPH in rabbit liver cells (Bhushan et al. 2003) and evidence of nitro formation includes the possibility of macrobiota acting as partial mineralizers. Similar metabolites have been measured via *Rhodococcus sp.* mediated metabolism of RDX with similar mechanisms proposed (Hawari et al. 2002). P450 has also been reported to biodegrade RDX derivatives MNX and TNX to similar metabolites in rabbit cells (Halasz et al. 2012). In this study, because the tissues were not extracted prior to bulk ^{15}N analyses, and derivatives other than the MNX, DNX, and TNX were not measured in the extracted fraction, any free derivative other than MNX, DNX, and TNX would be counted in the bulk ^{15}N measurement. Interestingly, because some of the nitroso breakdown pathways include denitration steps, it leaves open the possibility that macrobiota may also contribute to mineralization of RDX to DIN. (C) The third possible explanation is that further breakdown of the nitroso derivatives led to compounds that quickly formed adducts that are bound to specific tissue types. Bound adducts have been proposed in ^{14}C labelled munitions experiments as an unextractable fraction and used to explain discrepancies between the

measurable amount of munitions and the radio isotope label (Belden et al. 2011). As indicated by the model, (k_{pN} and k_{mN}) the ^{15}N was biotransformed into other compounds other than the three main RDX derivatives MNX, DNX, and TNX and both explanations B and C are supported by these models results. While these secondary products could take numerous forms (Crocker et al. 2006), they were nonetheless retained within the organism otherwise would not have appeared as a ^{15}N subsidy in the bulk EA analysis. (D) Finally a less likely but possible fourth explanation remains that the RDX is fully mineralized within macrobiota and the mineralized ^{15}N tracer is used in the biosynthesis of tissues. Several nitroso breakdown pathways yield variable oxidation state inorganic N compounds (Fournier et al. 2002). Although it is unclear if those reactions operate within macrobiota, and we do not propose a specific mechanism, this possibility cannot be wholly discounted.

RDX as a potential toxicant in marine biota depends on which pathway caused the discrepancy between the ^{15}N accounted for in RDX and the much larger amount of bulk ^{15}N-RDX. If the RDX is mineralized, either externally or internally, (options A and D) and then incorporated into tissue through natural biosynthesis pathways, then RDX is most likely not a large concern for organisms coastal marine environment. Similar pathways to A and D with low toxicological effect have been documented (Nipper et al. 2009). However if intra-organism transformations lead to derivative production other than MNX, DNX, and TNX and those products are either in the "free" state or as adducts (options C and D) and are more toxic than RDX or the nitroso derivatives then RDX could be of greater concern. RDX in general is associated with low toxicity, which leads to the inference that and "free" or adduct breakdown products do not substantially contribute to acute toxicological effects. However any long-term effect, particularly associated with production of adducts with DNA remain unknown.

4.2 Model toxicokinetics and BCFs

Distribution and movement of RDX, RDX derivatives, and ^{15}N were accurately described using the first order equations (Eqn. 3.2-3.4). The expansion of previously published models (Lydy et al. 2000; Nuutinen et al. 2003) allowed for a better understanding of the fate of RDX by tracking the biodegradation and metabolism of RDX derived N. The rates and rate constants reported in Table 3.1 are not markedly different across species though some patterns do emerge. The modeled k_u values derived from the model fall within the few reported values published (Belden et al. 2005a; Lotufo et al. 2009). The similarities between our k_u and previous published values is expected since the k_u is controlled by the physical partitioning of the RDX molecule into tissue rather than active assimilation. However stark differences arose in other terms in our model due to the inclusion of modeling the bulk ^{15}N tracer. The modeled elimination k_{ep} values derived here are smaller by 1-2 orders of magnitude than previously reported k_e values (Belden et al. 2005a; Lotufo et al. 2009). The difference in the k_{ep} values reported here is offset by the higher retention of ^{15}N (k_{pN} and k_{mN}) in this study's tracer model. The k_{pN} and k_{mN} are one order of magnitude larger than the elimination values k_{ep} and k_{em}. Since k_{pN} and k_{ep} pull from the same ^{15}N pool (Fig. 1) the ^{15}N is not being removed but retained by the organism. With k_{pN} and k_{mN} being so much larger than the elimination values for the those pools, the need to account for the total ^{15}N led to the low k_{eN} and $^{15}N_R$ values for biota suggests that ^{15}N is retained in tissue and not just removed as previous studies indicate.

The model provided an additional way to estimate BCF and for this study, we had a total of 4 options to estimate a BCF. (1) The ratio of the steady state concentration of tissue concentration divided by the aqueous munitions concentration (BCF_m, Eqn. 3.5). (2) The use of total ^{15}N values attributed to RDX (BCF_T, Eqn. 3.6). (3) The use of Log K_{ow} values as a proxy

for BCF (Eqn. 3.7). (4) Finally, the modeled derived rate balance was used to calculate a BCF (BCF_R, Eqn. 3.8). Generally our BCF values compared favorably to other reports for aquatic organisms derived with similar methods (Lotufo et al. 2009). BCFs calculated in previous studies have shown that BCF calculated with only the parent compound (BCF_m) are typically lower than estimates using Log K_{ow} values (BCF_{Kow}; Lotufo et al. 2009). Similarly BCFs calculated with total isotopes inventory (BCF_T) also yield a BCF much higher than estimates using Log K_{ow} as summarized by Lotufo et al (2009). Most toxicological studies have either used Log K_{ow} or BCF_m method. Either of these methods work well for studies that need to know only how much of the parent compound is in the species tissues for a given aqueous concentration. However, if the parent and derivatives are important (such as when breakdown products might have high toxicity) then a more complete BCF using total reactivity (BCF_T) should be utilized as it indicates other potentially unmeasured metabolites, adducts, or other compounds of similar toxicological relevance provided options B and/or C are dominant. Alternatively, if the BCF_T reflects tracer that has been liberated through mineralization and subsequent incorporation of N into tissue (options A and D), it may be a better indication of processing than as an indicator of the partitioning of an intact compound with some presumed toxicity.

Similar to other studies, the BCF_R calculated here from the modeled rate constants gave a larger BCF values relative to BCF_m method, but it was smaller than the BCF_T. The BCF_R as defined by Eqn. 3.8 functions as an aggregated BCF of RDX, its derivatives, and adducts assuming options B and C are the principle cause. Under these scenarios the BCF_R is not a unique metric for only the parent compound and/or its measured derivatives but instead captures all compounds derived from RDX that may retain some toxic properties, and reflects the balance

between uptake, elimination, and transformations of RDX. The value that is calculated for the BCF_R reflects the transformations and eliminations that the ^{15}N model captures and that the more simple BCF_m method does not take into account. If options A or D are correct from the previous section, then k_{eN} would need to be removed from Eqn. 3.8, because the accumulation of ^{15}N in DIN does not include tracer associated with derivatives. This adjusted BCF_R would still adequately characterize ratio of uptake to retention of RDX plus all metabolites.

Our model can accurately describe not only the experimental BCF_m but also the subsequent processing the RDX post uptake as it is transformed and subsequently retained by the organism. Even though our model can both track ^{15}N movement in the organism and accurately estimate BCFs that could be used for toxicological studies, the model cannot eliminate the possibility of some unknown derivatives or partial breakdown products with adducts. Resolving these questions should be part of future work since it would help better define the fate of RDX after uptake and useful for assessing the RDX effects on coastal biota.

5. Conclusions

The multi organism ^{15}N tracer experiment identified uptake, conversion of RDX into its primary derivatives, and retention of nitroso derived N into the macrobiota. The biota reached a steady state with respect to both RDX and ^{15}N although at much different rates. The different rate of retention of ^{15}N indicates that RDX is continually metabolized and the nitrogen was retained into tissue. While the rates to steady state varied, the larger ^{15}N bulk then ^{15}N attributed to RDX indicated that there are common pathways or mechanism to the biotransformation and retention of ^{15}N. The identification of the ^{15}N breakdown products is paramount of importance to knowing whether the unknown large ^{15}N subsidy measured in tissue is harmful. ^{15}N was instrumental in identifying the fact that much more compound was taken up and processed even though we don't

exactly know how. The use of ^{15}N constrain more traditional analytical chemistry approaches in this regard. The disadvantage of ^{15}N beyond additional cost and instrumental overhead is that N can be widely distributed among many pools, some associated with uptake and some not. It is sometimes difficult to isotopically characterize some specific compounds that are formed. The lack of compound identification can lead to large percentages of unknown in the ^{15}N tissue mass balance. The large percentages of unknown in ^{15}N tissue mass balance is both a boon (in that it can identify missing and possibly important processes seen here) and a difficulty because the optimum utility of the tracer often relies on analysis of many different N containing fractions. The value of using ^{15}N labeled munitions, as with many techniques, depends on whether it can yield information that cannot be derived through other means. For this study, it clearly did. Bioconcentration factors were calculated with 4 different methods. The different BCF methods add variety to the current published methods to allow for a more accurate measurement of BCF for different systems. Toxicokinetic modeling of the ^{15}N tracer, RDX, and derivatives revealed a more complete picture of the fate of the RDX. The new model was a good fit to experimental data and has the ability to estimate the amount of ^{15}N incorporated into a variety of coastal marine biota. The model simultaneously modeled the ^{15}N and calculated toxicological relevant BCF values by introducing a new ^{15}N rate term. Future works should include identification of the unknown breakdown products and adducts. ^{15}N labeled compounds can offer many insights to transport and fate studies and should be used in follow up studies specifically in other environments (aquatic and terrestrial), other nitrogen containing compounds, and identifying the unknown breakdown products formed.

6. Acknowledgements

We would like to acknowledge Strategic Environmental Research and Development Program No. ER-2122 for their support and funding. We also thank David Cady, Charlie Woods, and Veronica Rollinson for laboratory support.

References

Annamaria H, Manno D, Strand SE, Bruce NC, Hawari J. 2010. Biodegradation of RDX and MNX with rhodococcus sp. strain DN22: New insights into the degradation pathway. Environ Sci Technol 44(24):9330-6.

ASTM E1022-94 2013. Standard guide for conducting bioconcentration tests with fishes and saltwater bivalve mollusks. ASTM International, West Conshohocken.

Ballentine M, Tobias C, Vlahos P, Smith R, Cooper C. 2015. Bioconcentration of TNT and RDX in coastal marine biota. Arch Environ Contam Toxicol 68(4):718-28.

Belden JB, Lotufo GR, Lydy MJ. 2005a. Accumulation of hexahydro-1, 3, 5-trinitro-1, 3, 5-triazine in channel catfish (*Ictalurus punctatus*) and aquatic oligochaetes (*Lumbriculus variegatus*). Environmental Toxicology and Chemistry 24(8):1962-7.

Belden JB, Ownby DR, Lotufo GR, Lydy MJ. 2005. Accumulation of trinitrotoluene (TNT) in aquatic organisms: Part 2—Bioconcentration in aquatic invertebrates and potential for trophic transfer to channel catfish (*Ictalurus punctatus*). Chemosphere 58(9):1161-8.

Belden JB, Lotufo GR, Chambliss CK, Fisher JC, Johnson DR, Boyd RE, Sims JG. 2011. Accumulation of 14 C-trinitrotoluene and related nonextractable (bound) residues in *Eisenia fetida*. Environmental Pollution 159(5):1363-8.

Bentley R, Dean J, Ells S, Hollister T, LeBlanc G. 1977. Laboratory Evaluation of the Toxicity of Cyclotrimethylene Trinitramine (RDX) to Aquatic Organisms.

Bhatt M, Zhao J, Halasz A, Hawari J. 2006. Biodegradation of hexahydro-1, 3, 5-trinitro-1, 3, 5-triazine by novel fungi isolated from unexploded ordnance contaminated marine sediment. Journal of Industrial Microbiology and Biotechnology 33(10):850-8.

Bhatt M, Zhao J, Monteil-Rivera F, Hawari J. 2005. Biodegradation of cyclic nitramines by tropical marine sediment bacteria. Journal of Industrial Microbiology and Biotechnology 32(6):261-7.

Bhushan B, Trott S, Spain JC, Halasz A, Paquet L, Hawari J. 2003. Biotransformation of hexahydro-1,3,5-trinitro-1,3,5-triazine (RDX) by a rabbit liver cytochrome P450: Insight into the mechanism of RDX biodegradation by *Rhodococcus sp.* strain DN22. Appl Environ Microbiol 69(3):1347-51.

Burken JG and Schnoor JL. 1998. Predictive relationships for uptake of organic contaminants by hybrid poplar trees. Environ Sci Technol 32(21):3379-85.

Chai, T., Draxler, R. R., 2014. Root mean square error (RMSE) or mean absolute error (MAE)? - arguments against avoiding RMSE in the literature. Geosci. Model Dev. 7 (3), 1247-1250.

Clausen J, Robb J, Curry D, Korte N. 2004. A case study of contaminants on military ranges: Camp Edwards, Massachusetts, USA. Environmental Pollution 129(1):13-21.

Conder JM, Point TWL, Bowen AT. 2004. Preliminary kinetics and metabolism of 2, 4, 6-trinitrotoluene and its reduced metabolites in an aquatic oligochaete. Aquatic Toxicology 69(3):199-213.

Crocker FH, Indest KJ, Fredrickson HL. 2006. Biodegradation of the cyclic nitramine explosives RDX, HMX, and CL-20. Appl Microbiol Biotechnol 73(2):274-90.

Darrach M, Chutjian A, Plett G. 1998. Trace explosives signatures from World War II unexploded undersea ordnance. Environ Sci Technol 32(9):1354-8.

Fournier D, Halasz A, Spain J, Fiurasek P, Hawari J. 2002. Determination of key metabolites during biodegradation of hexahydro-1,3,5-trinitro-1,3,5-triazine with *rhodococcus sp*. strain DN22. Appl Environ Microbiol 68(1):166-72.

Halasz A, Manno D, Perreault NN, Sabbadin F, Bruce NC, Hawari J. 2012. Biodegradation of RDX nitroso products MNX and TNX by cytochrome P450 XplA. Environ Sci Technol 46(13):7245-51.

Harrison I and Vane C. 2010. Attenuation of TNT in seawater microcosms. Water Science & Technology 61(10).

Hawari J, Beaudet S, Halasz A, Thiboutot 3S, Ampleman G. 2000. Microbial degradation of explosives: Biotransformation versus mineralization. Appl Microbiol Biotechnol 54(5):605-18.

Hawari J, Halasz A, Groom C, Deschamps S, Paquet L, Beaulieu C, Corriveau A. 2002. Photodegradation of RDX in aqueous solution: A mechanistic probe for biodegradation with *Rhodococcus sp.* Environ Sci Technol 36(23):5117-23.

Holmes RM, Peterson BJ, Deegan LA, Hughes JE, Fry B. 2000. Nitrogen biogeochemistry in the oligohaline zone of a New England estuary. Ecology 81(2):416-32.

Houston JG and Lotufo GR. 2005. Dietary exposure of fathead minnows to the explosives TNT and RDX and to the pesticide DDT using contaminated invertebrates. International Journal of Environmental Research and Public Health 2(2):286-92.

Hovatter PS, Talmage SS, Opresko DM, Ross RH. 1997. Ecotoxicity of nitroaromatics to aquatic and terrestrial species at Army superfund sites. ASTM Spec Tech Publ 1317:117-29.

Jenkins TF, Hewitt AD, Grant CL, Thiboutot S, Ampleman G, Walsh ME, Ranney TA, Ramsey CA, Palazzo AJ, Pennington JC. 2006. Identity and distribution of residues of energetic compounds at army live-fire training ranges. Chemosphere 63(8):1280-90.

Just CL and Schnoor JL. 2004. Phytophotolysis of hexahydro-1, 3, 5-trinitro-1, 3, 5-triazine (RDX) in leaves of reed canary grass. Environ Sci Technol 38(1):290-5.

Korotenko K. 2003. Chemical warfare munitions dumped in the Baltic Sea: Modeling of pollutant transport due to possible leakage. Russian Academy of Sciences. Oceanology 43(1):16.

Lotufo GR, Gibson AB, Leslie Yoo J. 2010. Toxicity and bioconcentration evaluation of RDX and HMX using sheepshead minnows in water exposures. Ecotoxicol Environ Saf 73(7):1653-7.

Lotufo GR, Farrar JD, Inouye LS, Bridges TS, Ringelberg DB. 2001. Toxicity of sediment-associated nitroaromatic and cyclonitramine compounds to benthic invertebrates. Environmental Toxicology and Chemistry 20(8):1762-71.

Lotufo GR, Lydy MJ, Rorrer GL, Cruz-Uribe O, Cheney DP 2009. Bioconcentration, bioaccumulation, and biotransformation of explosives and related compounds in aquatic organisms. In: Sunahara GI, Lotufo G, Kuperman RG, Hawari J (eds) Ecotoxicology of explosives. CRC Press, Boca Raton, pp. 135-155

Lydy MJ, Lasater J, Landrum PF. 2000. Toxicokinetics of DDE and 2-chlorobiphenyl in *Chironomus tentans*. Arch Environ Contam Toxicol 38(2):163-8.

Meylan WM, Howard PH, Boethling RS, Aronson D, Printup H, Gouchie S. 1999. Improved method for estimating bioconcentration/bioaccumulation factor from octanol/water partition coefficient. Environmental Toxicology and Chemistry 18(4):664-72.

Miyares P and Jenkins T. 1990. Salting-out solvent extraction for determining low levels of nitroaromatics and nitramines in water. USA Cold Regions Research and Engineering Laboratory, Special Report :90-30.

Mukhi S and Patiño R. 2008. Effects of hexahydro-1, 3, 5-trinitro-1, 3, 5-triazine (RDX) in zebrafish: General and reproductive toxicity. Chemosphere 72(5):726-32.

Mukhi S, Pan X, Cobb GP, Patino R. 2005. Toxicity of hexahydro-1, 3, 5-trinitro-1, 3, 5-triazine to larval zebrafish (*Danio rerio*). Chemosphere 61(2):178-85.

Nipper M, Carr RS, Lotufo GR. 2009. Aquatic toxicology of explosives, In: Sunahara GI, Lotufo G, Kuperman RG, Hawari J (eds). Ecotoxicology of explosives. CRC Press, Boca Raton, pp 77-115.

Nipper M, Carr R, Biedenbach J, Hooten R, Miller K, Saepoff S. 2001. Development of marine toxicity data for ordnance compounds. Arch Environ Contam Toxicol 41(3):308-18.

Nuutinen S, Landrum PF, Schuler LJ, Kukkonen JV, Lydy MJ. 2003. Toxicokinetics of organic contaminants in *Hyalella azteca*. Arch Environ Contam Toxicol 44(4):0467-75.

Pennington JC and Brannon JM. 2002. Environmental fate of explosives. Thermochimica Acta 384(1):163-72.

Roh H, Yu C, Fuller ME, Chu K. 2009. Identification of hexahydro-1, 3, 5-trinitro-1, 3, 5-triazine-degrading microorganisms via 15N-stable isotope probing. Environ Sci Technol 43(7):2505-11.

Rosen G and Lotufo GR. 2007a. Toxicity of explosive compounds to the marine mussel, *Mytilus galloprovincialis*, in aqueous exposures. Ecotoxicol Environ Saf 68(2):228-36.

Rosen G and Lotufo GR. 2007b. Bioaccumulation of explosive compounds in the marine mussel, *Mytilus galloprovincialis*. Ecotoxicol Environ Saf 68(2):237-45.

Rosen G and Lotufo GR. 2010. Fate and effects of composition B in multispecies marine exposures. Environmental Toxicology and Chemistry 29(6):1330-7.

Rosen G and Lotufo GR. 2005. Toxicity and fate of two munitions constituents in spiked sediment exposures with the marine amphipod *Eohaustorius estuarius*. Environmental Toxicology and Chemistry 24(11):2887-97.

Sarrazin M, Dodard SG, Savard K, Lachance B, Robidoux PY, Kuperman RG, Hawari J, Ampleman G, Thiboutot S, Sunahara GI. 2009. Accumulation of hexahydro-1, 3, 5-trinitro-1, 3, 5-triazine by the earthworm *Eisenia andrei* in a sandy loam soil. Environmental Toxicology and Chemistry 28(10):2125-33.

Seth-Smith HM, Edwards J, Rosser SJ, Rathbone DA, Bruce NC. 2008. The explosive-degrading cytochrome P450 system is highly conserved among strains of *Rhodococcus spp.* Appl Environ Microbiol 74(14):4550-2.

Sheremata TW and Hawari J. 2000. Mineralization of RDX by the white rot fungus *Phanerochaete chrysosporium* to carbon dioxide and nitrous oxide. Environ Sci Technol 34(16):3384-8.

Simini M, Checkai RT, Kuperman RG, Phillips CT, Kolakowski JE, Kurnas CW, Sunahara GI. 2003. Reproduction and survival of *Eisenia fetida* in a sandy loam soil amended with the nitro-heterocyclic explosives RDX and HMX: The 7th international symposium on earthworm ecology· cardiff· wales· 2002. Pedobiologia 47(5):657-62.

Smith RW, Vlahos P, Tobias C, Ballentine M, Ariyarathna T, Cooper C. 2013. Removal rates of dissolved munitions compounds in seawater. Chemosphere 92(8):898-904.

Steevens JA, Duke BM, Lotufo GR, Bridges TS. 2002. Toxicity of the explosives 2, 4, 6-trinitrotoluene, hexahydro-1, 3, 5-trinitro-1, 3, 5-triazine, and octahydro-1, 3, 5, 7-tetranitro-1, 3, 5, 7-tetrazocine in sediments to *Chironomus tentans* and *Hyalella azteca*: Low-dose hormesis and high-dose mortality. Environmental Toxicology and Chemistry 21(7):1475-82.

Sweeney LM, Okolica MR, Gut CP, Gargas ML. 2012. Cancer mode of action, weight of evidence, and proposed cancer reference value for hexahydro-1, 3, 5-trinitro-1, 3, 5-triazine (RDX). Regulatory Toxicology and Pharmacology 64(2):205-24.

Talmage SS, Opresko DM, Maxwell CJ, Welsh CJ, Cretella FM, Reno PH, Daniel FB. 1999. Nitroaromatic munition compounds: Environmental effects and screening values. In: Reviews of environmental contamination and toxicology. Springer. 1 p.

Thompson KT, Crocker FH, Fredrickson HL. 2005. Mineralization of the cyclic nitramine explosive hexahydro-1,3,5-trinitro-1,3,5-triazine by *Gordonia* and *Williamsia spp*. Appl Environ Microbiol 71(12):8265-72.

Tobias CR, Macko SA, Anderson IC, Canuel EA, Harvey JW. 2001. Tracking the fate of a high concentration groundwater nitrate plume through a fringing marsh: A combined groundwater tracer and in situ isotope enrichment study. Limnol Oceanogr 46(8):1977-89.

Van Aken B, Yoon JM, Schnoor JL. 2004. Biodegradation of nitro-substituted explosives 2,4,6-trinitrotoluene, hexahydro-1,3,5-trinitro-1,3,5-triazine, and octahydro-1,3,5,7-tetranitro-1,3,5-tetrazocine by a phytosymbiotic methylobacterium sp. associated with poplar tissues (*Populus deltoides x nigra* DN34). Appl Environ Microbiol 70(1):508-17.

Vila M, Lorber-Pascal S, Laurent F. 2007. Fate of RDX and TNT in agronomic plants. Environmental Pollution 148(1):148-54.

Figure and Table Captions:

Table 3.1: Modeled rates and bioconcentration factors (BCFs): Uptake coefficients and rates for ^{15}N were modeled for each species individually using equations #'s 2-4. k_u = uptake clearance coefficient, k_{ep} = elimination rate constant, k_m = derivative uptake rate constant, k_{em} = metabolite elimination rate constant, k_{pN} = incorporation rate constant from parent compound, k_{mN} = nitrogen incorporation rate constant from metabolites, k_{eN} = nitrogen elimination rate constant, and k_{DN} = nitrogen uptake rate constant from DIN. BCF rates were calculated three ways. BCF_m was calculated using parent munitions concentrations, BCF_T was calculated using total ^{15}N measured in tissue, and BCF_R was calculated using modeled rates. BCF_{kow} values were previously reported in Lotufo et al. (2009) and represent the BCF values empirically derived from the Log K_{ow} of RDX. Root mean square error (RMSE) were calculated between the ^{15}N model data and the experimental values for each time point.

Figure 3.1: ^{15}N tracer three box model: Model structure representing uptake and movement of ^{15}N derived from within an organism. Box 1 is ^{15}N that attributed to RDX. Box 2 is the ^{15}N attributed to the sum of the nitroso derivatives (ie. metabolites TNX, DNX, and MNX). Box 3 represents the total ^{15}N in the organism not represented in box 1 or box 2.

Figure 3.2: Aqueous munitions concentration: Time series experimental aqueous data for munitions. Error bars are standard deviation (N=3). Predicted RDX concentrations were calculated from the initial spike and pumping rate of RDX into the experimental setup. DNX was not detected.

Figure 3.3: ^{15}N concentrations in biota tissue: Time series experimental biota data for munitions represented in ^{15}N units. $^{15}N_R$ and $^{15}N_D$ use the right axis while total ^{15}N uses the left axis. *F. heteroclitus* is not presented as data for $^{15}N_R$ and $^{15}N_D$ were lost.

Figure 3.4: ^{15}N in biota normalized to mass: Total ^{15}N measured in all species was normalized to total mass for each species. *M. edulis* died off after day 12. All *U. lactuca* samples were removed after day 19.

Figure 3.5: Partitioning of total ^{15}N: Total ^{15}N is represented in percentages. Pie chart A represents the total ^{15}N added to the experimental setup. The 'unknown' fraction is calculated by difference and could include sediment-bound munitions, mineralization products in sediments or aqueous phases, and other possible RDX derivatives not measured in this study. B shows how much of the ^{15}N found in biota can be accounted for as munitions species measured in tissues.

Table 3.1: Modeled rates and bioconcentration factors (BCFs)

	F. vesiculosus	*U. lactuca*	*M. edulis*	*M. mercenaria*	*C. virginica*	*L. littorea*	*C. maenas*	*P. americanus*	*F. heteroclitus*
k_u (mL g^{-1} day^{-1})	2.3	36.4	38.2	6.9	21.7	25	2.5	12.3	11.9
k_{ep} ($days^{-1}$)	0.05	0.5	0.4	0.5	0.2	0.5	0.7	0.03	0.5
k_m ($days^{-1}$)	0	5	0.8	1	1.5	1.5	0.4	3.5	2.5
k_{em} ($days^{-1}$)	0	0.5	0.5	0.5	0.5	0.5	0.04	0.4	0.5
k_{pN} ($days^{-1}$)	1.6	4	3.5	7	6	7	3	3	3
k_{mN} ($days^{-1}$)	0	3	2	2	2	2	0.8	3	2
k_{eN} ($days^{-1}$)	0.02	0.072	0.11	0.04	0.12	0.11	0.0047	0.022	0.04
k_{DN} ($days^{-1}$)	0.085	0.04	0	0	0	0.05	0	0	0
BCF_m (mL g^{-1})	0.57 (0.23)	5.90 (3.96)	4.36 (3.12)	1.44 (0.24)	1.21 (1.14)	3.37 (3.15)	0.35 (0.15)	1.67 (0.53)	N/A
BCF_T (mL g^{-1})	66.3 (12.7)	101.6 (51.6)	12.3 (7.42)	17.4 (7.50)	42.1 (10.2)	67.4 (24.8)	8.54 (3.16)	68.7 (74.7)	34.6 (23.0)
BCF_R (mL g^{-1})	32.9	33.9	37.8	6.6	26.5	22.5	3.3	27.2	11.4
BCF_{kow} (mL g^{-1})	2.3	2.3	2.3	2.3	2.3	2.3	2.3	2.3	2.3
RMSE (μg ^{15}N g dw^{-1})	1.3×10^{-2}	1.5×10^{-6}	1.6×10^{-6}	1.9×10^{-5}	2.0×10^{-3}	7.0×10^{-2}	6.0×10^{-3}	8.0×10^{-4}	2.0×10^{-3}

Figure 3.1: ^{15}N tracer three box model

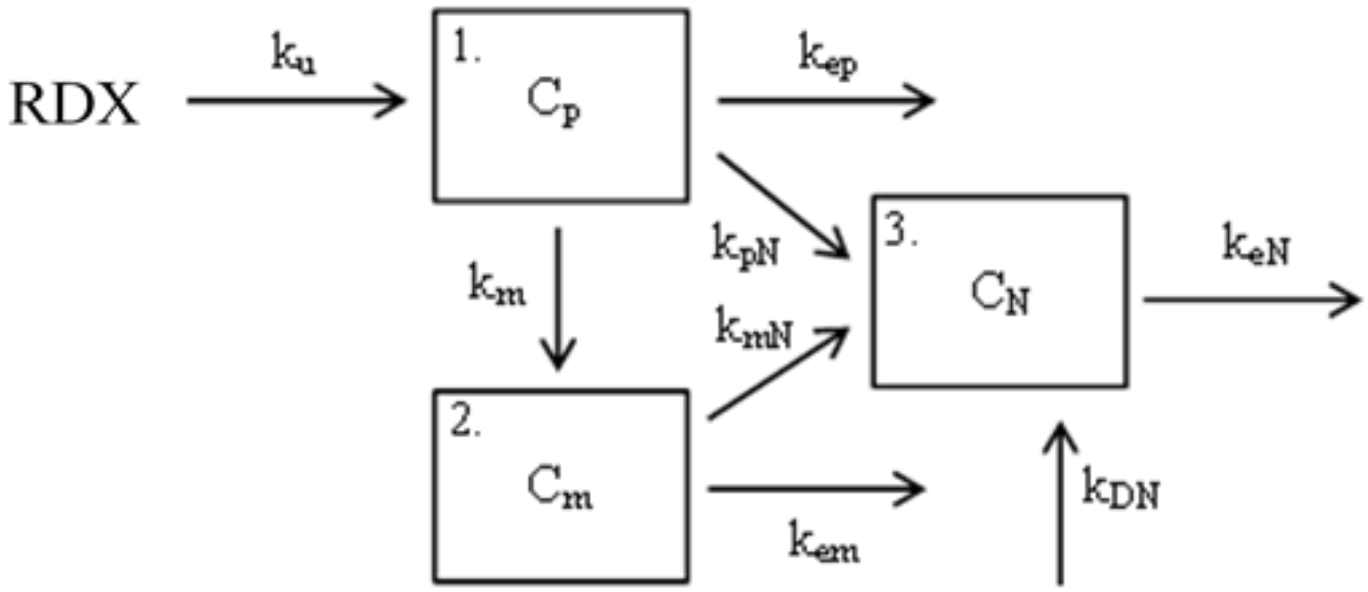

Figure 3.2: Aqueous munitions concentration

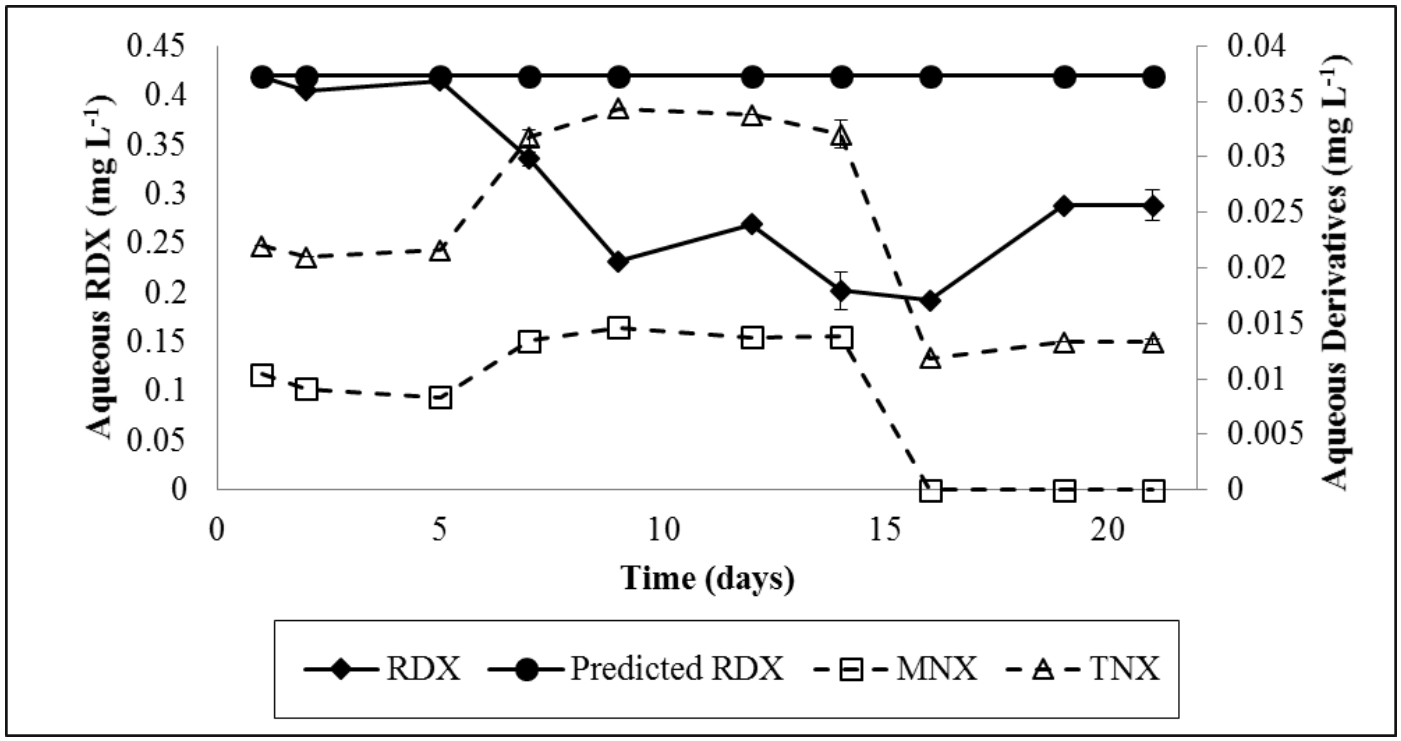

Figure 3.3: ^{15}N concentrations in biota tissue

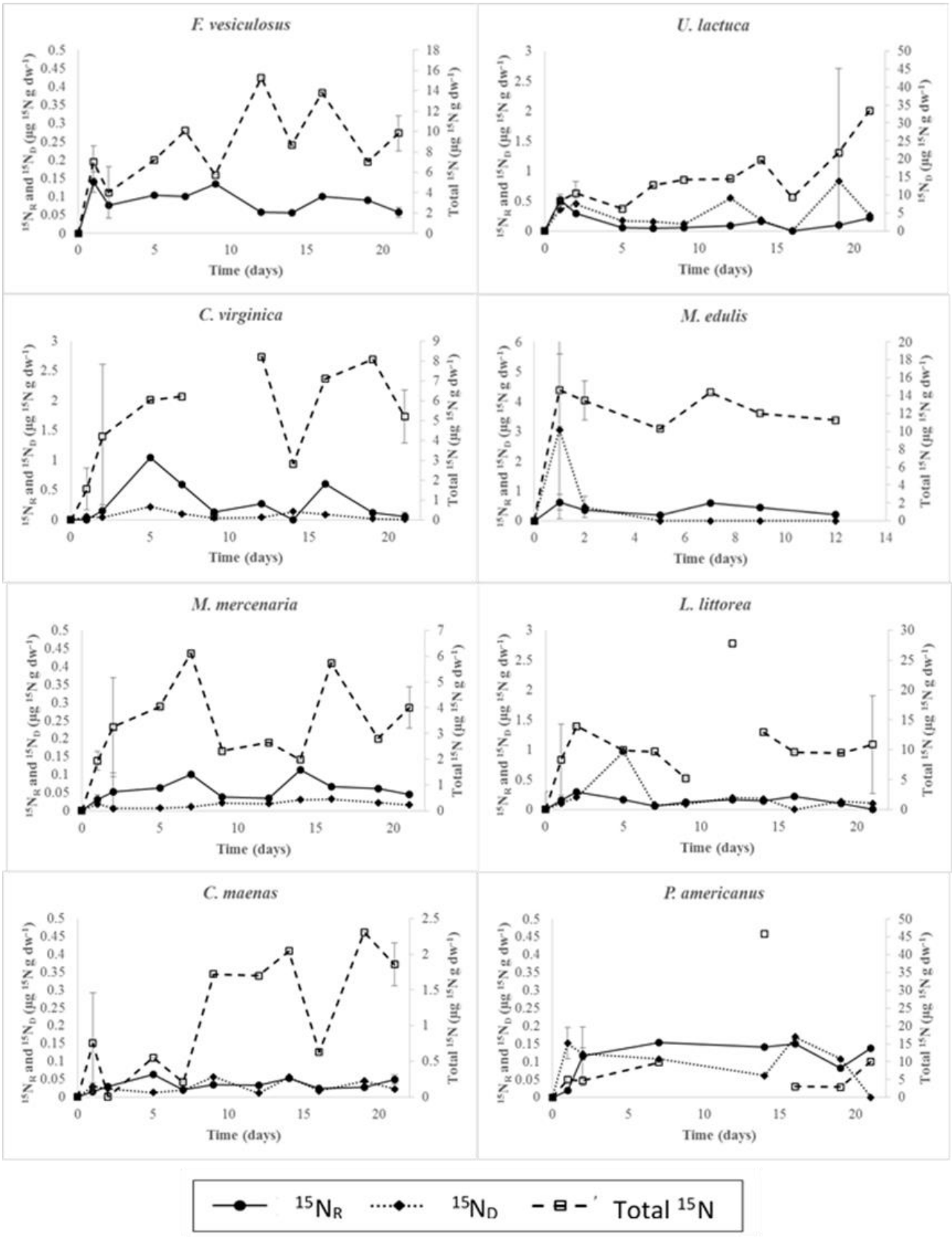

Figure 3.4: ^{15}N in biota normalized to mass

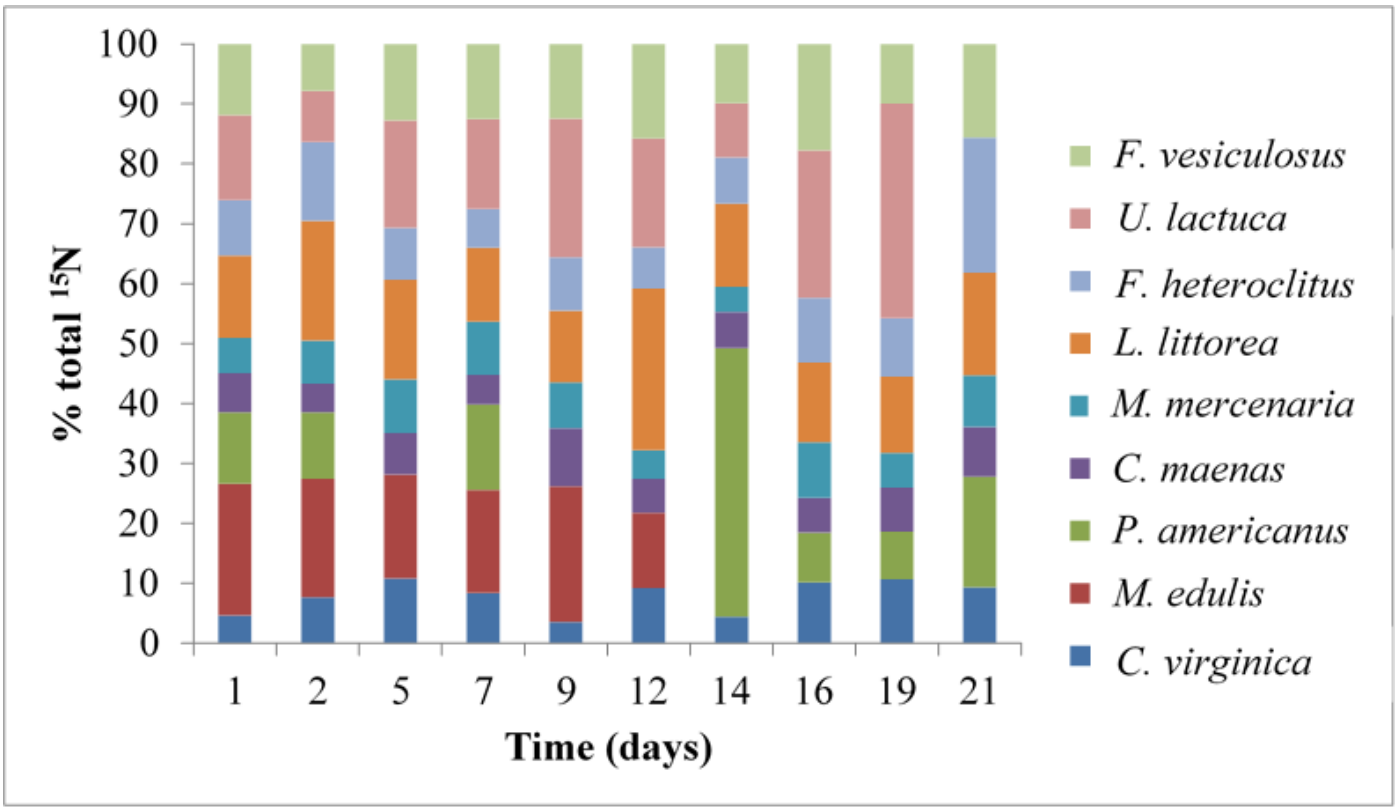

Figure 3.5: Partitioning of total ^{15}N

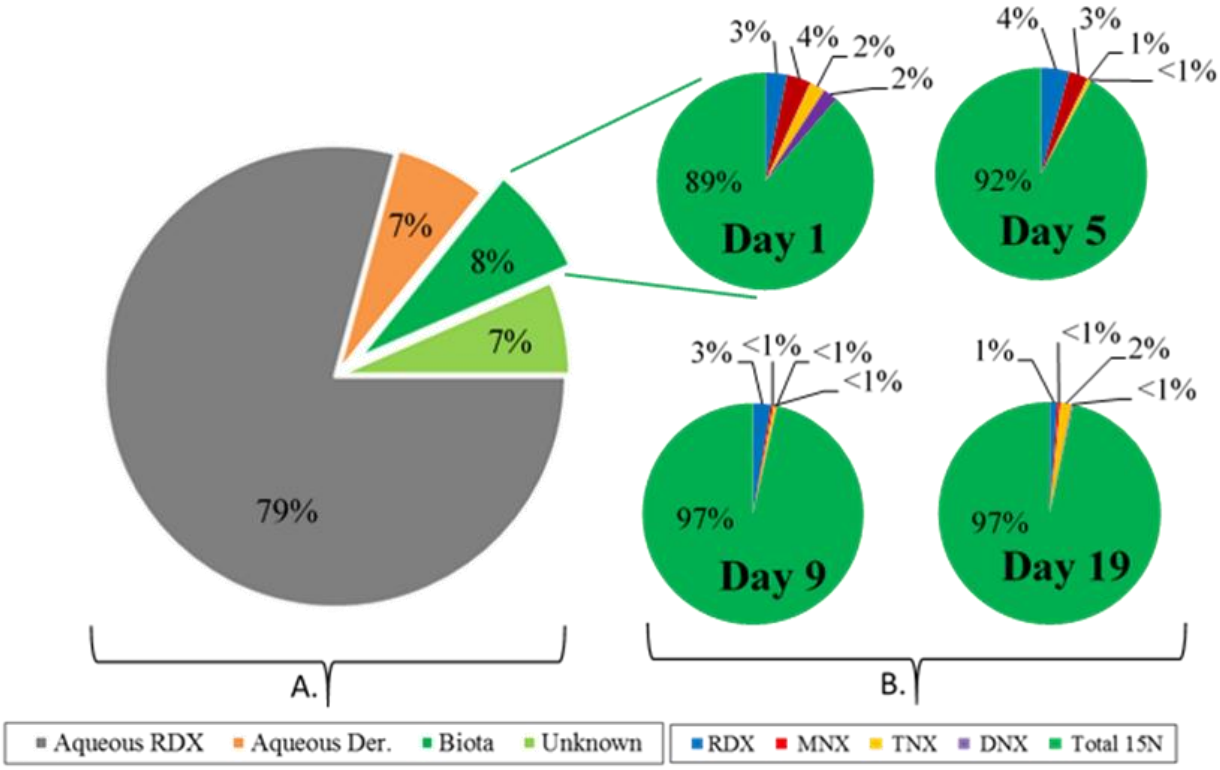

Chapter 4: Biotic uptake and retention of hexahydro-1,3,5-trinitro-1,3,5-triazine (RDX) derived nitrogen measured in three simulated coastal habitats[4]

[4] Ballentine, M., Ariyarathna, T., Smith, R. W., Cooper, C., Vlahos, P., Fallis, S., Groshens, T., Tobias, C. (2016). Biotic uptake and retention of hexahydro-1,3,5-trinitro-1,3,5-triazine (RDX) derived nitrogen measured in three simulated coastal habitats . *Envir. Toxicology and Chemistry*, Submitted

Abstract:

Hexahydro-1,3,5-trinitro-1,3,5-triazine (RDX) is one of the most commonly used munitions of the past century and remains an environmental contaminant of concern though little is known about its fate in coastal systems. ^{15}N nitro-labeled RDX was added to three marine mesocosm types, each simulating a different coastal environment. Uptake, retention, and transformation of the RDX and nitrogen derived from RDX was quantified in 13 different species. The amount of ^{15}N tracer in the organisms attributable to RDX and its primary derivatives MNX, DNX, and TNX was small (< 0.1 μg ^{15}N g dw^{-1}). It varied significantly between species in the same habitat, and was similar among the same species across different habitats. The tissue ^{15}N tracer concentrations associated with intact RDX were 1-2 orders of magnitude lower for all 13 species than the total ^{15}N measured in the biotic tissue indicating that the majority of the RDX uptake was biotransformed internally. There was limited correlation between aqueous RDX concentrations and RDX tissue concentrations suggesting that post uptake transformations are as important as aqueous RDX concentrations in setting tissue RDX levels. Extrapolating mesocosm results to ecosystem scales revealed that RDX retention in biota and macrobiotic processing scaled linearly with expected species biomass with "hot spots" of high retention and/or transformation in marsh macrophyte roots, and select filter feeding and oligochaete species.

1. Introduction

The explosive hexahydro-1,3,5-trinitro-1,3,5-triazine (RDX) is one of the most commonly used munitions of the past century (Darrach et al., 1998) and has caused the contamination of aquatic, terrestrial (Pennington & Brannon, 2002), and marine environments (Darrach et al., 1998). RDX can enter the marine environment through unexploded ordnance (UXOs), munitions disposed of at sea, nearshore storage, and ongoing training exercises (Harrison & Vane, 2010; Hovatter et al., 1997; Jenkins et al., 2006; Talmage et al., 1999). Most studies of RDX have mainly focused on biodegradation pathways (aerobic and anaerobic; Pennington & Brannon, 2002) and toxicological effects on aquatic (Bentley et al., 1977; Mukhi et al., 2005; Mukhi & Patiño, 2008; Steevens et al., 2002) and terrestrial (Simini et al., 2003) biota. Potentially high costs to remediate RDX contamination *in situ* serves as good motivation to research the fate of this and other of munitions in the marine settings (USA GAO 2003).

Most studies of biological effects of RDX have been done in short duration benchtop experiments using single species (Lotufo et al., 2010; Rosen & Lotufo, 2007). These studies resulted in very low uptake, retention, and toxicity of the parent compound, however these studies were of relatively short duration and isolated the species from their natural environments. This limitation can be overcome by using larger marine mesocosms that more closely simulate the complexities of marine systems. In this study, the uptake and retention of RDX is subject to competing uptake and mineralization pathways (Crocker et al., 2006), trophic interaction (Lotufo et al., 2009), and intra-organism turnover (Ballentine et al., 2016); all of which affect RDX water column concentrations, physical and chemical partitioning, and uptake. Closely mimicking the natural environments over an extended period of time permits a more realistic picture of RDX and breakdown product distribution among ecosystem compartments. The mesocosms types

used in this study represent three common shallow marine ecotypes: bare sand, silty vegetated sediment (eel grass), and an intertidal salt marsh. Each consists of different sediment types, levels of organic matter, and redox environments allowing for the possibility of different environmental interactions with RDX that could affect the uptake and retention of RDX within the biota.

The current literature suggests that aqueous concentration (Ballentine et al., 2015), partition coefficients (Belden et al., 2005), and lifestyles (e.g. benthic, pelagic, filter feeder) of the biota all play a role in biotic uptake, processing, and storage of munitions. For RDX, aqueous concentration is a good predictor of tissue concentrations, with ranges of bioconcentration factors (BCFs) for RDX indicating uptake is primarily through rapid physical partitioning (Ballentine et al., 2016; Lotufo et al., 2009), rather than bioaccumulation. Trophic level and/or organism lifestyle may account for interspecies differences. Large differences in uptake and bioconcentration have been found between autotrophs and heterotrophs derived from significant differential breakdown and storage of RDX (and its breakdown products) in autotrophs, particularly vascular macrophytes (Vila et al., 2007). Different marine settings are likely to impact aqueous concentrations, which are the net result of load and RDX mineralization, the species composition/interactions, and in turn set availability of RDX for further uptake.

The use of RDX labelled with the stable nitrogen isotope (^{15}N) allows for the tracking of nitrogen derived from RDX and thus its uptake and processing. Stable isotopes have been used previously for toxicological (Rosen & Lotufo, 2005), bioconcentration (Houston & Lotufo, 2005), and biodegradation studies (Annamaria et al., 2010; Smith et al., 2015; Van Aken et al., 2004). The objective of this study was to compare the biotic uptake and retention of RDX

derived nitrogen using ^{15}N nitro-labeled RDX in 13 different marine species of varying trophic levels and lifestyles. Patterns of biotic processing were compared across three common marine ecosystems in simulated mesocosms.

2. Material and methods

2.1 Experimental Design

Three experiments using 1000L mesocosms were conducted. Each experiment simulated one of three coastal ecosystems; sand, vegetated silt, and intertidal salt marsh. All experiments were conducted as steady state constant source RDX additions. These habitat types were selected to span the range of organic matter (OM) and redox conditions; two factors known to influence RDX processing. Two different designs were used in the construction of the mesocosms (Fig. 1). A single tank design was used for the sand and silt experiments. A two tank design was used for marsh experiment. For the sand and silt experiments, sediment (20 cm deep) was added first from coastal Long Island Sound (LIS). For the marsh experiment, *S. alterniflora* and associated sediment were added as intact sods. Water from LIS was then pumped through all mesocosms for an equilibrium period of 7 days. Following the equilibration period, macrobiota common to each habitat type (Table 4.1) were added and the system was switched to recirculation mode for a 24 hour acclimation period after which the addition of the ^{15}N RDX tracer commenced.

2.11 Mesocosm setup 1 – Sand and Silt Experiments

For the single tank design (Fig. 4.1A) that was used for two of the three mesocosms (sand and silt), raw seawater from LIS was pumped (Fig. 4.1A) through a coarse mesh filter to remove large particulates. Seawater was added to the experimental tank from this reservoir (Fig. 4.1A) using a peristaltic pump at an average rate of 180 mL min^{-1}. The turnover time of the seawater was 2.5 days in the experiment which was kept well mixed and aerated using 3 submersible

pumps. ^{15}N nitro labeled-RDX (^{15}N-RDX) was added to the experimental tank in a single 20.4 mL addition of methanol for an initial target tank RDX concentration of 1.0 mg L^{-1}, and then metered in throughout the time series experiment with the use of a peristaltic pump at a rate of 0.07 mL min^{-1} and 0.08 mL min^{-1} for sand and silt respectively. This analyte pump rate was set to maintain a steady state concentration between 0.5 and 1.0 mg L^{-1} based on seawater turnover time and previously measured rates of RDX removal (Smith et al., 2013).

2.12 Mesocosm setup 2 – Marsh Experiment

For the dual tank design (Fig. 4.1B) used in the intertidal marsh mesocosm (marsh) raw LIS seawater was pumped through the coarse filter into a tidal mixing tank (Fig. 4.1B) at a rate of 312 mL min^{-1} to produce a seawater turnover rate of 2.5 days. Tidal oscillations in water level was achieved using a combination of float switches and timers to move water between the tidal mixing and experimental tanks inducing marsh wetting and drying periods. Water between the tidal mixing and experimental tanks was constantly exchanged to insure a homogenous water mass using 2 submersible pumps at a rate of 1900 mL min^{-1}. ^{15}N-RDX was initially added to the tidal mixing tank in a single addition of 39 mL of methanol to bring the concentration of the entire system to 1.0 mg L^{-1}. After the initial single addition, the ^{15}N-RDX was metered into the tidal mixing tank using a peristaltic pump at a rate of 0.07 mL min^{-1} to reach an estimated ^{15}N-RDX aqueous concentration of between 0.5 and 1.0 mg L^{-1}. Time series samples were collected over 15 days for aqueous RDX, RDX biota concentrations, and total ^{15}N tracer.

During the experiments, biota were allowed free range of the mesocosm and could interact with the exception of *Carcinus maenas* and *Alitta virens*. Both *C. maenas* and *A. virens* were in cages with removable lids for sampling. Additionally, the *A. virens* cage did not have a bottom allowing for *A. virens* interaction with the sediments. Each mesocosm was placed in a

water bath and the experimental seawater temperature was kept between 19 and 21°C. A canopy was placed over the top of the experimental tanks to limit the exposure of the experimental tank to sunlight.

2.2 Aqueous sampling

Time series water column aqueous RDX samples (2 mL) were taken from the experimental tanks (Fig. 4.1A and B) and the tidal mixing tank (Fig. 4.1B). Water samples were measured for RDX, MNX, DNX, and TNX used a modified "salting out" technique adapted from Miyares and Jenkins (1990) and used by Ballentine et al. (2015). Briefly, the 2 mL of sample were added to 1.3 g of NaCl and shaken. American Chemical Society (ACS) – grade acetonitrile, 1.5 mL, was then added and shaken for 5 min. The separated acetonitrile was removed and the process was repeated two more times using 1 mL of ACS-grade acetonitrile. The final extract was then analyzed and run using a gas chromatograph (GC) equipped with an electron-capture detector (ECD) as detailed in Ballentine et al. (2015).

2.3 Biota sampling

Time series biota samples (Table 4.1) were removed from the experimental tank from both mesocosm setups then immediately rinsed for 5 min with clean filtered seawater to remove dissolved and weakly sorbed munitions from the tissue surfaces. The shells of *L. littorea, C. virginica, M. edulis, G. demissa,* and *M. mercenaria* were opened before being rinsed. *Z. marina* and *S. alterniflora* samples were separated into shoot and rhizome (*Z. marina*) or roots (S. alterniflora) after the rinse and were handled as separate samples. *S. alterniflora* and *G. demissa* were taken at both low and high tide. Once rinsed, tissues were removed, freeze-dried, and weighed. Freeze-dried samples were homogenized using a mortar and pestle and then separated into a fraction for measuring munitions concentrations in the tissue and a fraction for bulk ^{15}N

isotope. Samples analyzed for munitions concentrations were extracted using methods modified from Conder et al. (2004). ACS-grade acetonitrile, 10 mL, was added to the samples and then sonicated for 1 hour. The homogenate was then centrifuged for 10 min at 10,000 rpm. The supernatant was removed, filtered through 0.22-µm PTFE syringe-tip filter, and 0.01 mg L^{-1} of 3,4-dinitrobenzene (3,4-DNB) as a recovery standard. GC/ECD analysis was conducted with the same method as the water samples (Ballentine et al., 2015). Quantification was based on an external calibration curve of standard munitions RDX, MNX, DNX, and TNX (AccuStandard, New Haven, Connecticut, USA). The recoveries of munitions from tissue samples (n=3) ranged between 70 and 98% with a mean of 90% and standard deviation of 7% with a reporting limit for all compounds of 0.7 ng mL^{-1}. To account for various sizes of organisms extractable munitions concentrations were normalized to organism dry weight (g dw). In addition to munitions concentrations, biota were analyzed for total ^{15}N tracer.

2.4 ^{15}N analysis

Total ^{15}N in all solid samples were analyzed by elemental analyzer – isotope ratio mass spectrometry (EA/IRMS: Delta V, Thermofisher). Samples were freeze-dried and weighed into tin capsules. Sufficient sample mass was used to achieve 40-80 µg N for isotope analysis. Isotope values were normalized with a 2-endpoint correction using United States Geological Survey reference materials L-glutamic acid (USGS40 and USGS41) accompanying each analytical batch and also served as check standards for drift correction. Analytical precision on ^{15}N measurements was 0.3 per mil which is equivalent to approximately $1/9000^{th}$ of one percent excess ^{15}N. The µg ^{15}N g dw^{-1} was calculated by combining the ^{15}N mole fraction excess that was given from the EA/IRMS with the N content for each sample.

3. Results

3.1 Aqueous munitions

The measured inputs and outflow of RDX in each experiment was used to calculate a predicted RDX aqueous concentration assuming no reactive losses. In all three experiments aqueous RDX (RDX_{aq}) concentrations decreased from starting concentrations and remained below concentrations predicted by conservative mixing (Fig. 4.2). The silt and marsh experiments reached RDX_{aq} steady state concentrations of 0.50 ± 0.07 mg L^{-1} on day 3 (Fig. 4.2B) and 0.22 ± 0.04 mg L^{-1} on day 2 (Fig. 4.2C) respectively. The sand experiment did not reach an aqueous RDX steady state concentration (Fig. 4.2A) due to pumping irregularities. MNX and TNX were detected in all three experiments at concentrations 2 to 3 orders of magnitude lower than that of RDX_{aq} concentrations. DNX was detected sporadically and only within the first 9 days of the experiment at 3 orders of magnitude lower than RDX_{aq} concentrations. The difference between the predicted and measured aqueous concentrations indicated an RDX loss of 25%, 44%, and 50% in the sand, silt, and marsh experiment respectively. The total ^{15}N recovered in the biota accounted for a small percentage of the mass of RDX ^{15}N lost from the aqueous phase and was equivalent to 1.4, 0.5, and 0.01 percent in the sand, silt, and marsh mesocosms respectively.

3.2 Tissue concentrations – munitions and ^{15}N

For comparison to bulk ^{15}N tracer measured in biota, munitions concentrations measured in tissue were converted into ^{15}N units (μg ^{15}N g dw^{-1}) using the molar ratio of labeled ^{15}N to the whole RDX molecule (3:1). This conversion yielded the amount of ^{15}N tracer in tissues that could be attributed to intact RDX ($^{15}N_R$). A similar conversion was made for MNX + TNX + DNX to yield a measure of the amount of ^{15}N in tissues that could be attributed to these intact species ($^{15}N_D$). Total ^{15}N concentrations measured in the biota tissue by EA-IRMS will be

heretofore be referred to as $^{15}N_T$. The time weighted mean for $^{15}N_R$ and $^{15}N_T$ was calculated and used for comparisons between species and experiments. Comparisons were done using a statistical t test assuming unequal variances and assessed at the $p \leq 0.05$ level. Finally, the fraction of $^{15}N_T$ attributed to $^{15}N_R$ ($f^{15}N$) in the biotic tissue was calculated for each species.

3.21 Autotrophs

The $^{15}N_R$ in the tissues were similar for each of the autotrophic species (*F. vesiculosus, U. lactuca, Z. marina,* and *S. alterniflora*) across the different mesocosms as the $^{15}N_R$ increased quickly and remained relatively constant throughout the experiment. With the exception of *S. alterniflora* root samples with mean $^{15}N_R$ of 0.53 ± 0.15 µg $^{15}N_R$ g dw^{-1}, all other autotrophic $^{15}N_R$ ranged from 0.03 to 0.13 µg $^{15}N_R$ g dw^{-1}. *S. alterniflora* root and shoot $^{15}N_R$ showed no difference between high and low tide. The root $^{15}N_R$ were as much as one order of magnitude greater and significantly different ($p < 0.01$) than the shoot $^{15}N_R$ (Fig. 4.3). All other comparison between autotrophs in the same mesocosm or across different mesocosms experiments did not show significant difference for $^{15}N_R$. $^{15}N_D$ was not detected for any autotrophic species. While autotrophic $^{15}N_R$ was low and fairly consistent across species and mesocosms, $^{15}N_T$ was not.

Mean autotrophic $^{15}N_T$ was dissimilar between species and some habitats. *F. vesiculosus* was the only autotrophic species that was in more than one mesocosm experiment and the $^{15}N_T$ was 2 orders of magnitude greater in the sand than the silt and was significantly different ($p < 0.001$) between the two mesocosms (Fig. 4.3). The autotrophs (*F. vesiculosus* and *U. lactuca*) in the sand mesocosm had greater mean $^{15}N_T$ than all other autotrophs in the silt and marsh mesocosm experiments by a factor of 10 (Fig. 4.3). The $^{15}N_T$ in *F. vesiculosus* was large and significantly different than *U. lactuca* (sand) and *Z. marina* shoot (silt; p < of 0.01). All other mean $^{15}N_T$ values among autotroph species were not significantly different. *U. lactuca* had the

largest mean $^{15}N_T$ of all species across all experiments. This ^{15}N, ultimately derived from RDX, was equivalent to 0.1% of total N in *U. lactuca* tissue.

The fraction of total ^{15}N attributable to RDX ($f^{15}N$) was smallest for the autotrophs in the sand experiment with values less than 2% (Fig. 4.3). *F. vesiculosus* $f^{15}N$ increased to 23% in the silt experiment 4 times higher than *Z. marina* $f^{15}N$ fractions. The highest $f^{15}N$ of all autotrophs was *S. alterniflora* root samples at 44%, indicating large amounts of uptake with little internal RDX processing relative to its storage (Fig. 4.3).

3.22 Epifauna

The mean $^{15}N_R$ for the epifauna species varied from 0.06 to 0.24 µg $^{15}N_R$ g dw^{-1} with one notable exception, *C. virginica* had a mean $^{15}N_R$ of 0.80 µg $^{15}N_R$ g dw^{-1} in the silt experiment. *M. edulis*, *L. littorea*, and *C. maenas* were used in all three mesocosm experiments. Both *M. edulis* and *L. littorea* have similar mean $^{15}N_R$ across the mesocosms types of 0.11 ± 0.03 and 0.18 ± 0.02 µg $^{15}N_R$ g dw^{-1} respectively (Fig. 4.4). *C. maenas* $^{15}N_R$ declined from sand to silt to marsh with mean $^{15}N_R$ values of 0.25 ± 0.05, 0.14 ± 0.05, and 0.04 ± 0.01 µg $^{15}N_R$ g dw^{-1} respectively. Interesting, only *M. edulis* and *L. littorea* had a significant difference when comparing between their mean $^{15}N_R$ in the silt mesocosm ($p < 0.001$) and *C. maenas* and *G. demissa* ($p < 0.05$) had a similar significant difference in the marsh mesocosm. While many of the epifaunal species showed similar $^{15}N_R$, the $^{15}N_T$ was more variable.

The $^{15}N_T$ differed among the species and within the same species between mesocosm experiments by over 1 order of magnitude (Fig. 4.4). *M. edulis* mean $^{15}N_T$ was significantly higher ($p < 0.05$) in the silt mesocosm (18 ± 4.6 µg $^{15}N_T$ g dw^{-1}) than in the sand (3.5 ± 0.9 µg $^{15}N_T$ g dw^{-1}) and marsh (3.3 ± 0.5 µg $^{15}N_T$ g dw^{-1}; Fig. 4). Although the *L. littorea* mean $^{15}N_T$ was higher in the sand mesocosm (5.4 ± 1.3 µg $^{15}N_T$ g dw^{-1}) than the silt and marsh mesocosms

there was no significant difference in the $^{15}N_T$ mean values (Fig. 4.4). *C. maenas* $^{15}N_T$ varied significantly ($p < 0.01$) between mesocosms with concentrations ranging from 0.3 ± 0.2 µg $^{15}N_T$ g dw^{-1} in the marsh to 1.5 ± 0.3 µg $^{15}N_T$ g dw^{-1} in the silt mesocosm. *C. maenas* (sand and marsh) mean $^{15}N_T$ was higher than other epifaunal species ($p < 0.05$). Within the silt mesocosm, *M. edulis* mean $^{15}N_T$ was higher than both *L. littorea* ($p < 0.01$) and *C. maenas* ($p < 0.01$).

The epifaunal $f^{15}N$ values were similar in magnitude to autotrophs and ranged from 3% to 12% with only a few exceptions (Fig. 4.4). *C. maenas* (sand) had the highest $f^{15}N$ of 31% and *M. edulis* (silt) had the lowest $f^{15}N$ of 0.3%.

3.23 Infauna

Both infaunal species (*M. mercenaria* and *A. virens*) were used in more than one mesocosm type (sand and silt mesocosm) and $^{15}N_R$ varied between 0.02 and 0.63 µg $^{15}N_R$ g dw^{-1}. *M. mercenaria* and *A. virens* mean $^{15}N_R$ between the sand and silt mesocosm were similar (Fig. 4.5) and were not significantly different. When the mean $^{15}N_R$ values for both infaunal species were compared within the same mesocosm, the silt experiment infaunal species $^{15}N_R$ values varied significantly ($p < 0.01$) even though *A. virens* had a high concentration in both the sand (0.23 ± 0.17 µg $^{15}N_R$ g dw^{-1}) and the silt (0.63 ± 0.50 µg $^{15}N_R$ g dw^{-1}) mesocosms (Fig. 4.5).

Mean infaunal $^{15}N_T$ values for *M. mercenaria* and *A. virens* were 10 – 20 fold significantly higher for the mean $^{15}N_R$ in both the sand and silt mesocosms. The $^{15}N_T$ ranged from 1.4 to 6.0 µg $^{15}N_T$ g dw^{-1} and *A. virens* exceeded *M. mercenaria* ($p < 0.001$) by a factor of 3 in the sand, while *M. mercenaria* $^{15}N_T$ exceeded *A. virens* ($p < 0.001$) by a factor of 3.5 in the silt experiment.

The infaunal $f^{15}N$ values were all below 4% with the exception of *A. virens* (silt) that had among the highest $f^{15}N$ measured suggestive of high RDX uptake coupled with little post-uptake processing and retention of N-bearing transformation products. This value was similar to the autotroph *S. alterniflora* root (marsh) at 44% (Fig. 4.5).

3.24 Fish

Fish species $^{15}N_R$, $^{15}N_T$, and $f^{15}N$ were each roughly 2 times higher than both the epifauna and infaunal species in the sand and marsh mesocosms, while in the silt mesocosm the fish species had $^{15}N_R$ and $^{15}N_T$ values roughly 2 times less than the epifaunal and infaunal species. *F. heteroclitus* (pelagic) was used in all three experiments, while *P. americanus* (benthic) was used only in the sand and silt experiments. *F. heteroclitus* mean $^{15}N_R$ showed no significant difference between experiments with for the sand, silt, and marsh of ranging between 0.23 – 0.41 μg $^{15}N_R$ g dw^{-1} respectively (Fig. 4.5). Similarly, there was no significant difference in the $^{15}N_R$ of *P. americanus* between the sand and silt experiments. Between species, only the silt mesocosm had a significant difference between *F. heteroclitus* and *P. americanus* $^{15}N_R$ ($p < 0.01$) even though *F. heteroclitus* $^{15}N_R$ exceeded that of *P. americanus* in both mesocosm types (Fig. 4.5).

There was no significant difference between the silt and sand mean $^{15}N_T$ concentrations for *F. heteroclitus* but the *P. americanus* mean $^{15}N_T$ was higher in the sand (6.0 ± 0.24 μg $^{15}N_T$ g dw^{-1}) relative to the silt (0.38 ± 0.15 μg $^{15}N_T$ g dw^{-1} ; $p < 0.001$; Fig. 5). No differences in $^{15}N_T$ between the two species was measured regardless of mesocosm type.

The $f^{15}N$ in fishes were less than 6% in the sand and marsh mesocosms. But both species showed higher $f^{15}N$ values (17 – 20%) in the silt experiment (Fig. 4.5).

3.3 Tissue concentration correlation to aqueous RDX

The time series changes in aqueous RDX concentration in the mesocosms coupled with past evidence that tissue RDX rapidly responds to aqueous RDX concentration (Ballentine et al. 2016; Lotufo et al., 2009) permitted examination of the relationship between $^{15}N_R$, $^{15}N_T$, and the aqueous RDX concentration over the course of the experiments. Stepwise linear regressions between $^{15}N_R$ and RDX_{aq} and $^{15}N_T$ and RDX_{aq} were performed by species and by mesocosm type. For $^{15}N_R$ across all mesocosms the RDX_{aq} concentration explained more than 50% of the variance in $^{15}N_R$ for only 5 species correlations out of 26. All of those occurred in the sand mesocosm where RDX loss (presumably from mineralization) was smallest. Only two species (*P. americanus* and *F. vesiculosus*) had coefficients of determinations (r^2) above 0.65, while the majority of the species had r^2 of 0.40 and below (Table 4.2). When the mean of all coefficients of determination for each mesocosm were calculated, the $^{15}N_R$ variance attributable to RDX_{aq} (average r^2 of all species regressions) showed a decreasing trend from sand > silt > marsh.

For $^{15}N_T$ there were only 4 correlations where the RDX_{aq} explained more than 50% of the variance in $^{15}N_T$ over time (Table 4.2). These occurred in the sand and silt mesocosms with none in the marsh mesocosm. The low species-specific r^2 were most often below 0.3 (Table 4.2). Unlike the cross mesocosm regressions for $^{15}N_R$, the average $^{15}N_T$ r^2 did not show any significant patterns between mesocosms (Table 4.2).

4. Discussion

Results from the ^{15}N RDX multi mesocosm experiments support three major findings: (1) the habitat type controlled RDX_{aq}, but RDX_{aq} only partially explained variance found in biota concentrations particularly in more OM rich environments; (2) $^{15}N_R$ concentrations in biota was always less than $^{15}N_T$ concentrations indicating much more internal processing of RDX post-

uptake rather than retention of intact RDX; (3) the balance between retention of intact RDX and processing/throughput of RDX by macrobiota at the ecosystem scale is generally a function of ecosystem productivity (biomass), but some species represent hotspots of RDX uptake/processing that is disproportionately large relative to their species-specific biomass.

4.1 Mesocosm control of available RDX

Yields of RDX loss (predicted RDX_{aq} – measured RDX_{aq}; Fig. 4.2) in the three mesocosms was consistent with recent studies that found that aqueous RDX removal from seawater is in large part a function of sediment type (Ariyarathna et al., 2016; Smith et al., 2013). The differential loss of RDX and associated ^{15}N tracer relative to conservative mixing was the lowest in the sand mesocosm and highest in the marsh. Expressed as a percent of RDX loading 25%, 44%, and 50% was lost in sand, silt, and marsh respectively (Fig. 4.2).

This pattern of loss occurred likely as the result of higher RDX mineralization in the presence of higher concentration of sedimentary OM in the silt and marsh mesocosms (Sheremata et al., 2001). Further the presence of sharp redox gradients typical of vegetated sediments subtidal *Z. marina* and intertidal *S. alterniflora*, provides a suitable environment for aerobic and anaerobic mineralization pathways for RDX in close proximity. Unlike many past studies of RDX processing (Belden et al., 2005; Rosen & Lotufo, 2005), these mesocosm studies included varied biota as a potential sink for the ^{15}N-RDX. But the $^{15}N_T$ macrobiota values, when scaled to the total biomass in each of the mesocosms were not the cause of the differential RDX losses in the mesocosms. Macrobiota accounted for only small percentages of the observed total RDX ^{15}N loss from the aqueous phase (Sand 1.4%, Silt 0.5%, and Intertidal marsh 0.01%).

Variations in $^{15}N_R$ and $^{15}N_T$ among the three mesocosms was likely a function of RDX mineralization rates, which regulated the amount of RDX_{aq} available for biota to uptake. Yet

RDX_{aq} was not the sole determinant of either $^{15}N_R$ or $^{15}N_T$. The use of habitat appropriate fauna in each mesocosm type prevents a full crosswise comparison, but for the species common to all mesocosms and some pairwise comparisons indicate that correlations for the fish, non-filter feeding epifauna, and infauna vary widely across mesocosm type suggesting a significant environmental effect on both $^{15}N_R$ and $^{15}N_T$ aside from just RDX_{aq}. If $^{15}N_R$ was controlled solely by rapid partitioning of RDX_{aq} to tissues, and $^{15}N_T$ was controlled solely by $^{15}N_R$, then both $^{15}N_R$ and $^{15}N_T$ should, as BCF would predict, be highly correlated to RDX_{aq}. It was not. Based on controlled BCFs experiments (Ballentine et al. 2015), we would expect RDX_{aq} to be a better predictor of the variance in $^{15}N_R$ in the sand vs silt vs marsh, and we observed this in the mesocosms as evidenced by the distribution of the average coefficients of determination for linear regressions of $^{15}N_R$ vs. RDX_{aq} across mesocosm type (Table 4.2). Competing reactions for RDX within each system (e.g. mineralization) would be expected to increase from sand to silt to marsh, and this expectation is evidenced by the higher RDX_{aq} losses measured along this gradient. The mineralization of significant quantities of RDX could account for why RDX_{aq} is not a good predictor of $^{15}N_R$ or $^{15}N_T$ particularly in the high OM silt and marsh environments. Alternatively, higher amounts of intra-organism processing (Lotufo et al., 2009), lowering $^{15}N_R$, may be more efficient in the higher productivity silt and marsh mesocosms. If this is the mechanism behind the disconnect between RDX_{aq} and $^{15}N_R$ then such processing must be followed by elimination otherwise $^{15}N_T$ would be inversely related to $^{15}N_R$ across habitat types, which it is not. For $^{15}N_T$, there was no clear relationship to the RDX_{aq} within or across habitats. The role of intraorganism processing of RDX (affecting $^{15}N_R$) and the ultimate elimination of transformation products (affecting $^{15}N_T$) may be central to setting both $^{15}N_R$ and $^{15}N_T$. RDX biotransformation and breakdown pathways studies in microbiota have been shown to be

complex and to vary (Crocker et al., 2006), yet RDX transformation pathways in eukaryotes and specifically in macrobiota are presently ill-defined. If this explanation is correct, the data in Table 4.2 suggest that these removal mechanisms are of equal to or similar importance as uptake constants (e.g. BCFs) *in situ*.

4.2 RDX uptake, processing, and retention of tracer in biota

All $^{15}N_R$ values in heterotrophs, regardless of species type, lifestyle, trophic position, or experiment were small relative to $^{15}N_T$ (Fig. 4.3, 4.4, and 4.5). These mesocosm-scale observations mimic similar findings from lab experiments that were summarized by Lotufo et al. (2009). Time averaged $^{15}N_R$ for nearly all heterotrophic species regardless of experiments was close to 0.1 µg $^{15}N_R$ g dw^{-1}. Low RDX tissue concentrations are consistent with other reports for this relatively polar compound (Belden et al., 2005; Lotufo et al., 2009). Average heterotroph $^{15}N_T$ was generally close to 5.0 µg $^{15}N_T$ g dw^{-1} and the resulting $f^{15}N$ for heterotrophs were also low (< 20%) for all but two species (*C. maenas* and *A. virens*). The high $^{15}N_T$ indicated that a substantial amount of the RDX, internally processed, was retained in some unknown form. A striking difference from this study and others using RDX (Sunahara et al., 2009) is the lack of $^{15}N_D$ measured in any species throughout the time series other than a few small concentrations at random time points. This result suggested that biotransformation pathways did not lead to MNX, TNX, and DNX accumulation in any significant concentrations that could have had toxicological impacts on the biota.

Because heterotrophs are unable to take up $DI^{15}N$ released from ^{15}N-RDX mineralization (Smith et al., 2015), a precondition for high $^{15}N_T$ is high rates of encounter with ^{15}N-RDX. The amount of RDX encountered could be inferred from RDX_{aq} but not entirely depending on the mechanism of exposure. RDX_{aq} was only a poor to marginal proxy for $^{15}N_T$ for most species

(Table 4.2). The amount of exposure to RDX is likely as/more important than the RDX_{aq} concentration. *M. edulis* and *C. virginica* (among the highest $^{15}N_T$ for heterotrophs) both cycle through large amounts of seawater in the process of filter feeding allowing for a greater exposure of RDX_{aq} to tissues. Moreover, *M. edulis* had the larger mean $^{15}N_T$ in the silt experiment that was mostly due enhanced exposure to the resuspension of silt containing RDX, and/or enhanced filter feeding on elevated particulate organic matter (POM) in that experiment. Similarly higher $^{15}N_T$ in *L. littorea*, likely resulted from grazing of tank biofilms that were sites of RDX processing (Fournier et al., 2004; Thompson et al., 2005). Every species had a much larger mean $^{15}N_T$ than $^{15}N_R$ and a $f^{15}N$ typically < 20% indicating the RDX was being taken up and the biotransformed internally instead being retained unaltered. The total heterotrophic $^{15}N_T$ is small relative to the RDX loss in the mesocosm. The processing of the RDX is possibly still important for each individual organism, helping to set tissue RDX concentrations and the possibility that other biotransformation products containing tracer (inert or potentially toxic) may accumulate.

Autotrophs contrast with the heterotrophs in two important respects: some species are known to take up and store RDX intact (Thompson et al., 1999), and because they can assimilate DIN directly there is the potential for acquiring ^{15}N tracer that had originally been derived from RDX but was liberated as $DI^{15}N$ during mineralization. This ^{15}N uptake would increase $^{15}N_T$ values. An example of the direct uptake and storage of RDX by an autotroph was the large $f^{15}N$ (40%) by *S. alterniflora* root, yet the RDX was processed during translocation to the shoots as evident by a factor of 3 drop in the $f^{15}N$ in the *S. alterniflora* shoots. The high mean $f^{15}N$ for *S. alterniflora* root could also be due to a greater uptake of RDX as the sediments were recharged with a pulse of new RDX at each high tide. But unlike the high amount of RDX storage found in shoots/leaves of poplar trees (Thompson et al., 1999), RDX appears to be processed during

translocation from roots to shoots in *S. alterniflora*. In contrast, *Z. marina* had little intact RDX storage, either as a result of low uptake or fast processing, in roots and shoots which both showed low $f^{15}N$ values.

Some autotrophs, particularly macroalgae, have the ability to uptake DIN from the water column in excess of what is needed to maintain their N:P cellular ratio (Sterner & Hessen, 1994; Stelzer & Lamberti, 2001). This 'luxury uptake' of DIN may have included ^{15}N-DIN originating from RDX_{aq} via mineralization (Smith et al., 2015). The autotrophs, including the smallest $f^{15}N$ reported in *U. lactuca*, had smaller $f^{15}N$ values than the heterotrophs (Fig. 4.3). Interestingly, autotrophic $^{15}N_T$ concentrations decreased with mesocosm transition from sand to silt to tidal marsh as overall natural DIN availability increased, but $^{15}N_T$ results should be interpreted cautiously for macroalgae in settings where mineralization might be high and luxury uptake possible.

Generally, the autotrophic species compared closely to the heterotrophs in that the $^{15}N_R$ and $^{15}N_T$ values were relatively similar (Fig. 4.3, 4.4, and 4.5). Similar to the heterotrophic species no matter the experiment, $^{15}N_R$ values in autotrophs were much less than $^{15}N_T$ indicating the all species processed more RDX relative to RDX retention in tissue.

4.3 Scaling to the Ecosystems level

The mesocosms represent an intermediate step to scale from laboratory studies to intact ecosystems. Because $^{15}N_R$ was similar among species, the total amount of RDX within an ecosystem should be dependent on solely the amount of biomass (e.g. total RDX m^{-2} = $^{15}N_R$ x g biota m^{-2}), and the amount of RDX in any given species population will be a function of total population biomass. Similarities in $^{15}N_R$ between species despite disparate growth rates, lifestyles, and trophic position suggest that these factors are less important than total ecosystem

biomass for determining a collective steady state inventory of RDX in all biota. The mesocosm results coupled with typical biomass estimates of each species in coastal habitats show that higher productivity species (in terms of biomass) correspond to higher $^{15}N_R$ and $^{15}N_T$ m^{-2} (Fig. 4.6A and 4.6B) at the ecosystem level. The biomass effect on total RDX is generally linear across species and habitat type suggesting high productivity ecosystems (i.e. more biomass) will store more RDX in biota (Fig. 4.6, Tables 4.3 and 4.4). Because the largest standing stocks are typically autotrophs, these populations would be expected to harbor the most RDX mass within an ecosystem (Fig. 4.6, Table 4.3). While the mesocosm $^{15}N_T$ results show that the total RDX in biota is low relative to RDX load and RDX loss, it is important to examine how RDX and RDX transformations in biota would be distributed throughout the ecosystem. There are notable exceptions to the general linear effect of biomass on RDX storage and processing. *S. alterniflora* roots, the filter feeder *C. virginica*, and the infaunal polychaete *A. virens* all contain anomalously high ecosystem level RDX ($^{15}N_R$) retention relative to their typical population biomass. These hotspots for storage may reflect active uptake (*S. alterniflora*) and/or high aqueous or sediment throughput/exposure as a function of feeding (*C. virginica* and *A. virens*). The results for *S. alterniflora* are similar to those seen in phytoremediation studies (Best et al., 1997; Just & Schnoor, 2004) but the mesocosm results (low shoot $f^{15}N$) show the RDX in *S. alterniflora* is processed during translocation to shoots so the root storage of RDX is transient and a first step to further transformation. Typically macrobiota has been viewed as an ecological risk receptor. The high $^{15}N_T$ and low $f^{15}N$ values suggest they play an active role in transformation, but this transformation is not uniform among species. At the ecosystem level, a similar analysis of the biomass scaling for RDX transformation (derived from $^{15}N_T$), revealed the filter feeder *M. edulis* and the macroalgae *F. vesiculosus* and *U. lactuca* as ecosystem compartments that

disproportionately take up RDX, transform it internally, and retain the N-bearing transformation products (Table 4.4). *F. vesiculosus* and *U. lactuca* may also be active hotspots for processing although this conclusion should be considered cautiously due to a potential for luxury uptake effects on $^{15}N_T$.

The extrapolation of the mesocosm experiment results provided three metrics to gauge the role of different ecosystem compartments with respect to RDX. High $^{15}N_R$, low $^{15}N_T$, and high $f^{15}N$ identify primarily reservoirs for unaltered RDX. These compartments include *S. alterniflora* root, *A. virens*, and C. maenas (Fig. 4.3, 4.4, and 4.5; Table 4.3 and 4.4). Low $^{15}N_R$, high $^{15}N_T$, and low $f^{15}N$ consist of zones where internal transformations supersede storage and there is a disproportionate amount of macrobiotic processing of RDX. These compartments include *F. vesiculosus*, *U. lactuca*, and *S. alterniflora* shoots. These metrics may also apply to macroalgae that have utilized N liberated through mineralization of RDX. Finally, compartments with high $^{15}N_R$, high $^{15}N_T$, and low $f^{15}N$ would be the most active transformers in the ecosystem; representing high uptake and extensive processing. The translocation of RDX from *S. alterniflora* roots to *S. alterniflora* shoots reflects this transition from high $^{15}N_R$, low $^{15}N_T$, high $f^{15}N$ to low $^{15}N_R$, high $^{15}N_T$, low $f^{15}N$ compartment.

5. Conclusions

The amount of tissue bound ^{15}N tracer attributed to RDX constituted a small amount of total RDX loss in all marine mesocosms. Tissue ^{15}N levels varied by an average factor of 8 between species in the same habitat, and were similar among the same species across different habitats. For all biota, the tissue ^{15}N tracer concentrations associated with intact RDX were at least 1 order of magnitude lower than the total ^{15}N measured in biotic tissue indicating that the majority of the RDX uptake was biotransformed internally. Aqueous RDX concentration was only a modest

predictor of tissue RDX and total ^{15}N tracer derived from RDX. This observation coupled with the low fraction of total ^{15}N attributable to RDX suggests that post uptake biotransformation is equally important as gross uptake for setting tissue concentrations *in situ*. While the use of ^{15}N as a tracer for RDX showed a large amount of biotransformation in comparison to intact storage, the exact products formed are not known and warrants further study. Ecosystem level extrapolation of mesocosm results yielded a linear relationship between total biomass and RDX per area across species with hot spots for retention and/or transformation existing in marsh macrophytes roots, and select filter feeding and oligochaete species.

6. Acknowledgments

We would like to acknowledge Strategic Environmental Research and Development Program No. ER-2122 for their support and funding. We also thank David Cady, Charlie Woods, Veronica Rollinson, and Amanda Dostie for laboratory support.

References

Ale, M. T., Mikkelsen, J. D., & Meyer, A. S. (2011). Differential growth response of *Ulva lactuca* to ammonium and nitrate assimilation. *Journal of Applied Phycology, 23*(3), 345-351.

Annamaria, H., Manno, D., Strand, S. E., Bruce, N. C., & Hawari, J. (2010). Biodegradation of RDX and MNX with *Rhodococcus* sp. strain DN22: New insights into the degradation pathway. *Environmental Science & Technology, 44*(24), 9330-9336.

Ariyarathna, T., Vlahos, P., Tobias, C., & Smith, R. (2016). Sorption kinetics of TNT and RDX in anaerobic freshwater and marine sediments: Batch studies. *Environmental Toxicology and Chemistry, 35*(1), 47-55.

Ballentine, M., Ariyarathna, T., Smith, R. W., Cooper, C., Vlahos, P., Fallis, S., Groshens, T., Tobias, C. (2016). Uptake and fate of hexahydro-1, 3, 5-trinitro-1, 3, 5-triazine (RDX) in coastal marine biota determined using a stable isotopic tracer, 15 N–[RDX]. *Chemosphere, 153*, 28-38.

Ballentine, M., Tobias, C., Vlahos, P., Smith, R., & Cooper, C. (2015). Bioconcentration of TNT and RDX in coastal marine biota. *Archives of Environmental Contamination and Toxicology, 68*(4), 718-728.

Belden, J. B., Lotufo, G. R., & Lydy, M. J. (2005). Accumulation of hexahydro-1, 3, 5-trinitro-1, 3, 5-triazine in channel catfish (*Ictalurus punctatus*) and aquatic oligochaetes (*Lumbriculus variegatus*). *Environmental Toxicology and Chemistry, 24*(8), 1962-1967.

Bentley, R., Dean, J., Ells, S., Hollister, T., & LeBlanc, G. (1977). *Laboratory Evaluation of the Toxicity of Cyclotrimethylene Trinitramine (RDX) to Aquatic Organisms,*

Best, E. P., Zappi, M. E., Fredrickson, H. L., Sprecher, S. L., Larson, S. L., & Ochman, M. (1997). Screening of aquatic and wetland plant species for phytoremediation of explosives-contaminated groundwater from the Iowa army ammunition plant. *Annals of the New York Academy of Sciences, 829*(1), 179-194.

Crocker, F. H., Indest, K. J., & Fredrickson, H. L. (2006). Biodegradation of the cyclic nitramine explosives RDX, HMX, and CL-20. *Applied Microbiology and Biotechnology, 73*(2), 274-290.

Darrach, M., Chutjian, A., & Plett, G. (1998). Trace explosives signatures from World War II unexploded undersea ordnance. *Environmental Science & Technology, 32*(9), 1354-1358.

Fairchild, E. A., Sulikowski, J., Rennels, N., Howell, W. H., & Gurshin, C. W. (2008). Distribution of winter flounder, *Pseudopleuronectes americanus*, in the Hampton–Seabrook estuary, New Hampshire: Observations from a field study. *Estuaries and Coasts, 31*(6), 1158-1173.

Fell, P. E., Olmstead, N. C., Carlson, E., Jacob, W., Hitchcock, D., & Silber, G. (1982). Distribution and abundance of macroinvertebrates on certain Connecticut tidal marshes, with emphasis on dominant molluscs. *Estuaries, 5*(3), 234-239.

Fournier, D., Halasz, A., Spain, J., Spanggord, R. J., Bottaro, J. C., & Hawari, J. (2004). Biodegradation of the hexahydro-1,3,5-trinitro-1,3,5-triazine ring cleavage product 4-nitro-2,4-diazabutanal by *Phanerochaete chrysosporium*. *Applied and Environmental Microbiology, 70*(2), 1123-1128.

Harrison, I., & Vane, C. (2010). Attenuation of TNT in seawater microcosms. *Water Science & Technology, 61*(10)

Houston, J. G., & Lotufo, G. R. (2005). Dietary exposure of fathead minnows to the explosives TNT and RDX and to the pesticide DDT using contaminated invertebrates. *International Journal of Environmental Research and Public Health, 2*(2), 286-292.

Hovatter, P. S., Talmage, S. S., Opresko, D. M., & Ross, R. H. (1997). Ecotoxicity of mitroaromatics to aquatic and terrestrial species at army superfund sites. *ASTM Special Technical Publication,* (1317), 117-129.

Jenkins, T. F., Hewitt, A. D., Grant, C. L., Thiboutot, S., Ampleman, G., Walsh, M. E., Ranney, T. A., Ramsey, C. A., Palazzo, A. J., & Pennington, J. C. (2006). Identity and distribution of residues of energetic compounds at army live-fire training ranges. *Chemosphere, 63*(8), 1280-1290.

Just, C. L., & Schnoor, J. L. (2004). Phytophotolysis of hexahydro-1, 3, 5-trinitro-1, 3, 5-triazine (RDX) in leaves of reed canary grass. *Environmental Science & Technology, 38*(1), 290-295.

Lockfield, K. (2011). *Population-Level Responses of the Mummichog, Fundulus Heteroclitus, to Chronic Nutrient Enrichment in a New England Salt Marsh* (Doctoral dissertation, Faculty of the Louisiana State University and Agricultural and Mechanical College in partial fulfillment of the requirements for the degree of Master of Science in the Department of Biological Sciences by Konner Lockfield BS, Louisiana State University).

Lotufo, G. R., Gibson, A. B., & Leslie Yoo, J. (2010). Toxicity and bioconcentration evaluation of RDX and HMX using sheepshead minnows in water exposures. *Ecotoxicology and Environmental Safety, 73*(7), 1653-1657.

Lotufo, G.R., Lydy M.J., Rorrer G.L., Cruz-Uribe O., & Cheney D.P. (2009) Bioconcentration, bioaccumulation, and biotransformation of explosives and related compounds in aquatic organisms. In: Sunahara G.I., Lotufo G., Kuperman R.G., Hawari J. (eds) Ecotoxicology of explosives. CRC Press, Boca Raton, pp 123-155.

Lovely, C. M., O'Connor, N. J., & Judge, M. L. (2015). Abundance of non-native crabs in intertidal habitats of New England with natural and artificial structure. *PeerJ, 3,* e1246.

Mann, R., Southworth, M., Harding, J. M., & Wesson, J. A. (2009). Population studies of the native eastern oyster, Crassostrea virginica, (Gmelin, 1791) in the James river, Virginia, USA. *Journal of Shellfish Research, 28*(2), 193-220.

McGrorty, S., & Goss-Custard, J. (1991). Population dynamics of the mussel *Mytilus edulis*: Spatial variations in age-class densities of an intertidal estuarine population along environmental gradients. *Marine Ecology Progress Series, 73*, 191-202.

Mukhi, S., Pan, X., Cobb, G. P., & Patino, R. (2005). Toxicity of hexahydro-1, 3, 5-trinitro-1, 3, 5-triazine to larval zebrafish (*Danio rerio*). *Chemosphere, 61*(2), 178-185.

Mukhi, S., & Patiño, R. (2008). Effects of hexahydro-1, 3, 5-trinitro-1, 3, 5-triazine (RDX) in zebrafish: General and reproductive toxicity. *Chemosphere, 72*(5), 726-732.

Nikolaisen, L., Daugbjerg Jensen, P., Svane Bech, K., Dahl, J., Busk, J., Brødsgaard, T., Rasmussen, M., Bruhn, A., Bjerre, A., Nielsen, H., Albert, K., Ambus, P., Kadar, Z., Heiske, S., Sander, B., & Schmidt, E. (2011). *Energy Production from Marine Biomass (Ulva Lactuca),*

Pennington, J. C., & Brannon, J. M. (2002). Environmental fate of explosives. *Thermochimica Acta, 384*(1), 163-172.

Rosen, G., & Lotufo, G. R. (2005). Toxicity and fate of two munitions constituents in spiked sediment exposures with the marine amphipod *Eohaustorius estuarius*. *Environmental Toxicology and Chemistry, 24*(11), 2887-2897.

Rosen, G., & Lotufo, G. R. (2007). Bioaccumulation of explosive compounds in the marine mussel, *Mytilus galloprovincialis*. *Ecotoxicology and Environmental Safety, 68*(2), 237-245.

Santamaría-Gallegos, N. A., Sánchez-Lizaso, J. L., & Félix-Pico, E. F. (2000). Phenology and growth cycle of annual subtidal eelgrass in a subtropical locality. *Aquatic Botany, 66*(4), 329-339.

Schubauer, J., & Hopkinson, C. (1984). Above- and belowground emergent macrophyte production and turnover in a coastal marsh ecosystem, Georgia. *Limnology and Oceanography, 29*(5), 1052-1065.

Sheremata, T. W., Halasz, A., Paquet, L., Thiboutot, S., Ampleman, G., & Hawari, J. (2001). The fate of the cyclic nitramine explosive RDX in natural soil. *Environmental Science & Technology, 35*(6), 1037-1040.

Simini, M., Checkai, R. T., Kuperman, R. G., Phillips, C. T., Kolakowski, J. E., Kurnas, C. W., & Sunahara, G. I. (2003). Reproduction and survival of *Eisenia fetida* in a sandy loam soil amended with the nitro-heterocyclic explosives RDX and HMX: The 7th international symposium on earthworm ecology· Cardiff· Wales· 2002. *Pedobiologia, 47*(5), 657-662.

Smith, R. W., Tobias, C., Vlahos, P., Cooper, C., Ballentine, M., Ariyarathna, T., Fallis, S., Groshens, T. J. (2015). Mineralization of RDX-derived nitrogen to N_2 via denitrification in coastal marine sediments. *Environmental Science & Technology, 49*(4), 2180-2187.

Smith, R. W., Vlahos, P., Tobias, C., Ballentine, M., Ariyarathna, T., & Cooper, C. (2013). Removal rates of dissolved munitions compounds in seawater. *Chemosphere, 92*(8), 898-904.

Steevens, J. A., Duke, B. M., Lotufo, G. R., & Bridges, T. S. (2002). Toxicity of the explosives 2, 4, 6-trinitrotoluene, hexahydro-1, 3, 5-trinitro-1, 3, 5-triazine, and octahydro-1, 3, 5, 7-tetranitro-1, 3, 5, 7-tetrazocine in sediments to *Chironomus tentans* and *Hyalella azteca*: Low-dose hormesis and high-dose mortality. *Environmental Toxicology and Chemistry, 21*(7), 1475-1482.

Sunahara, G. I., Lotufo, G., Kuperman, R. G., & Hawari, J. (2009). *Ecotoxicology of explosives* CRC Press.

Talmage, S. S., Opresko, D. M., Maxwell, C. J., Welsh, C. J., Cretella, F. M., Reno, P. H., & Daniel, F. B. (1999). Nitroaromatic munition compounds: Environmental effects and screening values. *Reviews of environmental contamination and toxicology* (pp. 1-156) Springer.

Thompson, K. T., Crocker, F. H., & Fredrickson, H. L. (2005). Mineralization of the cyclic nitramine explosive hexahydro-1,3,5-trinitro-1,3,5-triazine by *Gordonia* and *Williamsia* spp. *Applied and Environmental Microbiology, 71*(12), 8265-8272. doi:71/12/8265 [pii]

Thompson, P.L., Ramer, L. A., & Schnoor, J. L. (1999). Hexahydro-1,3,5-triazine translocation in poplar trees. *Environmental Toxicology and Chemistry*, 18(2), 279-284.

Van Aken, B., Yoon, J. M., & Schnoor, J. L. (2004). Biodegradation of nitro-substituted explosives 2,4,6-trinitrotoluene, hexahydro-1,3,5-trinitro-1,3,5-triazine, and octahydro-1,3,5,7-tetranitro-1,3,5-tetrazocine by a pytosymbiotic *Methylobacterium* sp. associated with poplar tissues (*Populus deltoides* x *nigra* DN34). *Applied and Environmental Microbiology, 70*(1), 508-517.

Vila, M., Lorber-Pascal, S., & Laurent, F. (2007). Fate of RDX and TNT in agronomic plants. *Environmental Pollution, 148*(1), 148-154.

Wainright, S. (1990). Sediment-to-water fluxes of particulate material and microbes by resuspension and their contribution to the planktonic food web. *Marine Ecology Progress Series.Oldendorf, 62*(3), 271-281.

Walker, R. L., & Tenore, K. R. (1984). The distribution and production of the hard clam, *Mercenaria mercenaria*, in Wassaw Sound, Georgia. *Estuaries, 7*(1), 19-27.

Figure and Table Captions:

Table 4.1: Species List. Scientific and common names for each species by mesocosm.

Table 4.2: Species linear regression comparison: Coefficients of determination (r^2) for linear regressions of $^{15}N_R$ and $^{15}N_T$ tissue concentrations as a function of aqueous RDX. N/A denotes mesocosms where the species was not used and # indicates where species were used but a regression was not obtained do to missing species data for a mesocosm.

Table 4.3: Ecosystem level RDX ($^{15}N_R$): Average species biomass values are taken from the literature. The Intact RDX per area was calculated by multiplying the avg. biomass (gdw m^{-2}) by the RDX in tissue (µg RDX g dw^{-1}) derived from $^{15}N_R$ values for each species. Species codes apply to Figure 6A. na denotes when a species was not used in the mesocosm.

Table 4.4: Ecosystem level RDX ($^{15}N_T$): Average species biomass values are taken from the literature. The Total RDX per area was calculated by multiplying the avg. biomass (gdw m^{-2}) by the RDX in total tissue (µg RDX g dw^{-1}) derived from $^{15}N_T$ values for each species. Species code are a reference for Figure 6B. na denotes when a species was not used in the mesocosm.

Figure 4.1: Experimental Tank Setups A. Single experimental tank setup (sand and silt). Shaded areas are seawater. Arrows indicate direction of seawater flow. B. Two experimental tank setup (marsh). Double headed arrows indicate flow of seawater in both directions. The dotted line for the seawater indicates the high tide water level while the solid line indicates low tide level. The single arrowed dotted line indicates were ^{15}N-RDX was added. Lined rectangles indicate the location of sediments.

Figure 4.2: Aqueous RDX Concentrations. Solid lines are the measured aqueous RDX (RDX_{aq}) concentrations. The dashed line is the predicted aqueous RDX concentrations based on conservative mixing of RDX tracer with water volumes/inputs. Shaded area is the lost (missing) RDX. A. Sand mesocosm B. Silt mesocosm C. Tidal marsh mesocosm

Figure 4.3: Autotrophic ^{15}N concentrations. Temporal mean (se) ^{15}N tracer autotrophic tissue concentrations for each mesocosm (Sand, Silt, and Marsh). $^{15}N_R$ and $^{15}N_T$ tissue are represented by the gray and hatched bars. The solid black bar ($f^{15}N$) represents the percent of $^{15}N_T$ that can be attributed to $^{15}N_R$. N/A denotes organisms that were not used.

Figure 4.4: Epifaunal ^{15}N concentrations. Temporal mean (se) ^{15}N tracer epifaunal tissue concentrations for each mesocosm (Sand, Silt, and Marsh). $^{15}N_R$ and $^{15}N_T$ tissue are represented

by the gray and hatched bars. The solid black bar ($f^{15}N$) represents the percent of $^{15}N_T$ that can be attributed to $^{15}N_R$. *C. virginica* is missing $^{15}N_R$ data (#) due to high background in GC/ECD. N/A denotes organisms that were not used.

Figure 4.5: Infaunal and Fish ^{15}N concentrations. Temporal mean (se) ^{15}N tracer fish and infaunal tissue concentrations for each mesocosm (Sand, Silt, and Marsh). $^{15}N_R$ and $^{15}N_T$ tissue are represented by the gray and hatched bars. The solid black bar ($f^{15}N$) represents the percent of $^{15}N_T$ that can be attributed to $^{15}N_R$. *F. heteroclitus* $^{15}N_T$ tissue concentrations were not available for the sand mesocosm. N/A denotes organisms that were not used.

Figure 4.6: Storage of RDX on an Ecosystem Scale: Panel A. represents the intact RDX derived from the $^{15}N_R$ values for each species. The intact RDX storage values and the average biomasses are reported in Table 1S. While panel B. represents the processed and retained RDX derived from $^{15}N_T$ values for each species. The values for panel B are reported in Table 2S. The data points are represented by two digit letter code and a dash followed by a number denoting mesocosm type that is color coded (Sand-1 'blue', Silt-2 'red', and marsh-3 'green'). Values for *F. vesiculosus* (FV-1) and *U. lactuca* (UL-1) for the sand mesocosm were not plotted due to suspected high amounts of luxury uptake of $DI^{15}N$ produced from RDX mineralization (Table 2S).

Table 4.1: Species List

Scientific Name	**Common Name**	**Experiment**
Fucus vesiculosus	bladderwrack	sand, silt
Ulva lactuca	sea lettuce	sand
Zostera marina	marine eelgrass	silt
Spartina alterniflora	smooth cordgrass	marsh
Mytilus edulis	blue mussel	sand, silt, marsh
Geukensia demissa	ribbed mussel	marsh
Mercenaria mercenaria	hard clam	sand, silt
Crassostrea virginica	eastern oyster	sand, silt
Littorina littorea	common periwinkle	sand, silt, marsh
Alitta virens	sandworm	sand, silt
Fundulus heteroclitus	mummichog	sand, silt, marsh
Pseudopleuronectes americanus	winter flounder	sand, silt
Carcinus maenas	green crab	sand, silt, marsh

Table 4.2: Species linear regression comparison

Species	Sand		Silt		Marsh	
	$^{15}N_R$	$^{15}N_T$	$^{15}N_R$	$^{15}N_T$	$^{15}N_R$	$^{15}N_T$
F. vesiculosus	0.65	0.029	0.41	0.68	N/A	N/A
U. lactuca	0.52	0.11	N/A	N/A	N/A	N/A
Z. marina rhizome	N/A	N/A	0.48	0.24	N/A	N/A
Z. marina shoot	N/A	N/A	< 0.01	0.58	N/A	N/A
S. alterniflora root	N/A	N/A	N/A	N/A	0.43	0.18
S. alterniflora shoot	N/A	N/A	N/A	N/A	< 0.01	0.22
M. edulis	0.35	0.35	0.24	0.60	0.48	0.067
G. demissa	N/A	N/A	N/A	N/A	0.021	0.20
M. mercenaria	0.56	< 0.01	0.27	0.050	N/A	N/A
C. virginica	#	< 0.01	0.23	0.49	N/A	N/A
L. littorea	0.098	0.59	0.030	0.51	0.18	0.16
A. virens	0.60	0.32	0.16	0.21	N/A	N/A
F. heteroclitus	0.19	#	0.18	0.40	0.016	0.19
P. americanus	0.82	0.14	0.043	0.17	N/A	N/A
C. maenas	0.49	0.026	0.17	0.20	< 0.01	0.31
Average r^2 (±se)	0.47 (± 0.21)	0.19 (±0.19)	0.20 (± 0.14)	0.38 (± 0.20)	0.11 (± 0.17)	0.19 (± 0.07)

Table 4.3: Ecosystem level RDX ($^{15}N_R$)

Species	Species code	Avg. Biomass (gdw m^{-2})	Intact RDX per area (µg RDX m^{-2})			Reference
			Sand	Silt	Marsh	
F. vesiculosus	FV	750	335	123	na	Creed et al. 1996
U. lactuca	UL	206	64	na	na	Nikolaisen et al. 2011
M. edulis	ME	120	62	35	82	McGorty & Custard 1991
M. mercenaria	MM	33	12	3.9	na	Walker and Tenore 1984
C. virginica	CV	50	196	196	na	Mann et al., 2009
L. littorea	LL	50	43	63	60	Buschbaum 2000
A. virens	AV	65	74	202	na	Nielsen et al., 1995
F. heteroclitus	FH	0.34	0.61	0.68	0.38	Lockfield 2011
P. americanus	PA	0.49	0.19	0.19	na	Fairchild et al., 2008
C. maenas	CM	22.5	27	15	4.2	Lovely et al., 2015
POM	PM	5.2	16	2.8	67	Wainright 1990
Z. marina shoot	ZS	190	na	124	na	Santamaria-Gallegos et al. 2000
Z. marina rhizome	ZR	240	na	62	na	Santamaria-Gallegos et al. 2000
S. alterniflora root	SR	1000	na	na	2604	Schubauer and Hopkinson 1983
S. alterniflora shoot	SS	500	na	na	117	Schubauer and Hopkinson 1983
G. demissa	GD	228	na	na	132	Fell et al., 1982

Table 4.4: Ecosystem level RDX ($^{15}N_T$)

Species	Species code	Avg. Biomass (g dw m^{-2})	RDX equivalents processed and retained (µg RDX g m^{-2})			Reference
			Sand	Silt	Marsh	
F. vesiculosus	FV	750	20195	123	na	Creed et al. 1996
U. lactuca	UL	206	22777	na	na	Nikolaisen et al. 2011
M. edulis	ME	120	2060	10825	1938	McGorty & Custard 1991
M. mercenaria	MM	33	321	801	na	Walker and Tenore 1984
C. virginica	CV	50	703	2024	na	Mann et al., 2009
L. littorea	LL	50	1324	737	779	Buschbaum 2000
A. virens	AV	65	1912	478	na	Nielsen et al., 1995
F. heteroclitus	FH	0.34	3.9	3.9	6.5	Lockfield 2011
P. americanus	PA	0.49	15	0.94	na	Fairchild et al., 2008
C. maenas	CM	22.5	87	163	34	Lovely et al., 2015
POM	PM	5.2	58	17	35	Wainright 1990
Z. marina shoot	ZS	190	na	2432	na	Santamaria-Gallegos et al. 2000
Z. marina rhizome	ZR	240	na	1079	na	Santamaria-Gallegos et al. 2000
S. alterniflora root	SR	1000	na	na	4212	Schubauer and Hopkinson 1983
S. alterniflora shoot	SS	500	na	na	1858	Schubauer and Hopkinson 1983
G. demissa	GD	228	na	na	2445	Fell et al., 1982

Figure 4.1: Experimental Tank Setups

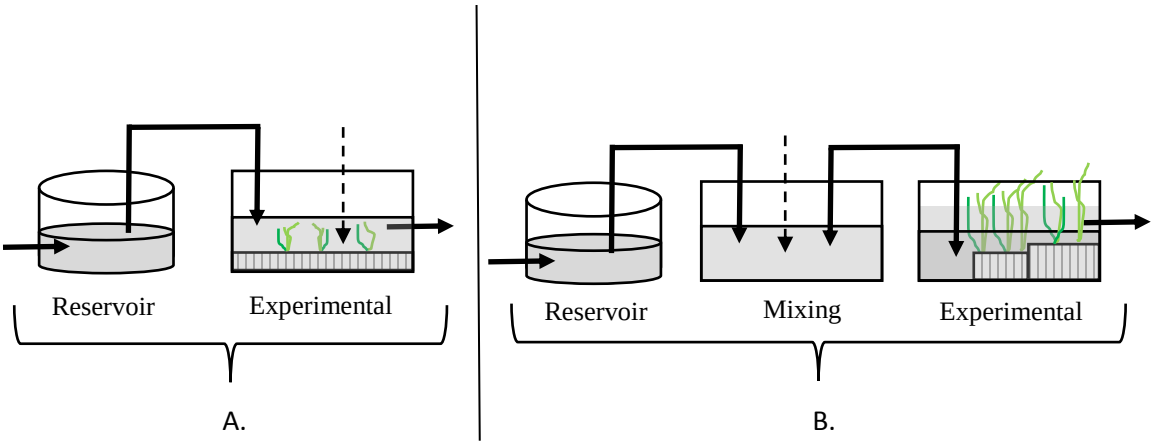

Figure 2: Aqueous RDX Concentrations

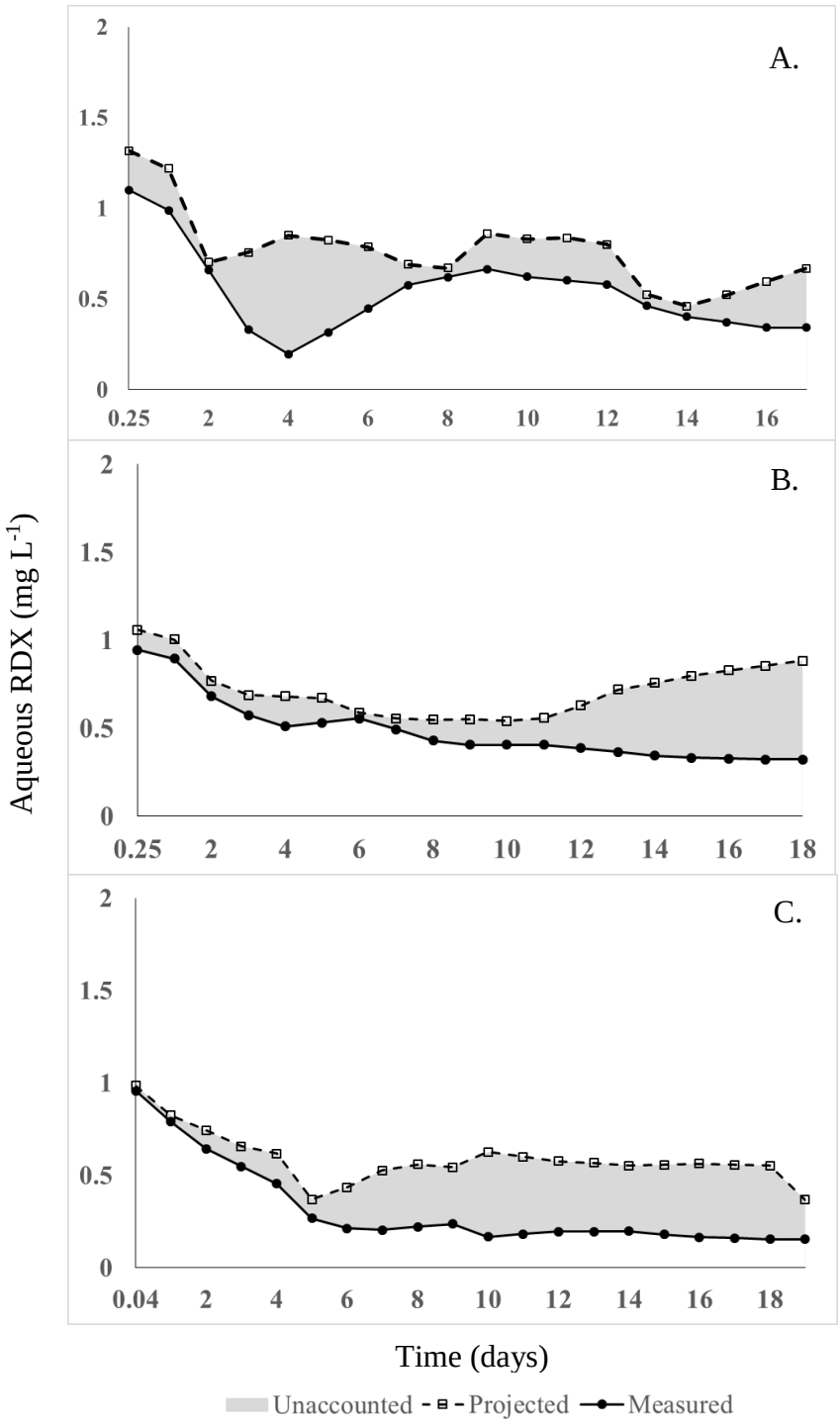

Figure 3: Autotrophic ^{15}N concentrations

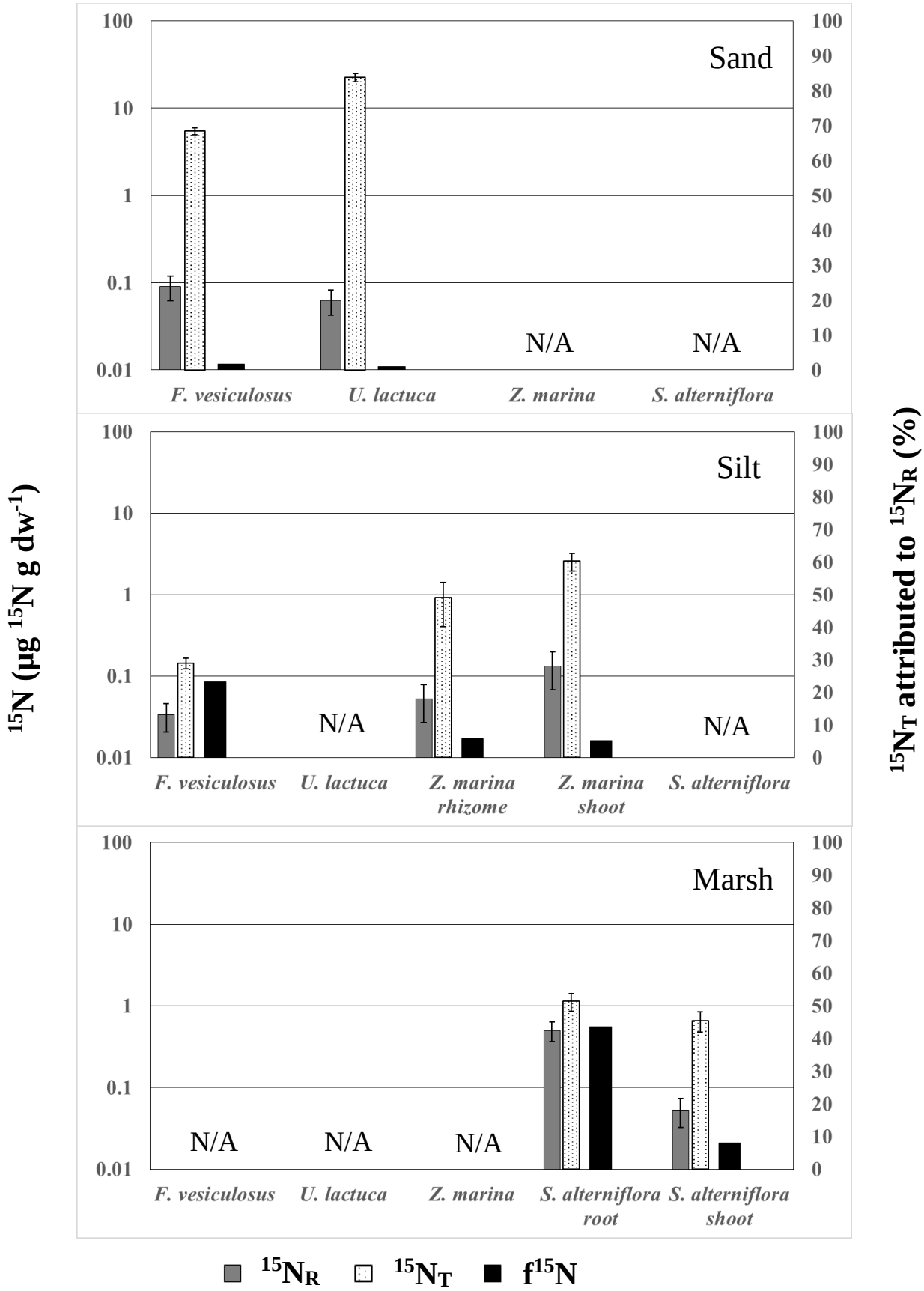

Figure 4: Epifaunal ^{15}N concentrations

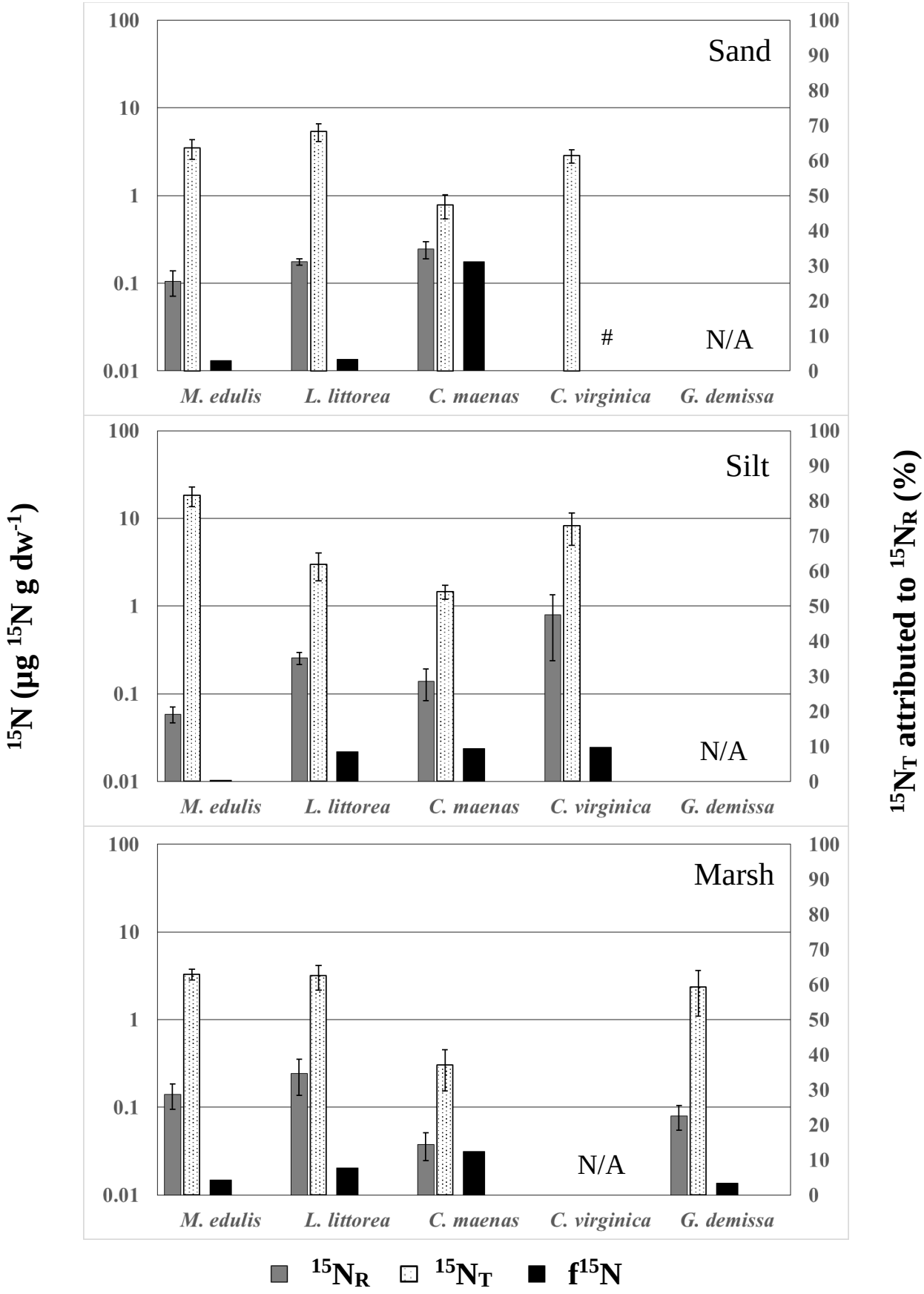

Figure 5: Infaunal and Fish ^{15}N concentrations

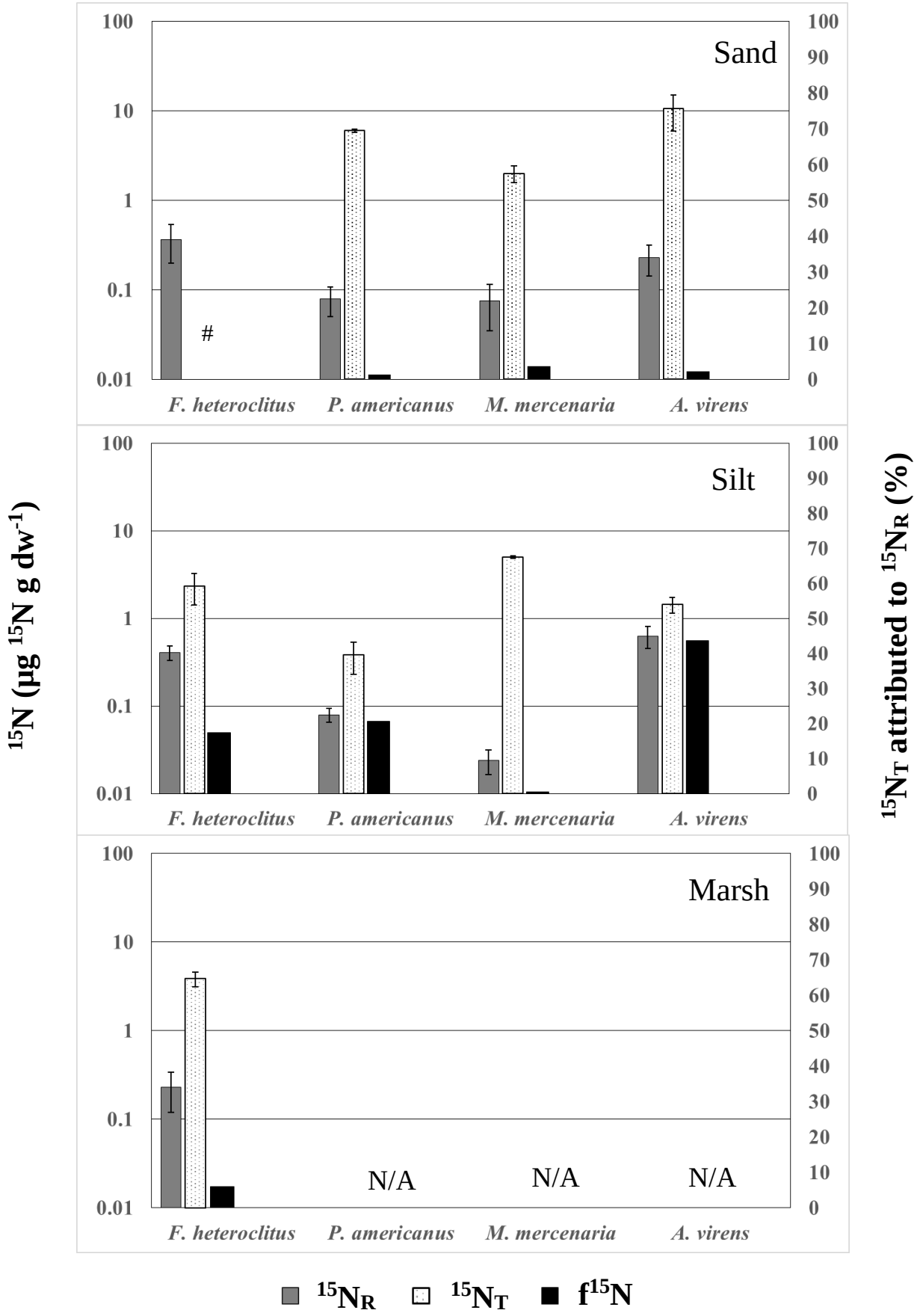

Figure 6: Storage of RDX on an Ecosystem Scale

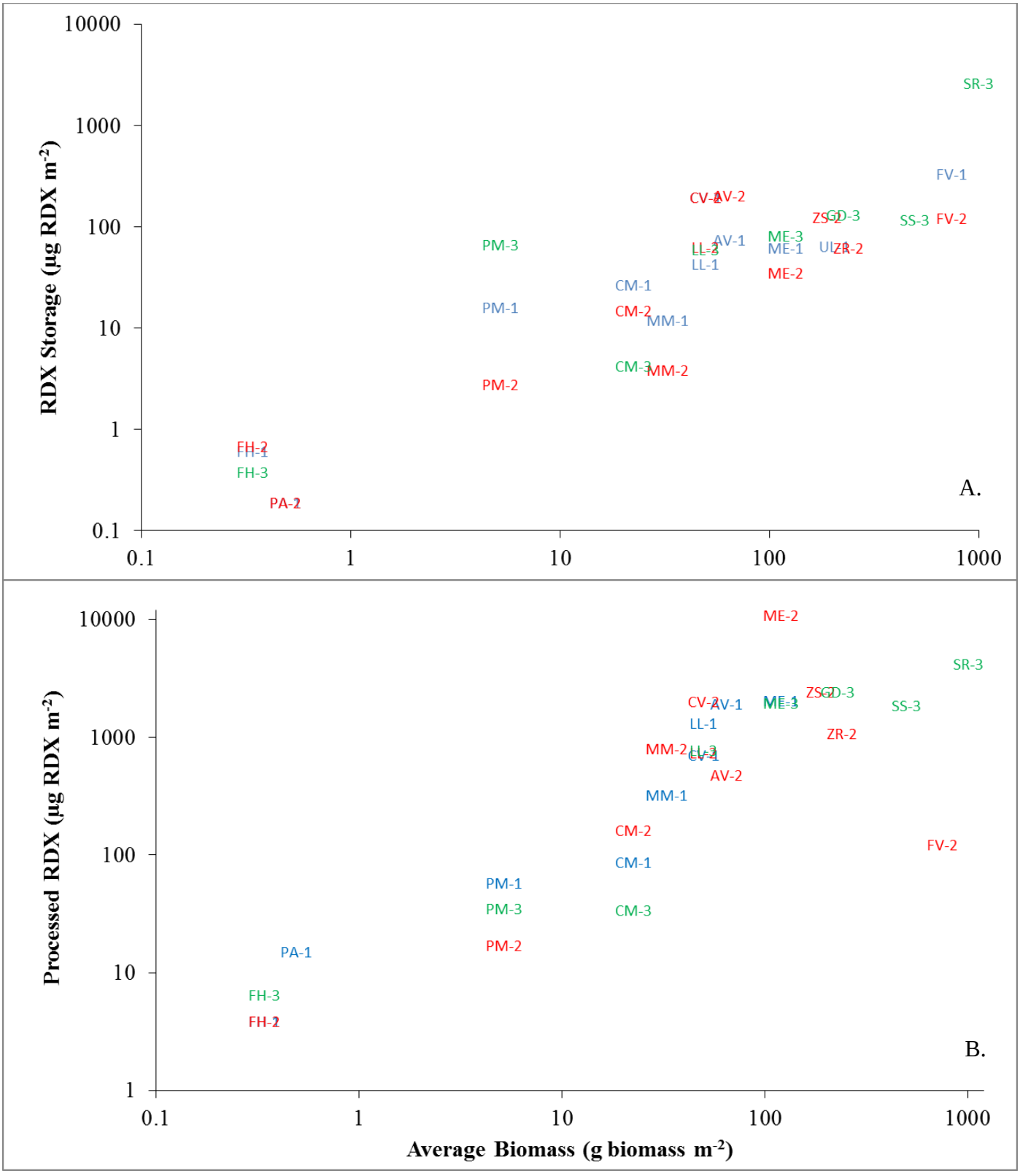

Chapter 5: Conclusion

General Conclusions:

This dissertation examined the uptake, elimination, retention, and biotransformation of TNT and RDX in coastal marine biota using ^{15}N stable nitrogen isotopes. Previous research of TNT and RDX focused primarily on terrestrial (Kuperman et al., 2009) and aquatic ecosystems (Lotufo et al., 2009) with the use of unlabeled TNT and RDX. Expanding the knowledge base of TNT and RDX behavior with the respect to marine organisms is necessary for developing relevant ecological risk profiles for these contaminants specific to coastal marine systems. Overall, TNT and RDX uptake, elimination, retention, and biotransformation in coastal marine biota was similar to aquatic measurements at the organismal level (Lotufo et al., 2009).

Fast uptake and elimination of TNT and RDX, paired with little variation of initial uptake rates between different marine fauna and flora species suggests that tissue concentration of TNT and RDX represents rapid chemical portioning into tissues followed by equilibrium steady state between elimination and additional partitioning. This steady state between uptake and elimination rates for TNT and RDX was similar across environments and species, suggesting applicability of bioconcentration factors (BCFs) established here to a wide variety of species across disparate habitats. Similar to BCFs both measured in aquatic species (Belden et al., 2005a; Belden et al., 2005b; Lotufo & Lydy, 2005), the marine BCFs derived here are low indicating that neither TNT nor RDX bioconcentrates in biotic tissues, and is not likely to bioaccumulate in marine flora or fauna.

The low potential for bioaccumulation of parent compounds, however is only one factor that may contribute to potential ecological risk. The use of ^{15}N labeled RDX in this dissertation provided the ability to measure retention of ^{15}N-containing breakdown products and model the movement of ^{15}N through the coastal marine biotic tissues. Previous use of ^{14}C and ^{15}N labeled

RDX focused either on single species uptake, or tracing mineralization of RDX to inorganic end products (Fournier et al., 2002; Sheremata & Hawari, 2000; Thompson et al., 2005). Experiments described in this dissertation allowed both microbial breakdown pathways to operate side by side with macrobiotic uptake and transformations as would be encountered *in situ*. The amount of ^{15}N in the biota tissue was 1-2 orders of magnitude greater than can accounted for by measureable tissue RDX indicating that a significant amount of RDX derived N was ultimately retained within tissues. While total ^{15}N retained in tissue constituted a small amount of the total RDX loss in the marine mesocosms, the retained N constituted the dominant fate of RDX uptake by the organism. This tight connection between uptake and ultimate retention of the RDX derived ^{15}N tracer was so strong that mesocosms aqueous RDX concentrations were only a modest predictor of tissue RDX and total ^{15}N tracer derived from RDX. This seeming disconnect between aqueous RDX and tissue concentration observed under conditions where organism uptake and mineralization pathways operate concurrently hint at the complexity of biotransformation pathways under natural conditions.

Both TNT and RDX have been shown to be degraded and biotransformed by various species and environments (Bhatt et al., 2005; Vila et al., 2007), and marine biota are no exception. The measurement and modeling of ^{15}N in biotic tissue in this dissertation suggests that there are four different pathways that the biotransformation products containing ^{15}N could be retained in marine biotic tissues. Some of these pathways may indicate that certain organisms could be using N released from RDX as a nutrient (e.g. macroalgae), while other pathways consist of accumulation of organic N containing derivatives that may have further toxicity. Identifying the specific ^{15}N containing breakdown products retained in tissues is an essential next step for determining whether or not there are unaccounted for ecological risks not addressed

by standard approaches such as BCFs, or if these munitions are actually supply N to organisms in this N-limited environment for growth.

This dissertation presented new and novel ways to measure and understand the uptake, elimination, retention, and biotransformation of TNT and RDX in a wide range of coastal marine biota. The use of ^{15}N as a tracer contributed to the existing literature by added the ability to measure biotransformation of TNT and RDX more completely. The knowledge that marine biota are taking up and retaining more TNT and RDX breakdown products than previously thought simultaneously resolved some questions about the removal of TNT and RDX from marine systems, and generated new questions about the impact of biotransformation products on coastal marine biota. Future work with munitions such as TNT and RDX should focus on identifying both the biotransformation products and their possible toxicological effects on coastal marine biota.

References

Belden, J. B., Lotufo, G. R., & Lydy, M. J. (2005a). Accumulation of hexahydro- 1, 3, 5-trinitro- 1, 3, 5- triazine in channel catfish (*Ictalurus punctatus*) and aquatic oligochaetes (*Lumbriculus variegatus*). *Environmental Toxicology and Chemistry, 24*(8), 1962-1967.

Belden, J. B., Ownby, D. R., Lotufo, G. R., & Lydy, M. J. (2005b). Accumulation of trinitrotoluene (TNT) in aquatic organisms: Part 2—Bioconcentration in aquatic invertebrates and potential for trophic transfer to channel catfish (*Ictalurus punctatus*). *Chemosphere, 58*(9), 1161-1168.

Bhatt, M., Zhao, J., Monteil-Rivera, F., & Hawari, J. (2005). Biodegradation of cyclic nitramines by tropical marine sediment bacteria. *Journal of Industrial Microbiology and Biotechnology, 32*(6), 261-267.

Fournier, D., Halasz, A., Spain, J., Fiurasek, P., & Hawari, J. (2002). Determination of key metabolites during biodegradation of hexahydro-1,3,5-trinitro-1,3,5-triazine with *Rhodococcus* sp. strain DN22. *Applied and Environmental Microbiology, 68*(1), 166-172.

Kuperman, R. G., Simini, M., Siciliano, S., & Gong, P. (2009). Effects of energetic materials on soil organisms. In: Sunahara G.I., Lotufo G., Kuperman R.G., Hawari J. (eds) Ecotoxicology of explosives. CRC press, Boca Raton, pp 35-76.

Lotufo G.R., Lydy M.J., Rorrer G.L., Cruz-Uribe O., Cheney D.P. (2009) Bioconcentration, bioaccumulation, and biotransformation of explosives and related compounds in aquatic organisms. In: Sunahara G.I., Lotufo G., Kuperman R.G., Hawari J. (eds) Ecotoxicology of explosives. CRC press, Boca Raton, pp 123-155.

Lotufo, G., & Lydy, M. (2005). Comparative toxicokinetics of explosive compounds in sheepshead minnows. *Archives of Environmental Contamination and Toxicology, 49*(2), 206-214.

Sheremata, T. W., & Hawari, J. (2000). Mineralization of RDX by the white rot fungus *Phanerochaete chrysosporium* to carbon dioxide and nitrous oxide. *Environmental Science & Technology, 34*(16), 3384-3388.

Thompson, K. T., Crocker, F. H., & Fredrickson, H. L. (2005). Mineralization of the cyclic nitramine explosive hexahydro-1,3,5-trinitro-1,3,5-triazine by *Gordonia* and *Williamsia* spp. *Applied and Environmental Microbiology, 71*(12), 8265-8272. doi:71/12/8265

Vila, M., Lorber-Pascal, S., & Laurent, F. (2007). Fate of RDX and TNT in agronomic plants. *Environmental Pollution, 148*(1), 148-154.